
**MODELING HIPPOCAMPAL THETA-COUPLED
GAMMA OSCILLATIONS IN LEARNING AND
MEMORY**

Author:

ASHRAYA SAMBA SHIVA

Supervisors:

PROF BRUCE GRAHAM

PROF CARRON SHANKLAND

PROF DAVID CAIRNS

*Thesis submitted for the
degree of Doctor of Philosophy*

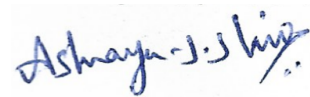
Division of Computing Science & Mathematics
School of Natural Sciences
University of Stirling
Stirling FK9 4LA
United Kingdom

30 SEPTEMBER, 2023

DECLARATION

I, Ashraya Samba Shiva, hereby declare that this thesis has been composed by me and that the research reported therein has been conducted by me unless otherwise indicated.

Tranby, Norway
January 25, 2024

A handwritten signature in blue ink that reads "Ashraya Samba Shiva". The signature is written in a cursive style with a horizontal line underlining the name.

Ashraya Samba Shiva

ACKNOWLEDGMENT

My research has been a long journey consisting of many interesting twists and turns. Some fortunate and many unfortunate.

Firstly, I would like to thank my supervisor Professor Bruce Graham, for his amazing guidance, patience and timely word of advice without which the whole ride would have been impossible. His expertise made me sharpen my understanding and his insightful feedback made me realize my mistakes and rectify them. Thank you for helping me make the right decisions at crucial moments which I will never regret, and thank you for being there throughout the toughest moments in my life, most of which happened in these 6 years. I would like to specially thank Professor Carron Shankland for her support, time and efforts in helping me write my thesis and pushing me to be on time. Your comments and questions helped me a lot in writing my thesis and to gain more understanding of my work. And lastly, thanks a lot to Professor David Cairns for his timely support.

Thanks a lot to Sam and Graham for their technical support.

I would like to thank all my professors, friends and colleagues for their timely support and encouragement.

I would like to thank the Department of Computing Science and Mathematics, University of Stirling, for granting me the Impact studentship without which I would not have been able to pursue my doctoral dream.

Finally, I would like to thank my parents, especially my Mom whose persisting questions led me to pursue this PhD in the first place. Her support and patience are endless which motivated me to keep going on even during hopeless circumstances. I would like to thank my Dad for his love, support and encouraging words in time of need. My special thanks and gratitude to my sister and brother-in-law for their support, patience and timely advice. I would like to specially thank my husband for helping me learn modeling of continuous models, without whose timely support and words of encouragement, my journey would have been really difficult. Both my Mom and Dad did not live to see me finish my PhD, nevertheless, I hope you feel happy and proud of my achievements wherever you are, Mom, Dad, and thanks a lot for being there for me every time, all the time. This thesis is a tribute to my Mom and Dad for their unconditional love and trust in me.

ABSTRACT

Two of the most researched domains in the hippocampus are the oscillatory activity and encoding and retrieval of patterns in the hippocampal CA1 and CA3 regions. They are, however, not studied together; and hence, the objective of our work is to study the cross-frequency coupling of theta-coupled gamma oscillations in CA1 and CA3 regions of the hippocampus while encoding and retrieving information. We have studied the cross-frequency coupling of theta-coupled gamma oscillations both individually and in our newly-proposed integrated model of CA1-CA3 to analyze the effects of Schaffer collaterals and CA1 back-projection cells on CA1 and CA3 regions of the hippocampus. Due to lack of literary evidence, we have also contributed our hypotheses about the effects of CA1 back-projection cells on CA1 and CA3 cell-types. Moreover, we have developed a deterministic rule-based cellular automata library to study cross-frequency coupling in single-neuron level and population neuronal networks at the same time. The discrete model is theta-oscillations-aware and hence encoding and retrieving of patterns takes place during the half-cycles of theta oscillations.

We have extended the septo-hippocampal population firing rate model proposed by Denham and Borisyuk (2000) to study (i) the influence of inhibitory interneurons, specifically PV-containing basket cells (BCs) and bistratified cells (BSCs) on theta and theta-coupled gamma oscillations in both CA1 and CA3 hippocampal networks; (ii) to study Schaffer collaterals from CA3 to CA1 and the influence of back-projection cells in CA1 on CA3; (iii) to analyze and compare the phases of cross-frequency coupling of theta-coupled gamma oscillations among the different cell types in CA1 and CA3 regions; (iv) to study the influence of external inputs on CA1 and CA3.

In our simulations, with constant external inputs, we identify the parameter regions that generate theta oscillations and that BCs and BSCs in CA1 are in anti-phase, as seen experimentally by Klausberger et. al (2008). Slow-gamma oscillations are generated due to the activity of BSCs and BCs in CA1 and CA3, and they are propagated from CA3 to CA1 through the Schaffer collaterals, as seen in Klausberger et. al (2008) where BSCs were observed to synchronize PC activity during theta-coupled gamma oscillations in CA1. In CA3, increasing excitation of CA3 pyramidal cells results in theta oscillations without the slow-gamma coupling. Increasing excitatory input to CA1 pyramidal cells results in steady state and decreasing the excitatory input, results in reduced oscillatory activity in both CA1 and CA3 due to Schaffer collaterals and the feedback projections from CA1 to CA3. This demonstrates that changes in input excitation can move the networks from oscillatory to non-oscillatory

states, comparable to the differences seen in animals between exploratory and resting state.

Further, Mizuseki et. al (2009) observed experimentally that CA1, CA3 and EC are out-of-theta-phase with each other and that the phase observed in CA1 pyramidal cells are not a result of a simple integration of phases from CA3, EC or the medial septum. We have thus, simulated theta-frequency sine-wave inputs from CA3 and EC of relative phases in the model and observed the same results in our CA1 individual and CA1-CA3 integrated model.

To study encoding and retrieval of patterns in an oscillating model, we took an engineering approach by developing a discrete modeling system using cellular automata (CA) derived from the models of Pytte et. al (1991) and Claverol et. al (2002). The aim of this model is to (i) replicate the oscillatory and phasic results obtained using the continuous modeling approach and (ii) extend the same model to study storage and recall of patterns in CA1 taking a theta-oscillations-aware approach.

Encoding and retrieval happen at different half-cycles of theta where information processing takes places in the sub-cycles of the slow-gamma oscillations in each half-cycle of theta oscillation (Cutsuridis et. al, 2010, Hasselmo et. al, 1996). A set of rules is developed to replicate this for the CA model of CA1. The encoding and retrieval half-cycles are identified using the basket cell activity, and hence synaptic learning is enabled during the encoding half-cycle of theta, and is disabled during the recall half-cycle of theta oscillations. This is also a biologically realistic enhancement for studying learning and recall in theta-coupled gamma oscillations using a discrete cellular automata approach.

CONTENTS

1	Introduction	14
2	Why study oscillations?	20
2.1	Behavioural states of oscillations	20
2.2	Role of hippocampus in learning and memory	22
2.2.1	Place cell formation	24
2.2.2	Encoding and retrieval of memories from the hippocampus and neo-cortex	25
2.2.3	Hebbian learning and associative memory	27
2.2.4	Encoding and retrieval of memories based on Hebbian learning	28
2.3	Theta and gamma oscillations in the hippocampus	29
2.3.1	Influence of hippocampal theta oscillations on other brain regions	30
2.3.2	External inputs and mechanisms of the hippocampal circuit	31
2.3.3	Comparison of CA1 and CA3	32
2.3.4	Role of oscillations in the encoding and retrieval of memories	33
2.4	Summary	33
3	Introduction to various types of models	34
3.1	Single-neuron models	35
3.1.1	Hodgkin-Huxley (HH) model	35
3.1.2	Fitzhugh-Nagumo model	38
3.1.3	Káli & Dayan hippocampal CA3 model	38
3.1.4	Leaky integrate-and-fire model	40
3.1.5	Non-linear integrate and fire model	42
3.1.6	Cellular automata approach for single neuron models	43
3.2	Continuous population models	46
3.3	Bifurcation analysis of non-linear systems	47
3.4	Conclusion	48
4	Theta-coupled gamma oscillatory model of the CA1-CA3 regions of the hippocampus	52
4.1	Introduction	52
4.2	Modeling CA1-CA3 integrated microcircuit	53

4.2.1	Basic theta oscillation circuit	58
4.2.2	Microcircuit of CA1-CA3 region of the hippocampus	60
4.2.3	Time constants of neuronal populations	65
4.2.4	Methods of analysis	66
4.3	Results	69
4.3.1	CA1 model with constant external inputs	69
4.3.2	CA3 model with constant external inputs	72
4.3.3	CA1-CA3 integrated model	77
4.3.4	Connection weights analysis	83
4.3.5	Oscillatory modes and bifurcation analysis	87
4.3.6	Effects of CA3 recurrent connections on CA1-CA3 neuronal network	89
4.3.7	Effects of CA1 back-projection cells on CA1-CA3 neuronal circuit	90
4.3.8	CA1-CA3 phase differences	95
4.4	Discussion	97
4.4.1	Comparison of CA1 and CA3 models	97
4.4.2	Comparison with experiments	98
4.5	Conclusion	100
5	Cellular automata model	102
5.1	Architecture of the cellular automata model	102
5.1.1	Elements in a cellular automata model	103
5.1.2	Stages in a cellular automata model	104
5.1.3	Inputs and outputs of the model	106
5.2	Theta and gamma oscillations in CA network models	109
5.2.1	Simulation of E-I model	109
5.2.2	Simulation of CA1 individual model	112
5.3	Large-scale simulations	114
5.4	Mechanism of pattern learning and recall in cellular automata model	117
5.4.1	Recall quality metric calculation	121
5.5	Simulations involving learning and recall of multiple intersecting patterns	121
5.6	Discussion	128
5.7	Conclusion	132
6	Conclusion and future work	133
6.1	Main contributions	133

6.2 Oscillations 134
6.3 Encoding and retrieval of memories 135
6.4 Future work 136

References **139**

LIST OF FIGURES

1	Pathways in the hippocampus	15
2	The different regions and the trisynaptic loop of the hippocampus	16
3	An E-I-E and E-E network of recurrent collaterals	17
4	Different types of synaptic plasticity taken from Sejnowski et. al. (1989)	17
5	Different frequency bands of the neural rhythmic oscillations explained	20
6	Hippocampus in a normal brain and after removal	23
7	Encoding and retrieval cycle proposed by Hasselmo et. al [1]	26
8	Simulation results for the Fitzhugh-Nagumo model	39
9	Simulation results for the Káli & Dayan hippocampal CA3 model	40
10	Simulation results for LIF neuron model	41
11	Simulation results for an E-I network using cellular automata model	45
12	Explanation of the different bifurcation stages in the FN model.	49
13	CA1-CA3 integrated microcircuit	53
14	Septo-hippocampal theta oscillation pacemaker circuit	54
15	Projections to CA1 and CA3 pyramidal cell	55
16	Projections to CA1 and CA3 basket cell	56
17	Projections to CA1 and CA3 bistratified cell	56
18	Projections to CA1 and CA3 other inhibitory interneurons	57
19	Activity dynamics of the hippocampal-septal pacemaker circuit	59
20	Explanation for getting frequencies from activity plots	68
21	CA1 microcircuit where CA3 and EC are constant inputs.	69
22	CA1 individual model simulation results	70
23	CA1 pyramidal, basket and bistratified cells are in-sync	72
24	CA3 microcircuit where CA1, EC and DG are constant inputs.	73
25	CA3 (left) 7Hz theta and (right) 50Hz theta-coupled slow gamma oscillations.	73
26	Effects on CA3 neuronal network as recurrent pyramidal excitation increases.	75
27	Effects on CA3 neuronal network as recurrent pyramidal excitation increases.	76
28	CA1-CA3 integrated model simulation results	78
29	Effect on CA1 pyramidal cells for different connection strength values.	79
30	Analysis of integrated model results	79
31	Analysis of CA1 bistratified cell to CA1 pyramidal cell connection strength changes	80
32	Analysis of CA3 basket cells and CA3 pyramidal cells for varying external inputs	82

33	Analysis of septal-loop changes	84
34	Effects of external inputs on CA1 and CA3 regions	85
35	Intermediate states when EC is low and connection weights of CA3 pyramidal to CA3 basket cells increases	88
36	CA1 and CA3 phase plots	88
37	Effects of CA3 recurrent collaterals on CA1	90
38	Analysis of CA1 pyramidal cells to CA1 back-projection cells connection weight changes	91
39	Analysis of CA1 back-projection cells to CA3 basket cells connection weight changes	92
40	Analysis of CA1 back-projection cells to CA3 bistratified cells connection weight changes	93
41	Analysis of CA1 back-projection cells to CA3 pyramidal cells connection weight changes	94
42	Analysis of CA1 back-projection cells to CA3 other inhibitory interneurons cells connection weight changes	95
43	CA1 phase changes with CA3 and EC sinusoidal input	96
44	CA1 phase changes with EC sinusoidal input in CA1-CA3 integrated model	96
45	Theta-coupled gamma oscillations in CA1 in the absence of CA3 input.	99
46	Neuronal network in a cellular automata model	104
47	Working of a cellular automata model derived from the work of Claverol et. al [3] . .	105
48	Architecture of the cellular automata model	106
49	Excitatory-inhibitory neuronal network in a cellular automata model	110
50	Cellular automata model simulation results for E-I network model	111
51	Cellular automata model simulation results for CA1 network model	113
52	Phases of pyramidal(E), basket(B) and bistratified(BS) populations	114
53	Theta and slow gamma frequency bands in pyramidal, basket and bistratified cell simulation	115
54	Attempts to synchronize pyramidal, basket and bistratified cells	116
55	Simulation results for large-scale network	118
56	Learning and recall phases in theta cycle	120
57	Simulation results without LTP and LTD	125
58	Simulation results with LTP and no LTD	126
59	Simulation results with both LTP and LTD	127
60	Effect on the population activity of pyramidal cells when basket cell population is completely removed from the network	129

61	Effect on the population activity when bistratified cell population is completely removed from the network	130
62	Effect on the population activity when other inhibitory interneuron cell population is completely removed from the network	131

LIST OF TABLES

1	Comparison of recurrent collaterals of different regions of the brain	31
2	Parameters used in Hodgkin-Huxley model	37
3	Types of bifurcations explained	50
4	CA1 connectivity matrix	60
5	CA3 connectivity matrix	61
6	Symbols definition	62
7	Time constants of cells in CA1 and CA3	66
8	Weights and external input values for CA1	71
9	Weights and external input values for CA3	74
10	Weights & external input values for CA1 integrated model	80
11	Weights & external input values for CA3 z integrated model	81
12	Effect of septo-hippocampal loop on CA1 and CA3 as shown in figure 34	86
13	Amplitude comparison between CA1 and CA3 individual and integrated models	98
14	Example of neuronal network input parameters in JSON files	108
15	Our implementation of the STDP learning algorithm	122
16	Our implementation of the STDP learning algorithm when basket cells are active.	123
17	Parameters for the cellular automata CA1 neuronal network	124

LIST OF PUBLICATIONS

1. Samba Shiva, A., and Graham, B.P., Population model of oscillatory dynamics in hippocampal CA1 and CA3 regions. BMC Neuroscience. 29th annual computational neuroscience meeting: Cns* 2020. BMC Neuroscience, 21(1):54, 2020.
2. Samba Shiva, A., and Graham, B.P., A cellular automata model of the hippocampal septal pacemaker circuit. 30th annual computational neuroscience meeting: Cns* 2021, In Journal of Computational Neuroscience, (Vol. 49, No. Suppl 1, pp. S77-S79), 2021.
3. Samba Shiva, A., and Graham, B.P., Population Model of Oscillatory Dynamics in Hippocampal CA1 and CA3 Regions. Under preparation to submit in Hippocampus.
4. Samba Shiva, A., and Graham, B.P., A cellular automata model of encoding and retrieval in hippocampal CA1 region. Under preparation to submit in Neural Networks.

1 INTRODUCTION

Mundane activities, some involuntary and some repetitive ones, such as breathing, blinking, locomotory activities, mastication, learning, memory, etc. are all related to the rhythmic oscillations in the brain. Rhythmic tremors observed in certain conditions such as epilepsy, Parkinson's, various sleep disorders [4, 5] are all related to various impairments to different oscillations. Brain oscillations are generated as a result of interactions between neurons or due to intrinsic activities in a neuron due to changes in membrane potential or evoking action potentials. The diversity of neuronal connections found in the brain has been widely studied and modeled. Neurons, the basic brain cells, communicate with each other, fire action potentials thus generating oscillations [6]. These oscillations can be regular or irregular, and yet have a well defined functionality. Due to an external stimulus, these oscillations can be perturbed, but they then return back to their initial cycle, perhaps with a phase difference [4]. The type of neurons interacting with each other determines the type of oscillatory activity. The high level question that we are trying to understand in this thesis is how these oscillations relate to encoding and retrieval of memories.

Oscillations are believed to coordinate the working of the different regions of the brain. In this work, we have considered the hippocampal region of the brain to study neuronal oscillations in encoding and retrieval. Physiologically, the hippocampus consists of CA1 to CA4 regions, subiculum and the dentate gyrus (DG), with major inputs coming from the entorhinal cortex (EC) and the medial septum. The projections from the EC to DG forms the perforant pathway, DG to CA3 forms the mossy fiber pathway, and from CA3 to CA1 forms the Schaffer collaterals, collectively called the trisynaptic loop, as shown in figure 1, and as explained in simple terms in figure 2. The CA3 region of the hippocampus has a recurrent neuronal structure wherein the excitatory pyramidal cells project onto themselves extensively. Such recurrent projections can be seen sparsely in CA1 as well. The interactions between neurons can be either from excitatory to inhibitory, inhibitory to excitatory or recurrent within the same population of neurons as shown in figure 3. When neurons in a population project onto themselves, recurrent collaterals are formed which can be either excitatory or inhibitory depending on the type of neurons involved. These recurrent collaterals aid in learning, memory and also provide computational capabilities [7]. Associative memories behave as such due to their large basin of attraction about each memory array in every region [8, 9]. In 1949, Donald Hebb proposed the "Hebb rule", which states that "*when an axon of cell A is near enough to excite cell B or repeatedly or persistently takes part in firing it, some*

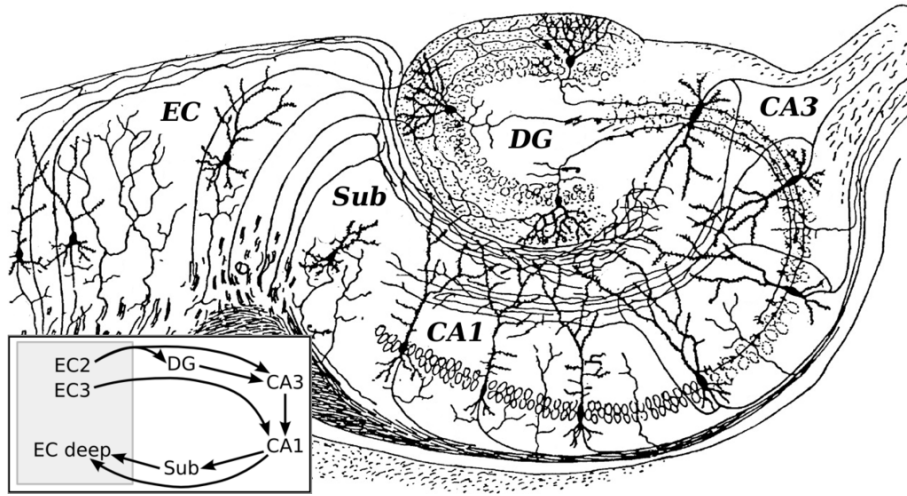


Figure 1: Drawing of the hippocampus with the different pathways by Drawing of the hippocampal regions by Santiago Ramón y Cajal, 1911, *Histologie du Système nerveux de l’Homme et des Vertébrés*, Paris

growth process or metabolic change takes place in one or both cells such that A’s efficiency, as one of the cells firing B, is increased” [10]. Three implementations of the Hebb rule are explained by Sejnowski et al. [11] for the implementation of synaptic plasticity —(i) A direct connection between two neurons *A* and *B* having a modifiable synaptic connection; (ii) a feedback connection from neuron *B* to *A* wherein the strength of the modifiable synaptic connection between them increases in proportion to the firing rates of the two neurons; and (iii) an intermediate neuron called the interneuron, *I*, which modifies the threshold needed for action potential generation, as the threshold decreases in proportion to the firing rate of the two neurons *A* and *B* as shown in figure 4.

These three implementations are found in the brain, wherein types (ii) and (iii) have recurrent collaterals. In type (ii), the recurrent excitation comes from the postsynaptic site projecting onto the projection from neuron *A* to neuron *B*, whereas in type (iii), the feedback comes from neuron *B* onto the intermediate inhibitory interneuron altering the threshold for further potentiation. We are more interested in the behaviour of neuronal networks where neurons in a population, either excitatory or inhibitory, project onto themselves, thus increasing either excitation or inhibition. Such projections in neuronal networks require an opposite force to regulate the behaviour of neurons in such circuits.

Functionally, the hippocampus plays an important role in memory consolidation of long-term memories or episodic memories stored in the neocortex [12]. Hippocampus is also a cognitive map wherein the primary cells of the hippocampus record the location of the sub-

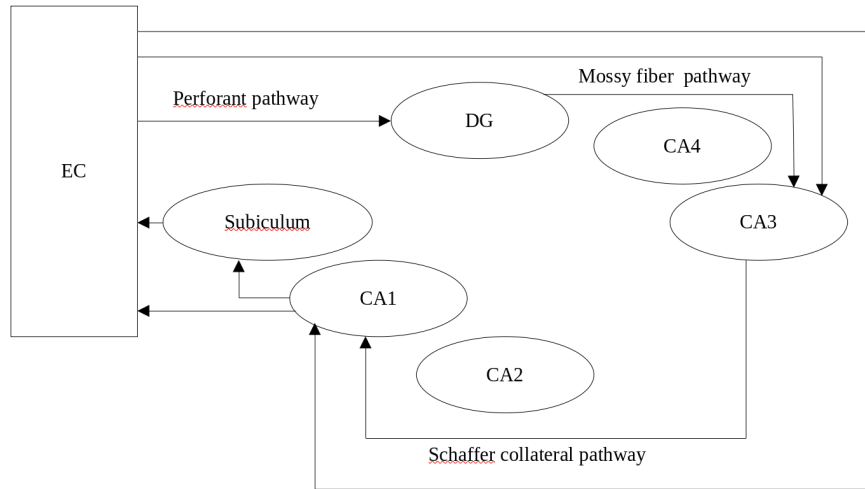


Figure 2: The different regions and the trisynaptic loop of the hippocampus

ject as the subject moves around [13, 14]. Hebb proposed that the synaptic connectivity between cells become stronger if they are active at the same time, which is termed as the “*coincidence-detection rule*” [10]. Modifiable synapses allow action potentials to persist for a longer duration and are required for remembering data that are learnt [15]. This is called long term potentiation (LTP) wherein a sustained increase in synaptic strength is observed following a high-frequency stimulus [16]. Whereas when the pre-synaptic neuron is not active but the post-synaptic neuron is active, it is called long term depression (LTD), and the corresponding projection strength decreases. The brain oscillations exhibited during such phenomenon are observed to be between 30-50Hz which is superposed on a 4-10Hz carrier.

Theta oscillations are rhythmic brain oscillations in the frequency range of 4-10Hz. The supra-mammillary bodies (SUM) via the medial septum-diagonal band of Broca (ms-dbb) propagate the rhythmic theta oscillations to the hippocampus [17]. Memory consolidation from the hippocampus to the neocortex is known to occur during rapid eye movement (REM) sleep [18]. Theta oscillations are known to be prominent during learning and recall of new location states, and during REM sleep in the hippocampus and neocortex [19]. Slow gamma oscillations are the rhythmic brain oscillations in the frequency range of 30-50Hz. These have been observed to process and encode data in subcycles encompassed in a single theta half cycle [20, 21]. It has been observed that the phase of theta oscillations decide the type of activity taking place between the pre- and post-synaptic neurons, whether it is an LTP or LTD [19].

Due to the recurrent collaterals in CA3, an autoassociative memory is formed, and due

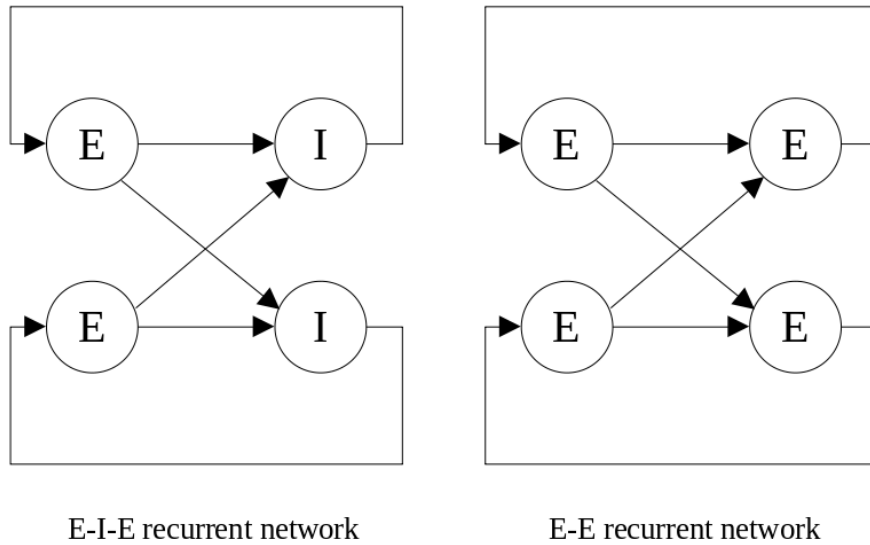


Figure 3: An E-I-E and E-E network of recurrent collaterals

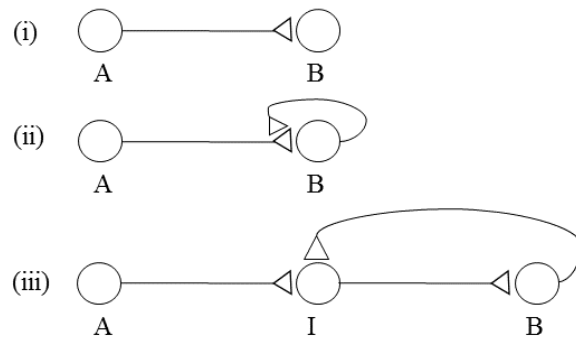


Figure 4: Different types of synaptic plasticity taken from Sejnowski et. al. (1989)

to the feedforward connectivity in CA1, a heteroassociative network is formed [22]. Active neurons representing learnt patterns are retrieved, and encoding of novel environments as new patterns occur in specific gamma cycles in different half cycles of theta oscillations, thus encoding and retrieval are temporally separated [22]. A brief explanation about oscillations is given in chapter 2.

The CA3 recurrent collaterals also behaves as a continuous point attractor network [23] having a large basin of attraction resulting in a pattern completion framework, given a part of the required pattern, due to the association of related memory segments in space and time. However, the relevance of memory segments in space and time can be determined from the

phase of oscillations [23]. The authors in [23] also show that the convergence to a particular pattern of space when small changes were introduced in the environment occurs in CA3 recurrent collaterals in the theta-phase firing of the CA3 pyramidal cells.

This thesis is an attempt *to understand the role of oscillations and recurrent collaterals in encoding and retrieval of information*. Taking inspiration from a continuous population model with a network of four coupled differential equations, known as the septo-hippocampal pacemaker circuit proposed by Denham et. al [2], we extended the model to incorporate additional neuronal populations in CA1. Inspired by this CA1 model, we developed a similar model for CA3 region by deriving structural information from biological results in the literature. We have also combined the models to propose the first CA1-CA3 integrated continuous model to understand the effects of the CA3 to CA1 Schaffer collateral projections, and to understand the inhibitory feedback received by CA3 from CA1. This also enables us to analyze the differences between basket and bistratified cells and the other inhibitory interneurons which are present in both CA3 and CA1.

We were able to reproduce results observed in several biological experiments including the phase differences between different cell types in CA1 and CA3, phase of CA1 pyramidal cells with respect to EC and CA3, the propagation of slow gamma oscillations from CA3 to CA1, effects of septal-pacemaker circuit. This validates both our model and the observations/contributions that come out of our simulations. Detailed explanations reproducing biological results are given in chapter 4.

With the results of the continuous population model as a baseline, we move on to study the mechanisms of encoding and retrieval in CA1 region of the hippocampus using the discrete cellular automata approach. With the cellular automata approach, we can also understand brain oscillations from a single neuron level. It is possible to model thousands of such single neurons and to encode and retrieve data during oscillatory activity. We study the recall of information learnt in the individual-based model of CA1 using the information encoded in single subcycles of gamma superposed in a half theta cycle carrier.

We have shown that a discrete modeling approach such as the cellular automata can be used to simulate neuronal models reproducing results from the continuous models, which enables us to study both single neurons and population networks at the same time. We have obtained the phase synchrony of different populations in the hippocampal CA1 region as in literature. In addition, an enhancement over the Cutsuridis et. al [24] model is that the recall of patterns in each of the gamma subcycle in each theta half cycle during our simulation times

are theta-oscillations-aware due to the activity of basket cells.

This thesis is organized to explain first about the importance of studying neuronal oscillations in chapter 2, followed by the various types of models present in chapter 3, and the ones which we have adopted in our study. This is followed by the modeling of population models in chapter 4, which is then followed by the cellular automata implementation in chapter 5, lastly followed by conclusion. Discussion of results from each model is also presented in the respective sections.

2 WHY STUDY OSCILLATIONS?

Oscillations can simply be defined as a periodic wave having an amplitude, frequency and phase recurring within a specified duration of time [25]. When neurons communicate with each other, or due to membrane potential changes, oscillations are generated and propagated across different regions of the brain. Oscillations can be short range, communicating with different neurons in the same region or long range, communicating with different regions of the brain. Multiple functionalities are associated with each oscillation frequency. Superposition of multiple frequency oscillations result in brain responses attributing to specific functional responses [25, 26] as shown in figure 5.

2.1 BEHAVIOURAL STATES OF OSCILLATIONS

Neuronal oscillations are a functionally essential part of the brain system for proper synchronization and coordination of different neuronal circuits. From synaptic plasticity to the communication of different neuronal assemblies to temporal ordering of encoding and retrieval of both short term and consolidated long term memories, are all facilitated by neuronal oscillations [27]. Frequency of brain oscillations can range from 0.5Hz to 500Hz depending on the region and context [27].

Different oscillatory ranges are associated with different behavioural states.

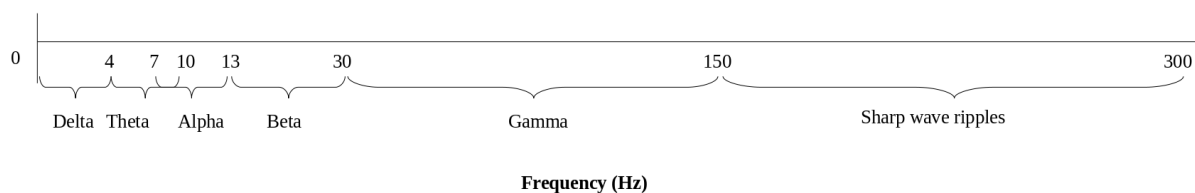


Figure 5: Different frequency bands of the neural rhythmic oscillations explained

1. Alpha band frequency (8-13Hz) is observed during sensory functions from the sensory areas, processing high cognitive loads in the frontal cortex, resting states from the occipital cortex, attention and alertness [26, 28, 29].
2. Gamma band frequency (30-150Hz) is attributed to perception, attention, memory and learning, and information processing [26, 29]. Depending on the temporal sequence of where it occurs, slow gamma (30 - 50Hz) oscillations are actively observed during both encoding and retrieval of information [30].

3. Delta band frequency (1-4Hz) is found when there is slow wave sleep and absence in motor activity [31, 32].
4. Theta band frequency (4-10Hz) is attributed to cognition, encoding and retrieval of information, memory formation and spatial navigation [33, 28, 29]. Theta frequency is also found during REM sleep when episodes from previous awake experiences are replayed for consolidation in the neocortex [29].
5. Beta band frequency (12-30Hz) is observed during awake conscious state just after sleep, in active concentrations, anxious moments, rewarding moments, awareness, processing novel information [34, 35].
6. Sharp wave ripples (140-200Hz) is observed in the hippocampal region during eating, drinking activities, and during memory consolidation to neocortex from the hippocampus. It is also hypothesized to be responsible for memory erasure due to its synchronized activity across CA3 to CA1-subicular-entorhinal complex [25].
7. Sleep spindles are found during stage 2 of the sleep cycle when both the cortical and thalamocortical neurons are active [25].

Cross-frequency coupling of oscillations occurs due to overlapping temporal dynamics which facilitates synchrony between different regions. Theta oscillations are said to be a global oscillator synchronizing and coordinating functionalities across different brain regions. Theta frequency oscillations are found to be coupled with fast gamma oscillations in the auditory cortex [36]. During different behavioural tasks fast gamma oscillations are coupled with higher theta amplitudes in the neocortex [37]. Alpha frequency oscillations are coupled with fast gamma oscillations during visual processing [38]. Alpha-beta frequency oscillations desynchronize during the formation of episodic memories in the neocortex, while the synchronization of hippocampal fast and slow gamma oscillations aid retrieval of information [39].

Theta-gamma cross frequency coupling occurs during short-term memory encoding and retrieval in the hippocampus. CA3 is observed to propagate slow gamma oscillations to CA1 via the Schaffer collaterals, while CA3 has local theta and gamma generating oscillators and also receives inputs from EC via the perforant pathway [40]. It is also hypothesized by Lisman and Idiart [20] that gamma subcycles are found superposed in theta oscillations, wherein seven gamma subcycles are found in each theta half cycle, and each gamma subcycle represents sequential memory items with each memory being triggered in each gamma subcycle

[21, 20, 36]. The intensity of theta-coupled gamma oscillations was found to be more strong during learning and recall mechanisms in the LFP of rats while studying the importance of theta-gamma coupling in the CA3 region of the hippocampus [41]. Theta rhythms were found to regulate learning in neurons, while gamma rhythms were found to bind events from memories, and lastly, the fast oscillatory sharp wave ripples were found to be stronger during consolidation process in the neocortex [42].

In this work, we are interested in studying the hippocampal theta coupled with slow gamma oscillatory activity which is observed during encoding and retrieval of memories between the CA1 and CA3 regions. It has been observed that the phase of theta oscillations decides the type of learning activity taking place between the pre- and post-synaptic neurons, whether it is strengthening or weakening of synaptic connections [19]. Information about the current position of the subject in space is stored in each theta phase [43]. The relationship between spatial exploration information and path integration information are linked together by theta waves [44]. Theta oscillations are used for communication and flow of information across different areas of the hippocampus. Theta acts as a global synchronizer organizing activity in each hippocampal region [45]. Synaptic potentiation is due to the inputs arriving in the positive phase of theta in the dendritic layer and synaptic depression is due to the inputs arriving in the negative phase of theta [46]. It can be said that theta oscillations are a periodic clock timing the spikes of the hippocampus [46].

2.2 ROLE OF HIPPOCAMPUS IN LEARNING AND MEMORY

In graph theory, there is the concept of *centrality algorithms* [47] describing the importance of a node in a network by various means such as, the number of incoming and outgoing projections from a node, if a node connects different populations in a network [48], if the node has the highest eigenvalue [49], etc. The importance of the presence of a node is felt by the network when the node is inactive or deleted or removed, depending on the context. In this context, removal of the hippocampus resulted in understanding its functionality.

The medial temporal lobe of a few patients was removed either partially or bilaterally to reduce symptoms of epileptic seizures, schizophrenia, etc [50] as shown in figure 6. Post-operative status was considered to be better than the patients' pre-operative state, resulting in considerable reduction in seizure medications that usually left the patients lethargic and confused. There was also no noticeable intellectual impairments, and patients showed no changes in personality [50]; however, there was an abrupt gap in the patients' memory time-

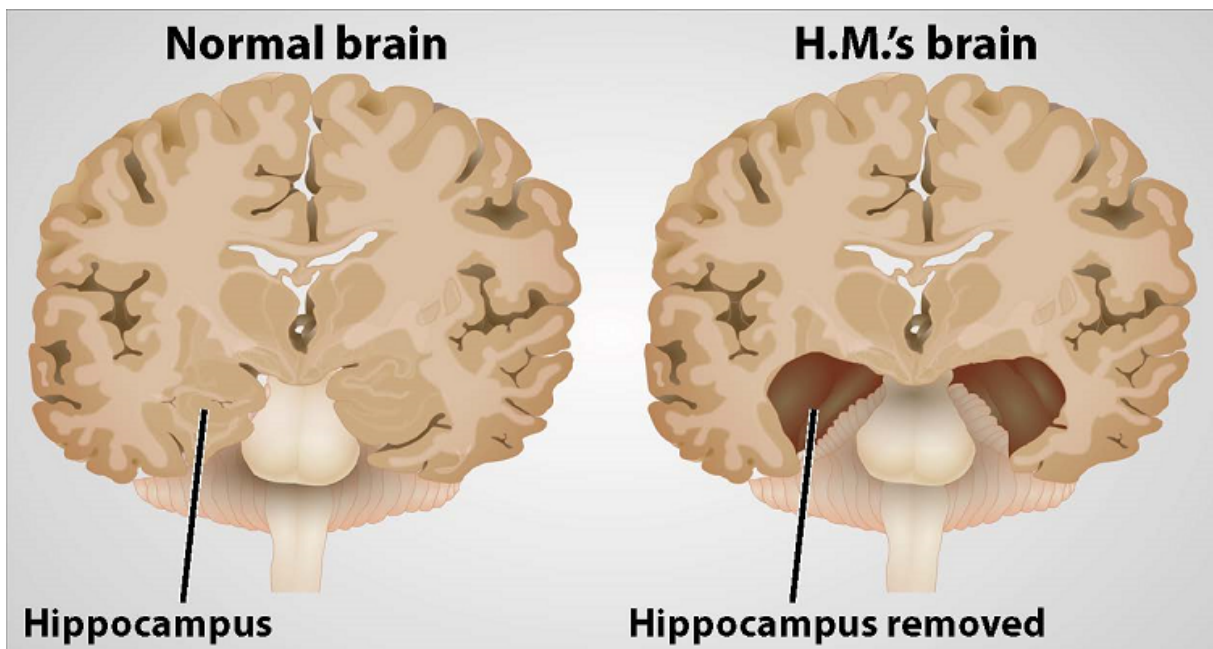


Figure 6: Comparison of a fully functional brain v/s the brain of a patient where hippocampal regions are surgically removed bilaterally. Courtesy: with permission: Rochelle Schwartz-Bloom, Duke University: <http://sites.duke.edu/a pep>

line. In patients where the hippocampus and the surrounding areas was bilaterally removed (about 8cm each on both the sides of the brain), memory about recent events seemed to be forgotten, although the patients could state almost accurately the events of their early life. The patients could not remember recent events in their life [50] which suggests loss of working memory or short term memory, to which the hippocampus is attributed. The patients also could not recall the map of their current environment [50] which also suggests loss of spatial navigation for which the hippocampus is held responsible. Since short-term memory is affected, none of the recent/current events could be stored for long-term recall, affecting memory encoding and memory consolidation.

Thus, hippocampus plays an important role in memory consolidation of short-term memories into long-term memories, or episodic memories which are stored in the neocortex [12]. Hippocampus also serves as a cognitive map wherein the primary cells of the hippocampus known as place cells, record the location of the subject as the subject moves around [13, 14]. Place cells are found to fire when the subject is in a particular environment or as the subject traverses a known environment. The afferents of the hippocampal CA1 area to EC contain information about patterns having relative facts that form the chain of elements of particular memories. Inputs from EC to CA1 has sensory information, inputs from CA3 to CA1

has conceptual information about a specific node, both of which converge in CA1 forming contextual memories. Firing of neurons in an associative manner retrieves memories from partial cues due to LTP, thus strengthening connections between neurons that fire consecutively [12, 51]. Many experiments including mazes, objects etc., are conducted on rats, cats, monkeys, rabbits, etc., to ascertain these observations [13].

Experiments are also conducted to analyze brain oscillations in order to understand more about encoding and retrieval processes. The types of oscillations generated or sustained during various activities of the subject is critical for the understanding of encoding and retrieval of information, which in our case are the theta and slow gamma oscillations in the hippocampus for learning and retrieving hippocampal dependent memories [52, 53, 54].

2.2.1 PLACE CELL FORMATION

It is a well-known observation that the hippocampus is responsible for spatial navigation. The patterns formed by the neurons in the hippocampus form a place field that is in fact overlapping for multiple patterns; i.e., the firing activity that occurs in the hippocampus while traversing environments is not a distinct non-intersecting set of neurons for every specific pattern. From various experiments involving attempts to study the firing patterns for recall of particular environments, it is found that while traversing specific areas in an environment, there is a transformation from a non-spiking neuronal cluster to a 100Hz spiking cluster indicating a strong existence of encoded patterns for those specific environments [13].

It is also observed that intersecting sets of neuronal clusters can represent the same environment encoded several times, each for a different scenario when the subject has traversed the same area [13]. Spatial maps inherit the characteristics of an attractor model wherein recurrent LTP in a particular set of neuronal trajectories get strengthened over time, and form a basin of attraction called a place field. Place cells in this place field converge to the same trajectory every time there is a partial spatial cue related to this firing pattern, thus following the Hebbian rule for associativity [13].

Events happening during a spatial navigation task to learn a specific map also includes many features such as the direction to take to reach the destination, the speed at which to traverse the map, the kind of reward that can be expected at the destination, etc. Each of these features are specific events which form a sequence of events for a particular navigation task. Each such sequence is unique when viewed as individual occurrences. When several such sequences have overlapping features, transitively the sequence map follows these nodal

properties which is also inferential learning. Thus when the nodal properties for certain inputs are activated, the sequences for more than a single chain of events can be seen to be activated owing to the inferential property of spatial representations. This shows that encoding of events represents conceptual and contextual associations between neuronal clusters converging towards an inferred state [13, 55].

Before proceeding further, it is worth mentioning that the memory unit of the brain includes neocortex, parahippocampal regions and the hippocampus which is the most significant region of the memory unit. While the hippocampus serves as a window for learning and creating novel pathways, the rest of the memory unit is busy consolidating the learnings of the hippocampus, which lowers the dependence on the hippocampus for such consolidated memories for retrieval [13].

The hippocampus functions as a working memory unit, to hold memories of events for a short period of time. How short depends on how frequently the memory is accessed, how frequently the same set of neurons in a cluster is activated which strengthens the pathways for specific sequences. Since the creation of such conceptual associations, they remain with the hippocampus for a short period of time, which is then propagated to the parahippocampal region in parallel while learning of new sequences still happens in the hippocampus [13]. The final step in memory consolidation is to propagate the consolidated memories from the parahippocampal cortex to the neocortex where memories are stored for a longer period, also known as the long-term memory, again depending on the retrieval frequency. Every event, the chain of events forming sequences and the nodal properties of such sequences are replayed in the same temporal order to get stored in the neocortex ultimately [13, 56, 57].

2.2.2 ENCODING AND RETRIEVAL OF MEMORIES FROM THE HIPPOCAMPUS AND NEO-CORTEX

The pathways present in the hippocampus play different roles in encoding and retrieval of memories. Considering the afferents to CA3, the perforant pathway (PP) coming from EC brings in multi-sensory information, while the mossy fiber (MF) pathway from the DG brings in novel information to encode [58]. Various experiments, mostly involving trials of learning, retrieval, reward sequences are conducted to test activation of pathways for encoding (PP) and retrieval (Schaffer collaterals). For example, the Hebb-Williams maze where the subject is trained (encoding of new spatial navigation information) to navigate through a maze from a starting point to a goal point to achieve rewards, or the T maze task or the radial maze task where all the paths lead to the center, and the reward can be present in the center

or the subject has to traverse the center to reach the reward location [51, 58, 59, 1, 60].

When it comes to CA1, as shown in figure 7, encoding of novel feed-forward multi-sensory input from EC takes place when the excitation from CA3 is inhibited, in the trough of theta cycle; whereas retrieval of information takes place when acetylcholine-mediated CA3 excitation propagates to CA1 in the peak of theta cycle [1, 61, 24].

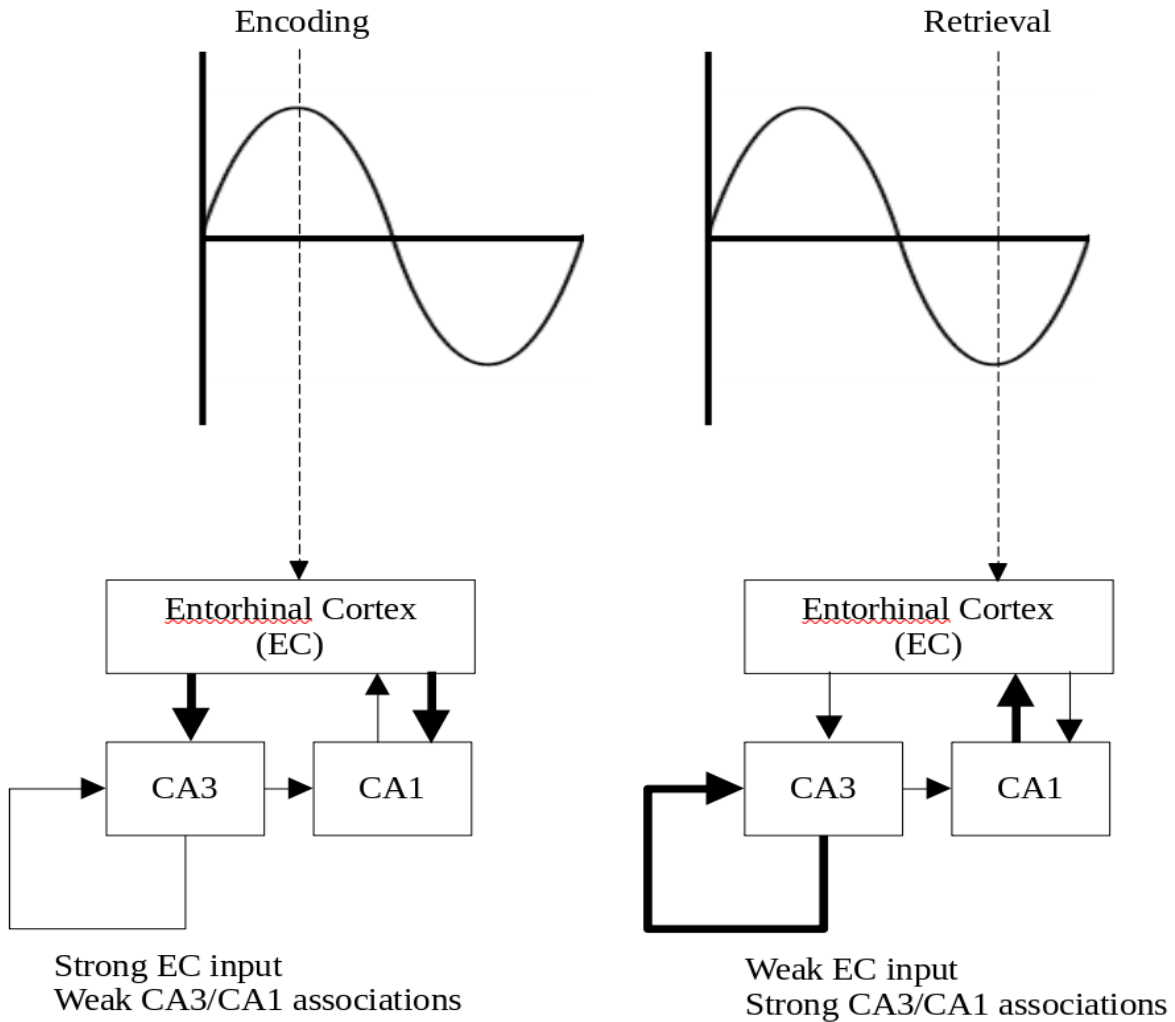


Figure 7: Encoding and retrieval cycle proposed by Hasselmo et. al [1]

The PP and MF pathways to the CA3 and CA1 regions of the hippocampus help encode sensory and spatial information forming episodic memories in the working memory. This information is then consolidated in the neocortex for long term retrieval of information through the hippocampo-neocortical and neocortico-hippocampal pathways respectively

[62, 63]. The hippocampo-neocortical pathway is excited by sharp wave bursts to store memories from CA3 to CA1 to EC to the neocortex during behaviours such as slow wave sleep. It is observed that the information learnt during wakeful behaviour of the subject in the theta-coupled gamma subcycles is compressed and replayed faster, during slow wave sleep exhibiting sharp wave bursts propagating information for consolidation to the neocortex [64]. Memories consolidated in the neocortex are independent of the hippocampus [64].

2.2.3 HEBBIAN LEARNING AND ASSOCIATIVE MEMORY

Hebb proposed that the synaptic connectivity between cells become stronger if they are active at the same time, which is termed as the “*coincidence-detection rule*” [10]. Modifiable synapses that persist action potentials for a longer duration are required for remembering data that are learnt [15]. This is called long-term potentiation (LTP) wherein a high-frequency stimulus is followed by a sustained increase in synaptic strength [16]. LTP is described by its cooperativity, associativity and input-specificity as defined below. A weak stimulus cannot cause LTP, rather a weak input in the presence of a strong impulse converges to evoke an action potential [16]. These synapses which display LTP activity are associative or Hebbian since post-synaptic depolarization and corresponding pre-synaptic activity strengthens the synaptic connectivity between the pre- and post-synaptic neurons [12]. This type of behavior is exhibited by neuronal networks which are responsible for learning and memory, such as the hippocampus [65].

Cooperativity is when the induction of an action potential in a set of synapses is a consistently increasing integrated function of a number of active synaptic afferents. Hence, a function that results in a weaker synaptic response fails to induce an LTP and that which results in a stronger synaptic response succeeds in inducing an LTP [66].

Associativity is when the induction of an action potential in a single neuron or in a neuronal cluster depends on both weak and strong synaptic inputs, where one influences the other quickly, strongly, persistently, conditionally and temporally. Such a form of associative LTP is observed in the Schaffer collaterals/commissural inputs to CA1 pyramidal cells [66].

From the experiments conducted by Barrionuevo et. al, associative LTP was experimentally induced in two excitatory monosynaptic inputs that shared a pathway in a hippocampal CA1 slice. One was given a weak electrical input and another a strong input to receive a weak and strong response respectively. When the synapses were individually stimulated, there was no noticeable effect in the weaker input, however, when both the synapses were stimulated

simultaneously, there was a long term synaptic response in the weaker input, thus exhibiting associative LTP [67].

The Hebb rule is temporal and is localized to specific cluster of neurons. A simple associative learning rule that follows the Hebb postulate is where the output is proportional to the integrated sum of synaptic strengths of inputs, as given in equation 1.

$$y_j = \sum_{i=1}^N w_{ji} * x_i \quad (1)$$

where y_j is the rate of activity of the output neurons, x_i is the rate of activity of the i^{th} input neuron, w_{ji} is the weight between the input neuron i to output neuron j and N is the total number of neurons.

The Hopfield learning algorithm is a simplistic example of Hebbian learning. Hopfield learning algorithm represents auto-associative memory structures that reach the local minimum of its Lyapunov function. The binary Hopfield learning algorithm is stated by the following equation

$$x_i(t+1) = \sum_{j \neq i} w_{ij} * x_j(t) \quad (2)$$

where $x_i(t)$ is ± 1 depending on the state of the neuron, w_{ij} is the weight matrix [68, 69]. When the learning rule is applied and the weight matrix is calculated for the network, the algorithm works such that given noisy input, the network will evolve to reach the stored patterns as represented by the learnt weight matrix.

Further enhancements can be made to the basic Hebb algorithm by having the integrated sum of synaptic inputs to be non-linear [70].

2.2.4 ENCODING AND RETRIEVAL OF MEMORIES BASED ON HEBBIAN LEARNING

Many experiments have confirmed that the associative recall functionality of the hippocampus follows the Hebbian rule of synaptic plasticity. As mentioned before, the MF pathways are found to encode novel memories and the PP pathways are found to recall learnt memories[58, 59, 71]. The Schaffer collaterals from CA3 to CA1 are observed to be important for retrieving contextual information when presented with a partial context [71]. Blocking the acetylcholine neuromodulator affects encoding of new memories [71].

Simple experiments are conducted to enforce repetitive learning such as the Hebb-William

maze tasks for rats wherein the rats are trained repetitively to memorize the map of the maze they traverse to find the reward. This experiment works because of the recurrent excitation of the same place cells resulting in the same basin of attraction [58]. Immediate retrieval tasks to recall lists of words or numbers that are presented repeatedly to the participants is another classic example of Hebbian learning [72, 73].

Complex experiments involve a distraction between the learning experiments, wherein learnt lists must then be recalled from the long term memory, called covert retrieval [72]. The Hebbian recall depends on how fast-paced the distractions are in the available time, and how much of the time is required for processing the distraction. If the distractions are slowly paced, then only a small percentage of the available time is needed to process the distraction; but if the distractions are fast paced, then all of the time is required to process the distraction thus placing heavy loads on the participant's attention [72]. In such scenarios, retrieval of the actual lists is poor due to the distractions [72]. It is also observed that if the distractions are during recall and not during learning, the recall quality is better as the lists are all already learnt [72].

Such experiments establish the existence of Hebbian rule for the working memory phenomenon. However, the actual communication amongst the working memory neuronal circuits to encode or recall memories, to convert data from the working memory to long term memory, and retrieval of the same back to working memory again, are facilitated by the propagation of neuronal oscillations, which will be looked into in the next sections.

2.3 THETA AND GAMMA OSCILLATIONS IN THE HIPPOCAMPUS

Among the different factors that are responsible for memory encoding and retrieval, rhythmic oscillations in the brain are a major factor. In the hippocampus, frequencies in the range 4-10 Hz (theta oscillations), 30-50 Hz (slow gamma oscillations) and 80-120 Hz (fast gamma oscillations) are observed to be responsible for memory encoding and retrieval. Hippocampal oscillations also synchronize and coordinate functionalities across different regions of the brain. Formation of memories in terms of maps of cell assemblies that get activated periodically during a repetitive task follows the 4-10 Hz rhythm of theta oscillations [74]. Theta oscillations have low frequency and high amplitude, and hence being able to reach farther regions of the brain [19].

During active behaviours such as exploring places or learning repetitive tasks, theta frequency oscillations can be observed; however, 30-60 Hz slow gamma frequency oscillations

were also observed [53]. Slow gamma oscillations have a relatively higher frequency and smaller amplitudes. Due to a higher frequency range, gamma oscillations contribute to processing information on a temporal basis, such as learning or encoding information and retrieval of information in a localized area. Slow or fast gamma oscillations are found in the hippocampal CA1 and CA3 regions due to the external inputs from EC, and also due to the recurrent collaterals of pyramidal cells present in CA3 region that act as local gamma oscillators. We can see this in literature in both biological studies [53] and reviews [54]. We aim to replicate these observations in our simulations of both continuous and discrete models of CA1 and CA3.

2.3.1 INFLUENCE OF HIPPOCAMPAL THETA OSCILLATIONS ON OTHER BRAIN REGIONS

Theta frequency oscillations act as a time-based carrier for other frequencies such as fast and slow gamma oscillations [36]. Each cycle of slow gamma oscillations is said to process an information element, repeatedly getting activated in each theta cycle [20]. Aside from influencing the hippocampal regions locally, hippocampal theta frequency oscillations influences many different brain regions such as the piriform cortex [75], striatum in the basal ganglia [76], neocortex [77], cerebellar purkinje cells [78], lateral geniculate nucleus [79], the sub-cortical central pattern generators [80], etc. These regions have a lot of other parameters in common, although they are present in very different regions of the brain. For example, recurrent collaterals are found in the CA3 region of the hippocampus, which also happens to oscillate in theta frequency. Such recurrent collaterals that also oscillate in theta frequency and have attractor dynamics are found in the inhibitory cerebellar purkinje cells [78], aspiny cholinergic interneurons in the striatum in the basal ganglia [76], the recurrent excitatory stellate cells network in layer IV of the neocortex [81], the fast and slow relay cells in the lateral geniculate nucleus (LGN) [82, 83], Renshaw cells in the motor network of the spinal cord [84, 85, 86], etc.

Another commonality found in these regions other than the presence of recurrent collaterals and the influence of hippocampal theta rhythms on their activity, is the presence of acetylcholine (ACh) neuromodulator. ACh alters the excitatory or inhibitory actions of neurons, affecting the release of the neurotransmitter in the region which is also described as changing the state of the neuron, synchronizing the firing of neuronal groups in different regions of the brain as stated by Picciotto et al [87]. From their work, such cholinergic networks are known to be found throughout the brain either as projection neurons or local interneurons. They have also indicated that ACh plays a vital role in synaptic plasticity which depends on

the timing of release of ACh. ACh has been found to be important for encoding new data, strengthening feedback inputs and its contribution to neuronal oscillations in the range of 4-10Hz [88]. Loss of acetylcholine in neurons results in symptoms of dementia [89]. It is interesting to observe the presence of such common features in the different regions of the brain and hence, a summary of these commonalities is presented in table 1.

Table 1: Comparison of recurrent collaterals of different regions of the brain

Region of the brain	Associated brain wave	Attractor type	Presence of ACh as a neuromodulator
Hippocampal CA3 region	Theta	Continuous point attractor	Yes
Piriform cortex	Theta, gamma	Fixed point attractor	Yes
Striatum in basal ganglia	Theta, gamma, beta	Saddle-node and stable node	Yes
Neocortex	Theta, gamma	Continuous point attractor	Yes
Cerebellar Purkinje cells	Theta	Saddle node & saddle homoclinic	Yes
LGN	Theta	Spike time attractor	Yes
Renshaw cells	Gamma	Fixed point attractor	Yes
Sub-cortical CPGs	Theta	Ring attractor	Yes

Here, we are more interested in the cross-frequency coupling of the theta and slow gamma oscillation types as these are more prominent during encoding and retrieval tasks in the hippocampus, and hence this is the focus of our study.

2.3.2 EXTERNAL INPUTS AND MECHANISMS OF THE HIPPOCAMPAL CIRCUIT

The hippocampus in general receives several external inputs namely, from EC during storage of memories causing fast gamma oscillations; from medial septum diagonal band of Broca (ms-dBB) which is known to propagate hippocampal theta oscillations affecting the amplitude of hippocampal theta oscillations; from supra-mammillary nucleus (SUM) in the hypothalamus that affects the frequency of hippocampal theta oscillations through ms-dBB;

from the nucleus reuniens (RE) of midline thalamus that helps in transferring information from medial pre-frontal cortex (mPFC) to the hippocampus aiding in functionalities that requires both mPFC and hippocampus [90].

It is found that if the ms-dBB is removed, then theta oscillations are absent in the hippocampus. If there are no theta oscillations, then encoding of new information does not happen in the hippocampus [90]. Fast gamma oscillations are propagated from EC to DG, and slow gamma oscillations are present in the CA3 region, both of which are then propagated to CA1. Synchronization of slow gamma oscillations from CA3 to CA1 with theta oscillations from ms-dBB is crucial for the successful retrieval of memories [54].

In the hippocampus, the CA3 region receives input from DG mossy fibers to retrieve information, and from EC to encode novel information. CA1 receives input from CA3 Schaffer collaterals for both encoding and retrieval, and from EC for information storage and retrieval [91, 92]. CA3 also receives back projection from CA1, the purpose of which is not fully known yet [17, 93].

2.3.3 COMPARISON OF CA1 AND CA3

Both CA1 and CA3 are involved in encoding and retrieval of memories. They both have almost the same kind of neuronal populations. Physiologically, the projections between the internal populations present in both CA1 and CA3 differ. CA3 has an extensive excitatory recurrent collateral formation which is only sparsely found in CA1. While CA3 to CA1 feedforward input is excitatory, the feedback from CA1 to CA3 is inhibitory from the back-projection cells. However, the external inputs to both differ as CA3 also receives input from DG to encode novel information [17]; and the only pathway present to communicate with the neocortex for long term consolidation of memories is through CA1 [60].

The kind of input afferents coming into CA1 and CA3 are different and, the purpose for the efferents from CA1 and CA3 is also different. While CA3 has compact place fields for different information, there are no contextual or sensory information associated with the place fields. This information is brought forward and sent to EC by CA1 neurons that perform the triangulation of various memories propagated by CA3, depending on the temporal context during retrieval tasks [60, 62] as mentioned in the previous section.

2.3.4 ROLE OF OSCILLATIONS IN THE ENCODING AND RETRIEVAL OF MEMORIES

As mentioned previously, theta oscillations from ms-dBB to CA1 and CA3 act as a carrier wave due to their low frequency and high amplitude nature, reaching different regions of the brain thus facilitating coordination and synchronization of processes across brain regions. Both slow and fast gamma oscillations from CA3 and EC are superposed in the hippocampal theta oscillations at different phases to converge sensory inputs and the temporal memories to retrieve the right contextual memory in CA1 [54].

Place cells in each place field of a map are activated successively as the subject traverses an already learnt environment, consecutively firing according to the theta cycle, wherein recently visited locations fire at early phases of theta, and places to be learnt firing at late phases of the theta cycle [57].

The phases of theta oscillations are more relevant in encoding spatial location information and much less relevant in encoding direction, temporal characteristics, etc., of an event [94]. Phase separation for encoding and retrieval is important so that retrieval doesn't get encoded again [1].

Nevertheless, when once the short term memories in the hippocampus are consolidated in the neocortex, those memories are independent of the hippocampal theta oscillations [74].

2.4 SUMMARY

So far we have explained the role of oscillations and how they affect encoding and retrieval of information in the hippocampus based on literature. In the next chapters, we can see from our simulations with both continuous and discrete modeling techniques how theta oscillations act as carrier for slow gamma oscillations to encode and retrieve information. We have integrated CA3 and CA1 models to have continuous input from CA3 to CA1 and vice-versa instead of having constant inputs from these external populations. This gives a better idea of how gamma oscillations are propagated from CA3 to CA1, and how basket and bistratified cells are required to oscillate in slow gamma frequency, that helps in information processing. With the inhibitory back-projection cells from CA1 to CA3, there is also a regulation of excitation and inhibition in CA3 from CA1.

In the next chapter, we look at the different ways of modeling neuronal networks that reproduce the biological results discussed in this chapter and more, and the models we have considered for our research with relevant explanations.

3 INTRODUCTION TO VARIOUS TYPES OF MODELS

A model is a simple way to represent a system that we have observed in nature. Scientific modeling can be categorized into two ways namely (i) descriptive modeling where researchers try to specify the system state at a particular point in time, and (ii) rule-based modeling where researchers try to come up with dynamical rules that would explain the observed phenomenon [95]. Descriptive modeling analyzes the external aspects of the system while rule-based modeling analyzes the behaviour of the system. An example of rule-based modeling is designing neuronal networks with its various properties, studying different oscillations and their interactions exhibited by these networks, etc.

In this chapter, we aim to provide a brief description of each of the modeling techniques, a couple of which we build upon with relevant explanations, so as to explain why we chose a particular model, what limitations we observed in them, and how we overcame those limitations. In the end, we explain the different kinds of dynamical states these models tend to settle in.

Modeling neurons can involve different methodologies depending on the aim of the research. To analyze individual neurons at a biologically-comparable level, we need to consider the different biological dimensions such as time constants, conductances, membrane potentials, representation of the various currents found in the different ion channels, etc. This results in a very complex model such as the Hodgkin-Huxley axon model [96, 97].

To reduce the complexity of such models and yet retain biological relevance, we have to reduce the dimensions considered, which results in a less-complicated solution such as the Morris-Lecar model or the Fitzhugh-Nagumo model, by considering the membrane potential of the neuron and a slow recovery variable that integrates over the activity of the membrane potential of the neuron.

An even simpler approach that reduces the complexities involved in the single neuron models is the spiking neuron models such as the linear integrate-and-fire neuron models or the time-dependent spike response models which depend on the previous output. It is possible to approximate out the results from a large number of identical neurons to study oscillatory properties of a model such as in population models.

Neurons having similar properties are clustered together forming a homogeneous population. The rate of firing activity of neurons in these population are averaged, rather than studying properties of every single neuron from the same homogeneous population. Such

population models are derived from the Wilson-Cowan model [98].

Another simplified computer science approach to modeling single neurons and populations simultaneously is the discrete method of cellular automata. Using messages or events at each time step, neurons are either activated or deactivated based on the comparison with the summed inputs of each neuron. Activation here could represent a binary state of on or off, a single action potential or a burst of action potentials. A random spike train input to the external inputs which in turn project to the populations initiate and sustain propagation of messages or events between neurons in different or same populations.

Some models generate action potentials or spikes based on a threshold value above which we consider the neuron to generate an action potential; some other models generate bursts of activity [99]. We can study models based on their spiking or bursting behaviour or based on their membrane potential changes. In our research, we have used continuous population model for studying oscillatory activity in CA1 and CA3 regions of the hippocampus, and spiking neuron models through a discrete state-based approach to study encoding and retrieval of memories in an oscillatory context. Our motive is to study oscillations in the hippocampus from a single neuron perspective in a homogeneous population model, while learning and recalling patterns, which fall in two superposing frequencies i.e., 4-7 Hz theta oscillations and 30-50 Hz slow gamma oscillations. To achieve this, we have used both continuous population models to study oscillatory properties of the hippocampus, and the discrete cellular automata approach in which we can model both single neuronal properties and population properties.

3.1 SINGLE-NEURON MODELS

3.1.1 HODGKIN-HUXLEY (HH) MODEL

The membranes of neurons have different types of currents that get activated and inactivated based on different mechanisms. In 1952, the Hodgkin and Huxley model was proposed for the sodium, potassium and leak chloride currents based on experiments conducted on the giant axon of a squid. The model consists of four non-linear differential equations as given in the set of equations 3a to 3k, wherein three equations represent the mechanism for the activation variables for the 3 different currents considered (3c to 3e), and the fourth equation represents the rate of change of membrane potential in the neuron (3a/b).

$$C \frac{dV}{dt} = I_{ext} - I_{K^+} - I_{Na^+} - I_L \quad (3a)$$

wherein, the currents can be expanded as,

$$C \frac{dV}{dt} = I_{ext} - g_K n^4 (V - E_K) - g_{Na} m^3 h (V - E_{Na}) - g_L (V - E_L) \quad (3b)$$

$$\frac{dn}{dt} = \alpha_n(V)(1 - n) - \beta_n(V)n \quad (3c)$$

$$\frac{dm}{dt} = \alpha_m(V)(1 - m) - \beta_m(V)m \quad (3d)$$

$$\frac{dh}{dt} = \alpha_h(V)(1 - h) - \beta_h(V)h \quad (3e)$$

where,

$$\alpha_n(V) = 0.01 \frac{10 - V}{e^{\left(\frac{10-V}{10}\right)} - 1} \quad (3f)$$

$$\beta_n(V) = 0.125 e^{\left(\frac{-V}{80}\right)} \quad (3g)$$

$$\alpha_m(V) = 0.1 \frac{25 - V}{e^{\left(\frac{25-V}{10}\right)} - 1} \quad (3h)$$

$$\beta_m(V) = 4 e^{\left(\frac{-V}{18}\right)} \quad (3i)$$

$$\alpha_h(V) = 0.07 e^{\left(\frac{-V}{20}\right)} \quad (3j)$$

$$\beta_h(V) = \frac{1}{e^{\left(\frac{20-V}{10}\right)} + 1} \quad (3k)$$

The parameters are explained in table 2. The n^4 , m^3 and h represents the four activation gates for K^+ , three activation gates for Na^+ and one inactivation gate for Na^+ respectively.

Applying an electric pulse to the neuronal membrane which is sufficient to increase the activation gates, m for the sodium current, I_{Na^+} , results in depolarization of the membrane by increasing the sodium current, I_{Na^+} . This creates a change in the membrane potential, V , leading to the generation of an action potential or a spike. As the membrane potential V increases, the activation gates for the potassium current, n , increase the potassium current, I_{K^+} , and the inactivation gates h , for the sodium current, I_{Na^+} decreases. The I_{K^+} and the leak

Table 2: Parameters used in Hodgkin-Huxley model

Parameter	Explanation
V	Membrane potential
$I_{ext}, I_{K^+}, I_{Na^+}, I_L$	Currents - external(ext), potassium(K), sodium(Na) and leak(L)
E_K, E_{Na}	Nernst potentials for potassium (K) and sodium (Na)
g_K, g_{Na}, g_L	Conductances - potassium (K), sodium (Na), leak (L)
n	activation gates for potassium
m	activation gates for sodium
h	inactivation gates for sodium

current I_L stabilize the membrane back to the resting membrane potential, V_{rest} .

The membrane time constants have a high value, and are sensitive to membrane potential changes, and hence, the K^+ current continues to activate even beyond V_{rest} , called membrane afterhyperpolarization. During the time when the I_{Na^+} inactivates, the membrane cannot fire another action potential. This duration when the membrane cannot generate an action potential while the Na^+ gates inactivate is called the refractory period.

The increase in I_{Na^+} causes the increase in the membrane potential, V , and the I_{K^+} and the leak current I_L can be seen as the recovery variables or the inhibition currents that get the membrane back to equilibrium, called repolarization. The concept of recovery variables can be understood in more detail in the following sections which discuss a couple of models that simplify the HH model.

The H-H model enables us to understand the ionic movements in the axonal section of a neuron. It has been applied to study thermally sensitive neurons [100], various phenomena in the squid nerve by altering the calcium and potassium ionic concentrations and temperatures [101]. The HH equations were further extended to understand and analyze the effects of sodium, calcium and potassium ionic channels in the cardiac tissues which led to the modeling of the pacemaker activity [102, 103].

Many models that are computationally simpler has emerged based on the Hodgkin-Huxley model. Undoubtedly the Hodgkin-Huxley model forms the basis for neuronal modeling, and is present in these simpler models since the fundamental concept on which the simpler models are derived is the activation of currents in low voltages [104, 105, 106].

3.1.2 FITZHUGH-NAGUMO MODEL

Let us consider the Fitzhugh-Nagumo model which is the simplified form of the Hodgkin-Huxley model by reducing the dimensions from 4 to 2. The model generated sharp peaks mimicking action potentials. It is defined by the 2 differential equations given in equations 4a and 4b, that generate oscillatory peaks, exhibiting limit cycles to converging spirals, as shown in figure 8. There are 2 differential equations, one for the membrane potential, u and another for a regulatory membrane potential w which controls u . I_{ext} is the external current and R is the resistance. The membrane potential V and potassium activation gate n from the HH model are combined and represented by u and the sodium activation gates, m , and inactivation gates, h , are combined and represented by w . τ is the membrane time constant, b_0 and b_1 are the constants.

$$F(u, w) = u - \frac{1}{3}u^3 - w + R * I_{ext} \quad (4a)$$

$$G(u, w) = \frac{(b_0 + b_1u - w)}{\tau} \quad (4b)$$

Many applications of the FN model exist including its applications in simulating action potentials in the cardiac tissues [107]. An extended FN model is used to model cortisol secretion in the hypothalamic-pituitary adrenal axis [108].

3.1.3 KÁLI & DAYAN HIPPOCAMPAL CA3 MODEL

An attractor model of the CA3 recurrent neuronal network to analyze the formation of place fields is proposed by Káli & Dayan in [109]. The model represents a system of coupled differential equations for the membrane potential u of neuron i as given in equations 5a and 5b.

$$\tau \dot{u}_i = -u_i + \sum_j J_{ij} g_u(u_j) - h g_v(v) u_i + I_i^{PP} + I_i^{MF} \quad (5a)$$

$$\tau' \dot{v} = -v + w \sum_j g_u(u_j) \quad (5b)$$

As seen previously in the Fitzhugh-Nagumo model, the model has v as a slow recovery variable that integrates over the activity of u , the membrane potential, τ and τ' is the membrane time constant of the excitatory and inhibitory cells, J_{ij} is the connection strength or weight from neuron j to i . I_i^{PP} and I_i^{MF} are the inputs from perforant path and mossy fibers from the dentate gyrus. The function $g_u(u)$ is the threshold linear activation function defined

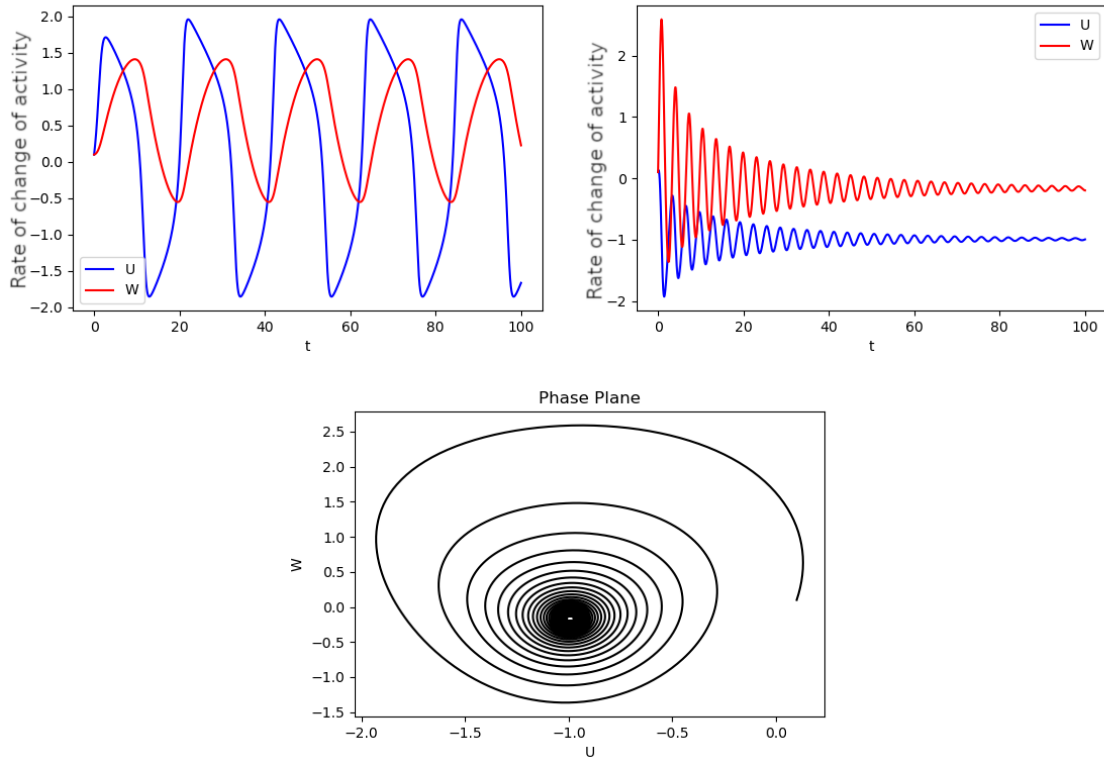


Figure 8: Fitzhugh-Nagumo model (left) activity dynamics when $b_0 = 0.1$ and $b_1 = 2$, $I_{ext} = 0.5$. (right) damping activity dynamics that converges representing a stable spiral as shown in the bifurcation plot & (bottom) phase plane when $b_0 = 49.5$ and $b_1 = 50$, $I_{ext} = 0.5$ showing a converging stable spiral.

as $\beta[u - \mu]_+$ where, the function evaluates to zero for values less than or equal to zero; $g_v(v)$ is defined as $\gamma[v - v]_+$.

The recovery variable acts as a global inhibitory neuron here, which can be clearly determined from the activity of the model as given in figure 9, wherein the activity of the neuron and the activity of the recovery variable are clearly out of phase.

The activity dynamics shown also depicts that the model can generate oscillations and converge to a point representing a stable spiral. The initial conditions used for simulating this model is 0mV which is why the activity dynamics reaches a membrane potential of +35mV. This model follows the Wilson-Cowan model [98], but is interpreted at a single neuron level, rather than at a population level and it represents the average membrane potential of a neuron.

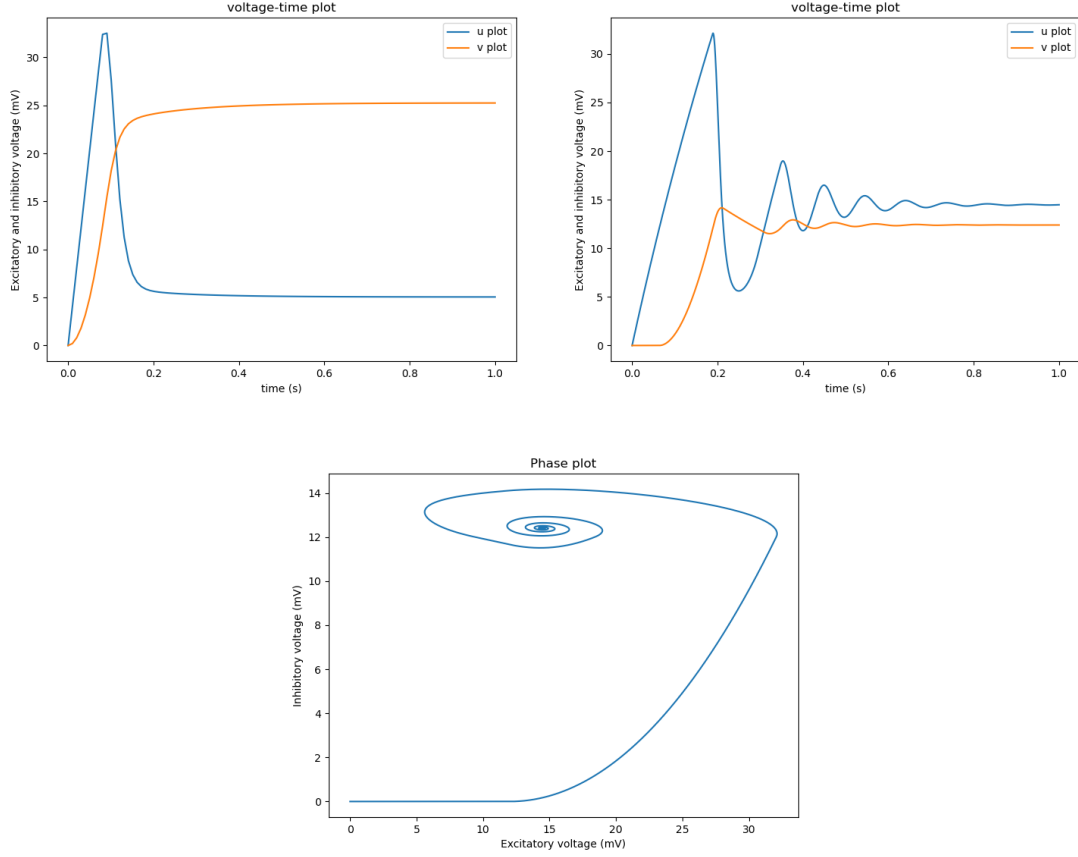


Figure 9: (left) Activity dynamics of the Káli & Dayan hippocampal CA3 model that converges to steady state [109] (right) damping oscillatory activity & (bottom) phase plot showing a converging stable spiral.

3.1.4 LEAKY INTEGRATE-AND-FIRE MODEL

Next, we consider the leaky integrate-and-fire neurons, or the LIF neurons, to study spiking neuron models [110]. Here, the neuron is considered to be an electrical circuit with resistance and capacitance, described by the first order linear differential equation given by equation 6.

$$\tau_m \frac{du}{dt} = -(u - E_l) + R_m * I(t) \quad (6)$$

where τ_m is the membrane time constant which is the product of membrane resistance R_m and membrane capacitance C_m , and $I(t)$ is the current flowing into the neuron.

Depending on if the neuron is excitatory or inhibitory, the projection between excitatory and inhibitory neurons is positive or negative. There is a membrane time constant which de-

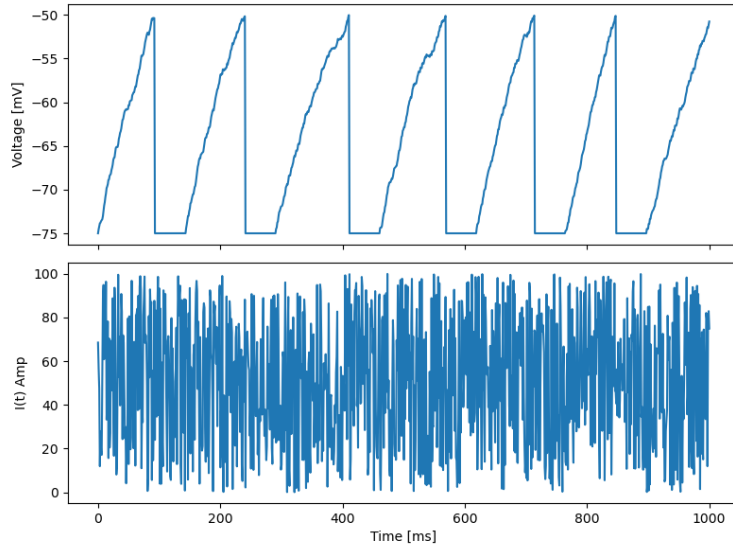


Figure 10: Activity dynamics of a simple LIF neuron with refractory period = 50ms, membrane time constant = 15ms and a random external current.

termines the rate of change to input currents below the action potential threshold. Once the spiking threshold is reached, the neuron fires an action potential and the membrane potential is instantly returned to its equilibrium (rest) potential.

The LIF neurons are easy to implement as defined in equation 6 and the activity dynamics is as shown in figure 10, implemented using the forward-Euler method. A refractory period during which the neuron does not emit an action potential can be added to the model, if required, as an exponential function of time.

Populations of such LIF neurons can be used to study individual neuron and population dynamics. For example, one such population modeling that uses integrate and fire neurons was applied for studying orientation tuning in the visual cortex [111].

The activity dynamics includes the rate of change of membrane potential of a single neuron with a membrane time constant defined by τ_m which determines the gap between the action potentials as given in the activity plot 10. Adding a recovery variable that regulates the firing of the actual neuron will generate results similar to the Káli & Dayan hippocampal CA3 model explained previously. The membrane potential of the neuron is the fast variable u which represents the potassium activation current K^+ and the recovery variable is the slow variable which represents the sodium inactivation current Na^+ .

The LIF neurons have binary states; the neurons either fire or do not fire based on the

spiking threshold, exhibiting class I neural excitability which has a direct relation between the external input current and the generated membrane potential or spiking frequency [112, 113].

Another linear extension of the LIF model is the resonant and fire model which has complex values as states variables and acts as a resonator. The model requires an input close to the resonant frequency which is close to the eigen value frequency of the neuron to generate an action potential. The resonators are the simplest model to produce damped oscillations [114].

3.1.5 NON-LINEAR INTEGRATE AND FIRE MODEL

The simple leaky integrate and fire model is said to have an action potential if the integrated input is greater than the threshold. The model has no spike-generating mechanism as such and hence is not a truly spiking neuron model. The non-linear integrate and fire models integrate each input pulse until they reach the threshold value to generate an action potential. This is the major difference between the linear integrate and fire models and non-linear integrate and fire models.

To account for the slow recovery variable representing the sodium activation dynamics, a nonlinear model extending the linear integrate and fire model is proposed [115]. There are two popular models in this category: quadratic integrate and fire model [116] and exponential integrate and fire model [117].

Quadratic integrate and fire model has the following equation form wherein u is replaced with u^2 .

$$\tau_m \frac{du}{dt} = a_0(u - u_{rest})(u - u_c) + R * I \quad (7)$$

where $a_0 > 0$ and $u_c > u_{rest}$. u_c is set to $+\infty$ or a large finite value for simulation purposes. The model has a saddle node bifurcation on an invariant circle. The spiked action potential approaches the resting state, merges and gets canceled out leaving behind a limit cycle. It is class I excitable and is the closest simplified model of Hodgkin-Huxley model [118, 112]. The system is the most suitable for large scale simulations both for the biological relevance and cost.

Exponential integrate and fire model has the following equation form

$$\tau_m \frac{du}{dt} = -(u - u_{rest}) + \Delta_T \exp\left(\frac{u - \Theta_{rh}}{\Delta_T}\right) + R * I \quad (8)$$

where Δ_T is the slope factor and Θ_{rh} is the threshold. The second term introduces the exponential or non-linear factor in the equation, while the first term is the passive membrane potential leak as in the previous equation. The system is expensive to simulate and is not used for large scale simulations [118].

3.1.6 CELLULAR AUTOMATA APPROACH FOR SINGLE NEURON MODELS

The cellular automata approach is a simplified way of representing the various parameters present in a differential equation describing the characteristics of a neuron by building a deterministic state machine. Every neuron has certain properties that have to be described, and every projection between two neurons has certain properties that have to be described separately. Although the projections between the populations are stochastically determined, the model follows a deterministic approach thereafter.

The properties to be described for a neuron include the refractory period, duration of an action potential, duration of synaptic delay, the synaptic duration for an impulse to reach another neuron, and the threshold for comparing the integrated sum of inputs to determine if an action potential occurred or not. The connection weight has to be specified for the projections between two neurons.

CA further simplifies the LIF approach by using simple square-wave summing of inputs, instead of integrating ODEs. Also that CAs are very flexible in terms of the rules that can be used to represent neural activity such as single APs, bursts of APs or just on/off activity.

An example of a simple excitatory-inhibitory(E-I) network, with 100 neurons in each population, simulated using the cellular automata approach is as shown in figure 11. The working of a CA model can be designed differently based on the requirement of the model or the research question. We found a lot of models using cellular automata approach in literature, which were used to establish the fact that such modeling technique exists and can be used to model large scale neuronal networks. However, we couldn't find a lot of models that actually simulates regions of the brain for different purposes. Hence, we have taken inspiration from two models that have actually implemented regions of the brain such as the CA3 model of the hippocampus implemented by Pytte et.al [119] and the piriform cortex model implemented by Claverol et. al [3].

In the model proposed by Pytte et. al for the CA3 region of the hippocampus, the authors have considered three types of neurons, excitatory, slow inhibitory and fast inhibitory. The projections between neurons are made randomly and there is a time delay for the signal to

propagate from one neuron type to the other. Excitatory neurons fire spontaneously every $(\tau_s + 1)$ time units after the last burst. All neurons receive inputs which are summed up and compared against a threshold to determine if a neuron should fire or not, which is called the stimulated firing of neurons. An activated neuron remains as such for a specified duration. Since this is a CA3 model, the excitatory neurons also have self-projections.

The Claverol et. al model of the piriform cortex is an event-driven message based approach that has four blocks of processing. The messages consist of the time to reach the destination neuron, the type of message and another additional field for extra information to be passed from one neuron to another. The different blocks in the model are the synapse block, threshold block, oscillator block and the burst-generator block.

The synapse block receives a message to activate a specific neuron at time t which is broadcast to the threshold block. The synapses are activated after a delay of t_{del} and are deactivated after $t + t_{del} + t_{dur}$ where $t + t_{dur}$ is the active time duration of the synapse.

The threshold block computes the weighted sum of inputs, compares the sum against excitatory and inhibitory threshold, and if the sum exceeds the excitatory threshold, an activation message is sent to the burst generator block; if the sum exceeds the inhibitory threshold, a deactivation message is sent to the burst generator block.

The oscillator block sends an activation message every t_{osc} time units to the burst generator block to generate oscillatory rhythms in the population of neurons.

The burst generator block activates a neuron if the neuron is off, changes the state of the neuron to refractory after t_{ap} time units for the neuron, and deactivates the neuron after t_{ref} time units.

An extension of these two CA models is what we have developed which is explained in chapter 5.

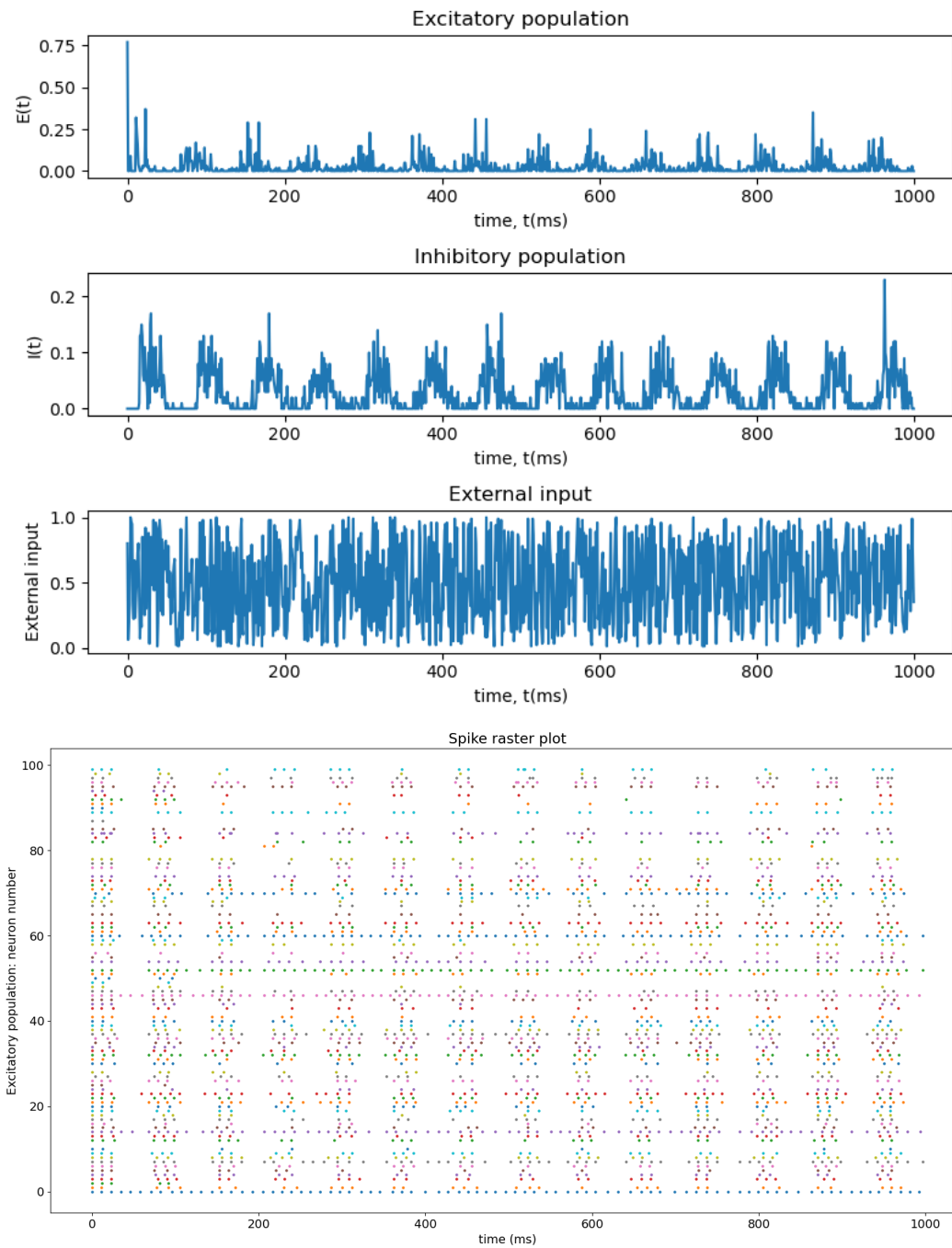


Figure 11: (left) Activity plot of a 10 excitatory and 10 inhibitory neurons; (right) Raster plot of the excitatory population over time that shows the neurons that are active at a specific time step.

3.2 CONTINUOUS POPULATION MODELS

When a stimulus approaches the regions of the brain, a considerable patch of neuronal network gets affected, not just a single neuron. Averaging the result of a spatially localized cell assembly of a region provides a chance to study the brain as a large scale network and is computationally efficient. Many different models have been proposed to study cell assemblies or populations of neuronal networks such as Beurle [120], Wilson-Cowan [98], Griffith [121], etc. The models that considered only the excitatory population of neurons displayed unstable dynamics. As such, inhibitory population of neurons were introduced in the network to regulate the firing of the excitatory neurons [121]. Hence, the Wilson-Cowan model operates based on the initial fundamental assumption that any neuronal processing is dependent on the communication between excitatory-inhibitory populations.

For an excitatory population $E(t)$ and inhibitory population $I(t)$, with a refractory period $\alpha(t)$, the average activity at time t is,

$$\int_{-\infty}^t \alpha(t-t') [c_1 E(t') - c_2 I(t') + P(t')] dt' \quad (9)$$

where c_1 and c_2 are the number of synapses per neuron and $P(t')$ is the external input. If the number of neurons in refractory period, r is $\int_{t-r}^t E(t') dt'$, then the number of neurons that can be activated is $1 - \int_{t-r}^t E(t') dt'$. At any given time, the sub-population of neurons that will be active is given by $S_e(x)$ for excitatory population and $S_i(x)$ for inhibitory population, which are sigmoidal. Thus, the activity dynamics of the neuronal populations are given by,

$$E(t + \tau) = [1 - \int_{t-r}^t E(t') dt'] \cdot s_e \left\{ \int_{-\infty}^t \alpha(t-t') [c_1 E(t') - c_2 I(t') + P(t')] dt' \right\} \quad (10)$$

for excitatory populations. For inhibitory populations,

$$I(t + \tau) = [1 - \int_{t-r}^t I(t') dt'] \cdot s_i \left\{ \int_{-\infty}^t \alpha(t-t') [c_3 E(t') - c_4 I(t') + Q(t')] dt' \right\} \quad (11)$$

The Káli & Dayan model [109] seen in the previous sections, the septal pace-maker circuit we shall discuss in the chapter 4 are derived from the Wilson-Cowan model described here.

The neurobiological models we have seen so far are non-linear systems, wherein the output is not directly proportional to the input, instead they can be described by a set of non-linear differential equations. Usually such systems tend to settle in multiple states depending on the initial state of the system. A brief explanation of the states non-linear

systems can exhibit is given in the next section.

3.3 BIFURCATION ANALYSIS OF NON-LINEAR SYSTEMS

Bifurcation is defined as “a qualitative, topological change of a system’s phase space that occurs when some parameters are slightly varied across their critical thresholds” [95]. Bifurcations are exhibited by non-linear systems such as a spring-mass system, or oscillations of a pendulum, etc. Different bifurcation methods exist depending on the nature of stability of the dynamical non-linear system. It is important to understand the different effects the variable parameter space can exhibit in a dynamical system, which is explained by bifurcation analysis. In this section, we discuss some of the bifurcations exhibited by the non-linear models such as the neuronal models we have discussed in the previous subsections.

In this section, we will use the popular Fitzhugh-Nagumo (FN) model which we discussed in section 3.1.2 to illustrate the different bifurcations in dynamical systems of neuronal networks. The model exhibits different bifurcations according to the external input.

The variable for membrane potential u allows for self-excitation and the regulatory membrane potential variable or the recovery variable w allows for a slower inhibitory feedback. This coupled dynamical system demonstrates bifurcations such as Hopf bifurcation, saddle-node and saddle-homoclinic bifurcations [122].

When the system is stable, it exhibits a closed trajectory path called a *limit cycle*. The system remains in a limit cycle when the external input is in the range $[-3, 3]$. Any values outside this range transforms the system to a stable spiral according to *Hopf bifurcation*. Hence, the system begins from a stable spiral, transforms to an unstable homoclinic bifurcation, to a saddle node, then to a limit cycle, and again to a stable spiral, as the external input increases as shown in figure 12.

In simple terms, *saddle node* bifurcations exhibit instability where some trajectories converge towards the equilibrium, while others diverge from the equilibrium. *Stable nodes* are those where all trajectories converge towards the equilibrium point. *Unstable nodes* are those where all trajectories diverge from the equilibrium point. A *neutral center* or a *limit cycle* is a periodic trajectory which revolves around the equilibrium point, until one of the trajectories converge towards the equilibrium. *Andronov-Hopf bifurcation* is an asymptotically stable or unstable spiral trajectory that either converges or diverges from the equilibrium, respectively.

These stability properties are described by the eigenvalues of the dynamical system.

Whether the eigenvalues are real or complex, the stability of a system is determined by the real part of the eigenvalues. If the eigenvalues are negative, the system exhibits stability; if the eigenvalues are positive, the system exhibits instability. Saddle node is case where the system has both positive and negative eigenvalues. The system exhibits a limit cycle when the real part of the eigenvalues become zero as explained in the case in table 3.

3.4 CONCLUSION

One way to model the brain is using non-linear dynamics, with a system of continuous differential equations describing neural activity at the individual neuron and population levels, wherein the rate of change of firing activity or the membrane potential depends on more than a single parameter at the same time step, such as the opening of different ionic channels or gates, the time constants, integrated sum of inputs from different sources, etc. Such a model is the Hodgkin-Huxley model [97] which with just four differential equations where the working of ionic gates in a single compartment of the giant axon of a squid is analyzed [97], and it is still complicated to work with four variables, and a number of constants.

Simpler models from thereon emerged, such as the Morris-Lecar model, Fitzgugh-Nagumo model, and lastly, the integrate and fire model, which is widely used to model single neurons, called the LIF or leaky integrate and fire neuronal model. While models built using the LIF neurons are continuous, cellular automata models are discrete trying to achieve the same goals using a deterministic finite automata approach.

The type of model chosen depends on the research question, and the feasibility of computational time and efficiency, availability of resources and simulating a biologically realistic model that adheres to the findings in literature, as proposed by Izhikevich in [99]. The Hodgkin-Huxley model is a more biologically plausible model but is not computationally efficient. An integrate-and-fire model is computationally very efficient, but is not a biologically plausible model in terms of the number of features that can be adopted [99]. Continuous population models are good to analyze oscillatory states as they average the activity of neurons in each population. The CA model is better to study encoding and retrieval since every neuron activity is needed to study encoding and retrieval of patterns. The CA model is a simple message based deterministic approach to model populations of single neurons to analyze oscillatory states and to study encoding and retrieval of patterns in our research.

Accordingly, we have investigated our research goals in each of the single neuron models, population models and discrete modeling approaches. With continuous population models

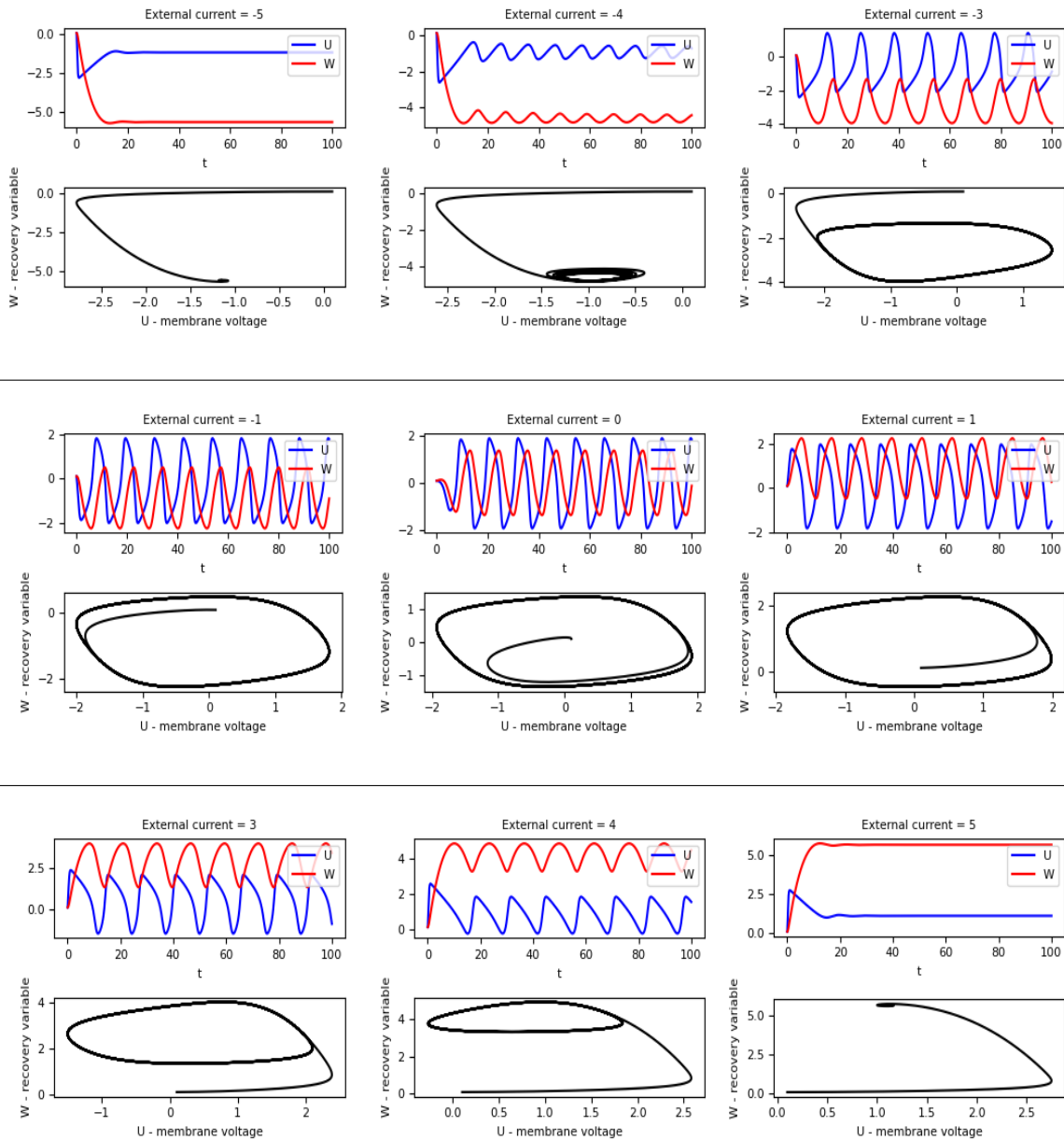
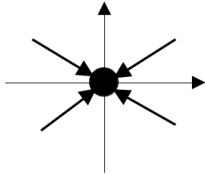
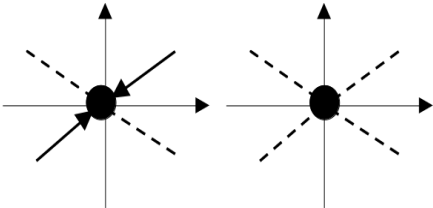
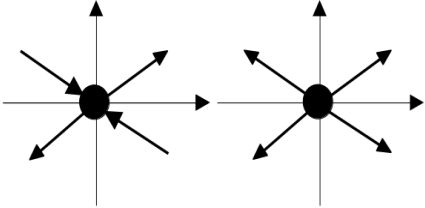
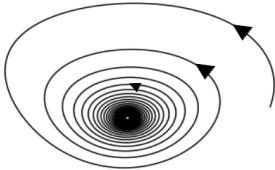
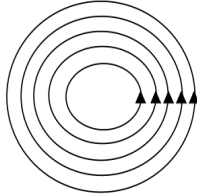
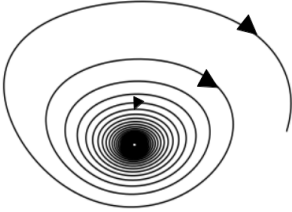


Figure 12: Bifurcation stages as the external input increases in the Fitzhugh-Nagumo model. Each figure comprises of the activity dynamics of the rate of change of membrane potential and its corresponding phase plot below. The parameters are $b_0 = 0.1$, $b_1 = 5$, $R = 1$, $\tau = 12.5$ and the external input, $I_{ext} = [-5, 5]$

Table 3: Types of bifurcations explained

Explanation	Type of bifurcation	Description
Real eigen values with $Re(\lambda) < 0$	Stable point	
Real eigen values with $Re(\lambda) = 0$	Neutral point	
Real eigen values with $Re(\lambda) > 0$	Unstable point	
Complex conjugate eigen values with $Re(\lambda) < 0$	Stable point	
Complex conjugate eigen values with $Re(\lambda) = 0$	Neutral point	
Complex conjugate eigen values with $Re(\lambda) > 0$	Unstable point	

we could study oscillatory behaviour of CA1 and CA3 regions of the hippocampus. With the results of the continuous population models as a baseline for oscillatory behaviour, we chose the discrete cellular automata model to study encoding and retrieval of patterns in an oscillatory model.

In chapter 5 we have developed an oscillatory model for encoding and retrieval of patterns using the discrete cellular automata approach. As pattern storage and recall relates to the activity of a specific subset of neurons in a population, we analyze the activity of single neurons in a population network, study oscillatory states and recall quality after learning a pattern using the cellular automata approach. With a cellular automata approach, we have attempted to find a balance between biological plausibility and computational efficiency.

4 THETA-COUPLED GAMMA OSCILLATORY MODEL OF THE CA1-CA3 REGIONS OF THE HIPPOCAMPUS

4.1 INTRODUCTION

In this chapter, we look into the individual and integrated models of CA1 and CA3 regions of the hippocampus to analyze and understand the effects of oscillatory behaviour of different population of excitatory and inhibitory neurons on one another. The network dynamics of pyramidal cells in CA1 and CA3 regions of the hippocampus are well-studied [60] concluding that there exist stable place fields in CA3 than in CA1, with more distinct phase precession than in CA1. The synchrony between hippocampal theta oscillations and other regions of the brain is necessary to prevent formation of incorrect synaptic projections in functional neuronal networks. Even small changes in inputs to interneurons in CA1 and CA3 can lead to variations in gamma oscillatory patterns which result in the formation of incorrect synaptic projections [123]. Different temporal sequences of patterns are assembled together in the correct order in different gamma cycles aggregated in a single theta cycle [123].

In this chapter, we have used population modeling approach to study oscillatory behaviour and the phase synchronization of different populations in CA1 and CA3 by extending the septo-hippocampal model proposed by Denham et. al [2] which is in turn derived from the Wilson-Cowan model [98]. The CA1 microcircuit is a combination of both Denham et. al [2] model and the model proposed by Cutsuridis et. al [24] and, the CA3 model is derived from the observations of several biological experiments producing a concise microcircuit (which is explained in section 4.2) as shown in figure 13.

Our objective in this chapter is to find the differences between CA1 and CA3 inhibitory interneurons, specifically PV-containing basket cells and bistratified cells, and to study the emergence of theta and theta-coupled gamma oscillations in both CA1 and CA3 networks. Interneurons involved in these regions are well-studied only in CA1 region and lack proper data for CA3 region. The phase relationships of the neurons considered in this model are by the afferent and efferent connections of PV-containing basket and bistratified cells in both CA1 and CA3 as described by Belluscio et. al [124].

We also contribute a new combined model of CA1 and CA3 regions, as shown in figure 13, which helps explain the propagation of signals from CA3 to CA1 via the Schaffer collaterals and from CA1 to CA3 through the back-projections cells. From the simulation results

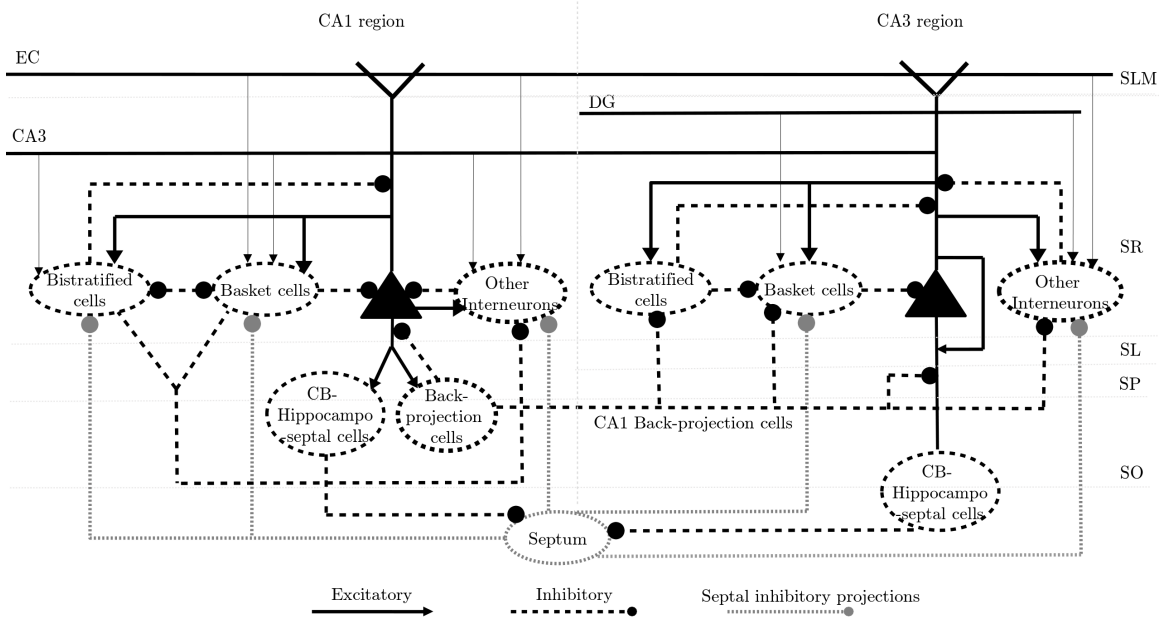


Figure 13: CA1-CA3 integrated microcircuit

and their correlation with experimental results, we intend to shed some light on the possible CA1 back-projection cell afferents on CA3 interneurons, the effects of external inputs in both the regions as explained in section 4.3.

Initially, we discuss the structural properties and time constants, the computational model and the analysis methods we have used, in section 4.2. Following which we will then discuss the effects of external inputs on the individual models, the simulation results of the individual and integrated model, analyze the results with bifurcation analysis, and consider the effects of various structural projections considered in the model in section 4.3. Lastly, we have a discussion section where we compare the CA1 and CA3 regions with each other and conclude with the comparison of the experimental results observed in literature in section 4.4. We do not simulate encoding or retrieval of patterns in this model; however, this model serves as the basis for the encoding and retrieval of patterns using the discrete cellular automata model discussed in the next chapter. Hence, the neuron populations chosen in the CA1 and CA3 regions relate to this in the big picture.

4.2 MODELING CA1-CA3 INTEGRATED MICROCIRCUIT

The different layers in EC from I to V are afferents to different regions of the hippocampus, and to different layers in the hippocampal pyramidal cell. EC stellate cells in layer

II projects to dentate gyrus and CA3, and EC layer III projects to CA1 [125], and in both CA3 and CA1, they project in the stratum-lacunosum moleculare layer of the pyramidal cells [126]. EC lies in-between the hippocampus and other cortical regions, where sensory inputs converge on the superficial layers of EC and which is propagated to the different regions of the hippocampus such as the dentate gyrus, CA3, CA2, CA1 and subiculum, and the processed outputs from the hippocampal CA1 region project onto EC layer V [127].

The internal connections in CA3 and CA1, the projections from CA3 to CA1 via the Schaffer collaterals and the CA1 to CA3 projections are all depicted in the CA1-CA3 integrated microcircuit as given in figure 13. We have considered PV-containing basket cells and bistratified cells as the major inhibitory interneurons in CA1 and CA3 regions, mainly to analyze the phase shifts between them and the pyramidal cells in CA1 and CA3 regions. Also, a single population of inhibitory septal input is received by both CA1 and CA3 regions in this model.

The septo-hippocampal loop as shown in figure 14 projects from excitatory pyramidal cells to septum via the calbindin-containing hippocampo-septal projection cells, and back to pyramidal cells via the GABAergic inhibitory interneurons. The proposal for this loop in

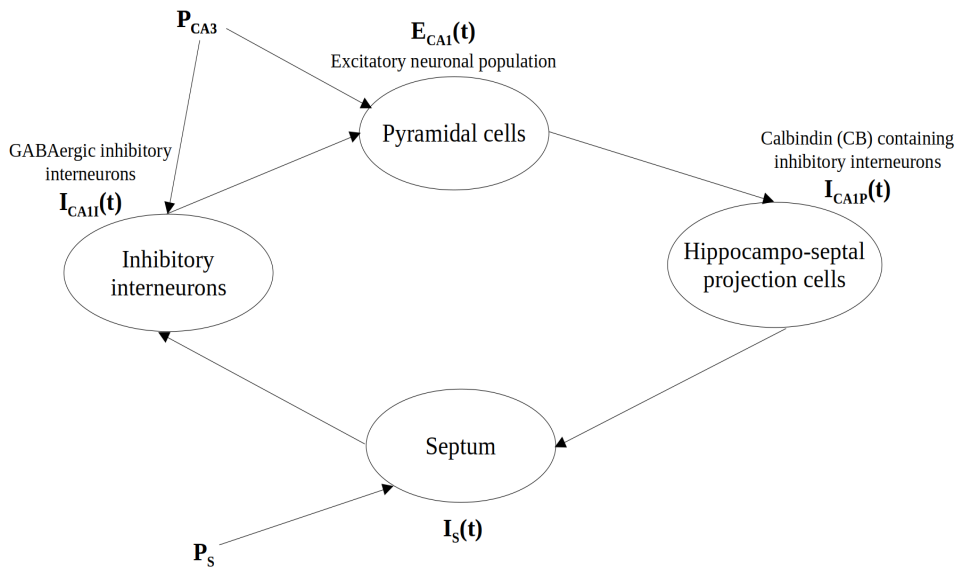


Figure 14: Septo-hippocampal theta oscillation pacemaker circuit as proposed by Denham et. al with the different populations of neuronal afferents and efferents to and from CA1 regions of the hippocampus with the external inputs [2]

CA1 is modeled by Denham et. al [2] which has been investigated for anatomical evidence

by Sans-Dublanc in [128]. For CA3, similar anatomical data is summarized by Witter [129].

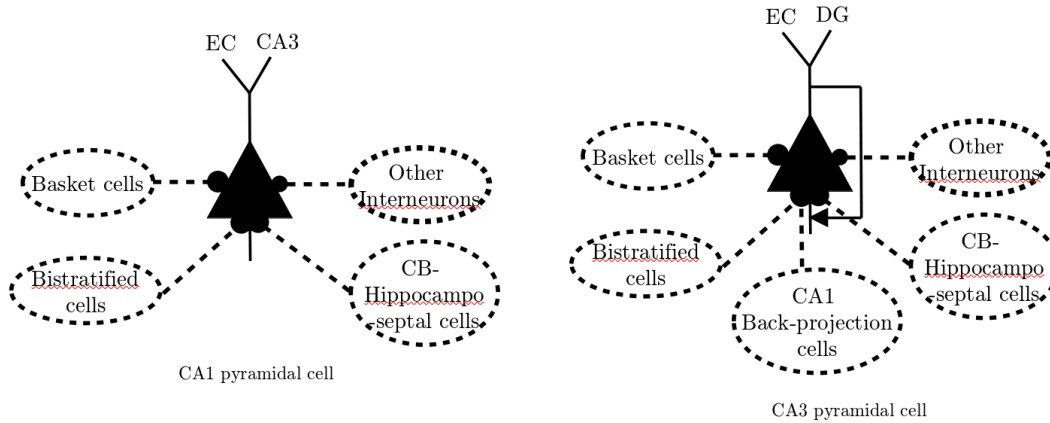


Figure 15: Projections to CA1 and CA3 pyramidal cell

Pyramidal cells (PCs): In CA1 and CA3, PCs are the major source of excitatory inputs to other interneurons and project onto themselves sparsely in CA1 and densely in CA3 [130]. The sparse recurrent excitatory connections in CA1 is not considered in our model, but we consider the dense recurrent excitatory connections in CA3. In CA1, PCs receive excitatory input from EC and CA3 PCs; while in CA3, they receive excitatory inputs from themselves, DG and EC. PCs in CA1 receive inhibitory inputs from CA1 BCs, CA1 BSCs, and other CA1 inhibitory interneurons; in CA3, PCS receive inhibitory inputs from BCs, BSCs, CA1 BPs and other CA3 inhibitory interneurons [130, 24, 71, 91]. The projections to CA1 and CA3 pyramidal cells are as shown in figure 15.

Basket cells (BCs): PV-containing BCs are present in both CA1 and CA3 regions which are responsible for generating gamma oscillations coupled with theta oscillations. BCs activity is noticed to occur while *learning* patterns in both CA1 and CA3 regions in Cutsuridis et. al [24] and Hasselmo et. al [71] simulation models respectively. In addition, BCs in CA1 also receive EC input [24], however evidence for such an external input for both CA1 and CA3 BSCs is absent in literature. BCs in CA1 receive excitatory inputs from CA1 PCs, CA3 PCs and EC [24, 130, 91, 131] and inhibitory inputs from CA1 BSCs [130, 91, 131] and septum [24, 131]; whereas CA3 BCs receive excitatory input from CA3 PCs [71, 130] and DG [130] and inhibitory input from CA3 BSCs and septum [71] and CA1 BPs [93]. The projections to CA1 and CA3 basket cells are as shown in figure 16.

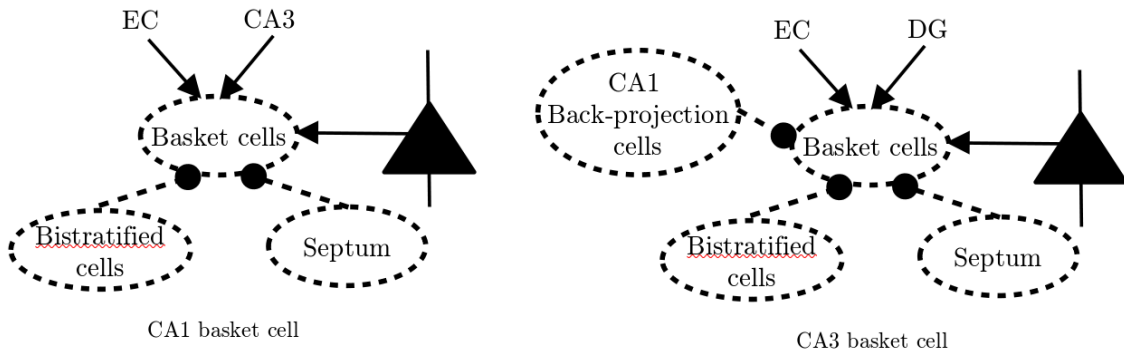


Figure 16: Projections to CA1 and CA3 basket cell

Bistratified cells (BSCs): PV-containing BSCs are present in both CA1 and CA3 regions. In CA1, they are observed to suppress unwanted PCs activity, excited by CA3 excitatory projections, during recall of patterns in Cutsuridis et. al [24] simulation model. O-LM cells are also active during recall of patterns to suppress unwanted pyramidal cell activity excited by EC projections as explained in Cutsuridis et. al model [24]. We have considered BSCs here instead of O-LM cells as we are modeling CA3 and have EC as a constant external input to both CA1 and CA3. In CA1, BSCs receive excitatory input from CA3 PCs [24], CA1 PCs and inhibitory input from BCs and septum [24, 130, 91, 131], while in CA3, BSCs receive excitatory input from CA3 PCs and inhibitory input from CA1 BPs [93]. Other external connections as seen in CA1 BSCs are not found in CA3 BSCs as we could not find evidence for such projections in literature. The projections to CA1 and CA3 bistratified cells are as shown in figure 17.

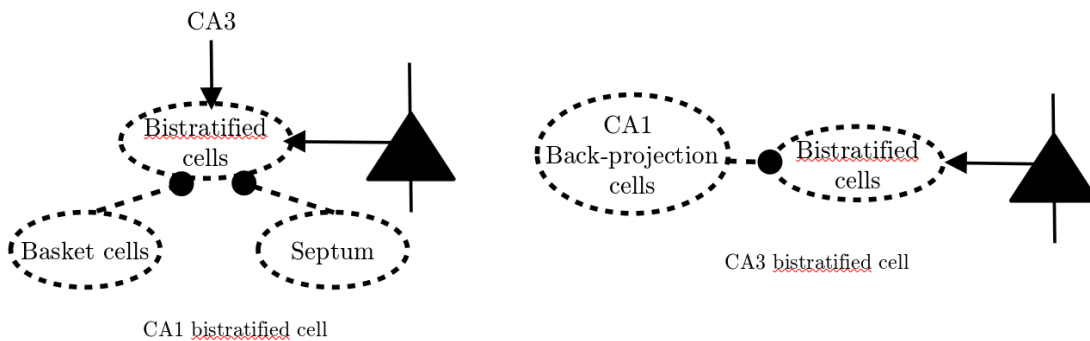


Figure 17: Projections to CA1 and CA3 bistratified cell

Other inhibitory interneuron population: There are many other inhibitory interneurons

in CA1 and CA3 such as the O-LM cells, axo-axonic cells, CA3 granule cells, etc., which we have not considered individually in our model. Instead, we consider all the other inhibitory interneurons as a single population of inhibitory interneurons, both in CA1 and CA3. Collectively, in CA1, we have considered excitatory inputs from CA1 PCs, CA3 PCs and EC; and inhibitory inputs from CA1 BCs, CA1 BSCs [132] and septum [24, 130, 91, 131]. In CA3, we have considered excitatory inputs from CA3 PCs [71], DG and EC [130, 91, 131]; and inhibitory inputs from septum [129] and CA1 BPs [93]. The projections to CA1 and CA3 other inhibitory interneurons are as shown in figure 18.

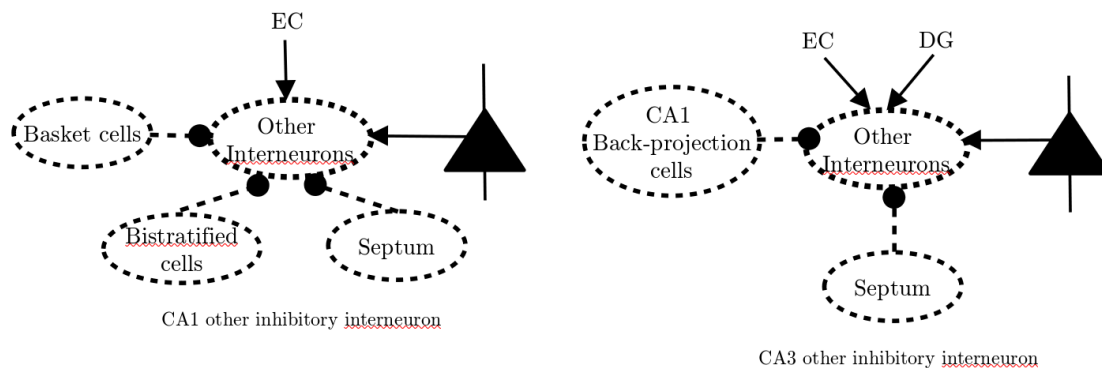


Figure 18: Projections to CA1 and CA3 other inhibitory interneurons

CA1 back-projection cells (BPs): We understand from Sik. et. al [93] about the projections from CA1 to CA3 interneurons. The CA1 back-projection cells receive excitatory projections from CA1 pyramidal cells and synapse on CA3 pyramidal cells and interneurons, and the hilar region in the DG. The CA1 back-projections cells are observed to terminate in the stratum-oriens (SO) and stratum-radiatum (SR) where pyramidal, basket, bistratified and other interneurons also have projections. However, there is not much information about the effects of CA1 back-projection cells on CA3 interneurons and hence, we have modeled projections from CA1 back-projection cells to CA3 pyramidal cells and inhibitory interneurons.

This completes the septo-hippocampal loop in CA1 and CA3 to propagate theta oscillations from the septum, the hippocampal loop between CA3 and CA1 propagating feed-forward information through Schaffer collaterals, and feedback information from CA1 to CA3 from the back-projection cells in CA1.

4.2.1 BASIC THETA OSCILLATION CIRCUIT

We take a population activity approach to modeling the microcircuit shown in figure 13. As mentioned before, we have extended the septo-hippocampal pacemaker circuit proposed by Denham et. al [2] which explains the propagation of theta frequency oscillation from septum to the CA1 region of the hippocampus. We found anatomical evidence for the existence of the septo-hippocampal loop in CA1 as described by Denham et. al, and we found that the same septo-hippocampal loop is present in CA3 as well as explained in the previous section.

The purpose of using the Denham et. al model is to simulate CA1 and CA3 regions using the septal input for which, the model serves as a basic foundation to build upon to study cross-frequency coupling of other frequency oscillations with theta frequency oscillations, with other populations of neurons.

We have thus, extended the same model to CA3 and have integrated both CA1 and CA3 regions, with time constants for each type of neuron chosen as close to the anatomical data available.

The basic model from Denham et. al primarily focuses on the GABAergic calbindin (CB)-containing hippocampo-septal projections in CA1, GABAergic projections from septum to CA1 and GABAergic CB-containing cells in CA1, as shown in figure 14. The defining equations of this model are as follows.

$$\begin{aligned} \tau_{E_{CA1}} \frac{dE_{CA1}}{dt} &= -E_{CA1}(t) + (k_e - E_{CA1}(t)). \\ &Z_e(-w_{E_{CA1} \leftarrow I_{CA1I}} I_{CA1I}(t) + P_{CA3}(t)) \end{aligned} \quad (12a)$$

$$\begin{aligned} \tau_{I_{CA1P}} \frac{dI_{CA1P}}{dt} &= -I_{CA1P}(t) + (k_i - I_{CA1P}(t)). \\ &Z_i((-w_{I_{CA1P} \leftarrow E_{CA1}} E_{CA1}(t))) \end{aligned} \quad (12b)$$

$$\begin{aligned} \tau_{I_{CA1I}} \frac{dI_{CA1I}}{dt} &= -I_{CA1I}(t) + (k_i - I_{CA1I}(t)). \\ &Z_i((-w_{I_{CA1I} \leftarrow I_S} I_S(t)) + P_{CA3}(t)) \end{aligned} \quad (12c)$$

$$\begin{aligned} \tau_{I_{SEPT}} \frac{dI_S}{dt} &= -I_S(t) + (k_i - I_S(t)). \\ &Z_i((-w_{I_S \leftarrow I_{CA1P}} I_{CA1P}(t)) + P_S(t)) \end{aligned} \quad (12d)$$

where $E_{CA1}(t)$, $I_{CA1P}(t)$, $I_{CA1I}(t)$ and $I_S(t)$ are the average activity of CA1 pyramidal cell population, average activity of CA1 hippocampo-septal projections, average activity of CA1 in-

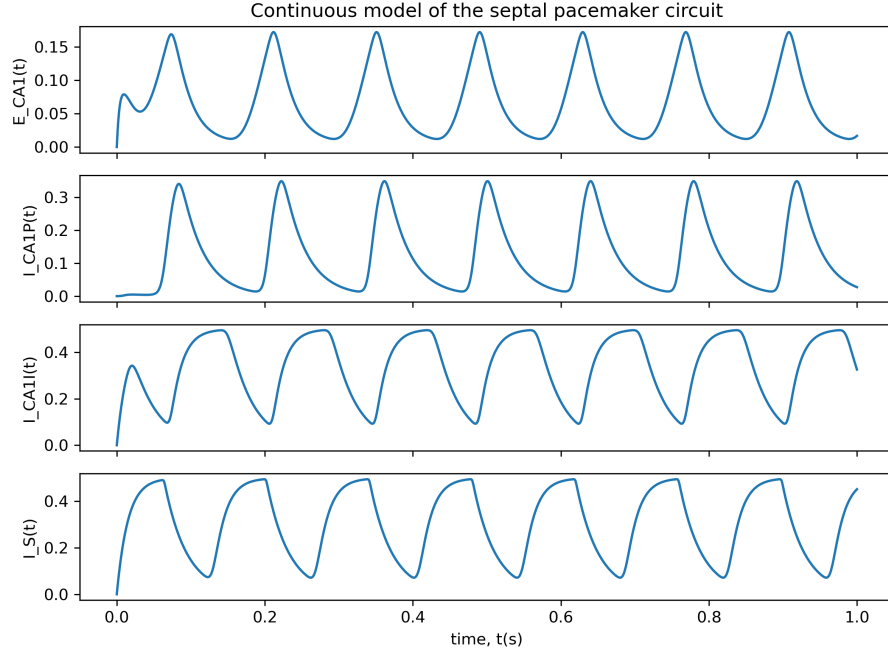


Figure 19: Activity dynamics of the hippocampal-septal pacemaker circuit proposed by Denham et. al [2] which is recreated here.

terneuron population and average activity of ms-dB septo-hippocampal projections respectively. $w_{X \leftarrow Y}$ are the strength of connections from Y population to X population cells. $P_{CA3}(t)$ is the constant activity of pyramidal cells of CA3 and $P_S(t)$ is the constant inputs from posterior hypothalamus and supra-mammillary nucleus (SUM). The response functions, $Z_p(x)$ are sigmoidal, which represent the fraction of active population for a given value x , described by,

$$Z_p(x) = \frac{1}{(1 + \exp(-b_p(x - \theta_p)))} - \frac{1}{1 + \exp(b_p \theta_p)}$$

where, $p \in e, i$, b_p and θ_p are constants, and $k_p = \frac{1}{Z_p(\infty)}$. The logistic function is chosen as given by the Wilson-Cowan model [98] such that the function $Z_p(0) = 0$. The parameters b_p and θ_p provide the position and value of the maximum slope of the model respectively. The activity is as given in figure 19. The external inputs are constants in the model.

In the model extended in this work, the inhibitory interneuron equation I_{CA1I} is dissected to include PV-containing basket cells, bistratified cells and back-projection cells in the CA1 region. Hence, I_{CA1I} equation will later represent the population of inhibitory interneurons which are not explicitly included in the equations such as the axo-axonic cells, O-LM cells, ivy cells, neurogliaform cells, etc.

Table 4: CA1 connectivity matrix. Pyr: Pyramidal cells; BC: Basket cells; BSC: Bistratified cells; ICAI: Other inhibitory interneurons; ICAP: CB-containing hippocampo-septal projections; BP: CA1 back-projection cells; EC: Entorhinal cortex. ✓ specifies that a projection exists between the two populations.

From \ To	PC	BC	BSC	ICAI	ICAP	BP	Septum
PC		✓[91]	✓[131]	✓[131, 133]	✓[128]	✓[131, 128]	
BC	✓[131]		✓[131, 91]	✓[132]			
BSC	✓[131]	✓[131, 91]		✓[132]			
ICAI	✓[131, 128]						
ICAP							✓[128]
BP	✓[93, 131]						
CA3: Pyr	✓[91]	✓[131]	✓[131, 133]	✓[131]			
Septum		✓[131]	✓[131]	✓[131, 128]			
EC	✓[130]	✓[131]		✓[131]			

4.2.2 MICROCIRCUIT OF CA1-CA3 REGION OF THE HIPPOCAMPUS

The inputs from perforant path propagates from EC layer III to the distal dendrites of CA1 pyramidal cells while the inputs from EC layer II propagates to CA3 pyramidal cells via mossy fibers in DG and to the proximal dendrites of CA1 pyramidal cells via the Schaffer collaterals. The timing of inputs from EC layer II and layer III are important since the order of arrival of signals to the soma of the CA1 pyramidal cells determines the order of input to be integrated for meaningful information processing [134]. It is also estimated that the perforant path input comes before Schaffer collateral input to CA1 pyramidal cells in order for the signal to reach soma from the distal dendritic synapse [134] since the information present has to be processed in the hippocampus within the gamma cycle duration. On the other side, experimentally the existence of feedback signals propagating from CA1 to the interneurons in CA3 and hilar region is found [93, 17] to synapse in stratum radiatum. Taking these inputs into account, the microcircuit in figure 13 is proposed. The model equations for CA1 are as

Table 5: CA3 connectivity matrix. Pyr: Pyramidal cells; BC: Basket cells; BSC: Bistratified cells; ICAI: Other inhibitory interneurons; ICAP: CB-containing hippocampo-septal projections; EC: Entorhinal cortex; DG: Dentate gyrus; BP: CA1 back-projection cells. The black dots (•) for the projections from CA1 BP to BC, BSC and ICAI in CA3 is due of the inconclusive proof for the existence of such projections which we have included in our model to explore their effects on these populations. ✓ specifies that a projection exists between the two populations.

From \ To	PC	BC	BSC	ICAI	ICAP	Septum
PC	✓[131, 91]	✓[131, 91]	✓[93]	✓[131]	✓[129]	
BC	✓[131, 91]					
BSC	✓[131, 91]	✓[131, 91]				
ICAI	✓[131, 129]					
ICAP						✓[129]
CA1: BP	✓[131, 93]	•[131, 93]	•[131, 93]	•[131, 93]		
Septum		✓[131]		✓[129]		
EC	✓[131, 129]			✓[131]		
DG	✓[131]	✓[130]		✓[91]		

Table 6: Symbols definition

Symbols	Definition	Symbols	Definition
$E_{CA1}(t)$	Excitatory CA1 pyramidal cells	$E_{CA3}(t)$	Excitatory CA3 pyramidal cells
$I_{CA1I}(t)$	Inhibitory CA1 interneurons	$I_{CA3I}(t)$	Inhibitory CA3 interneurons
$I_B(t)$	PV-containing basket cells	$I_S(t)$	Septo-hippocampal input
$I_{BS}(t)$	Bistratified cells	$P_{EC}(t)$	Entorhinal cortex external input
$I_{CA1P}(t)$	CA1 Hippocampo-septal input	$w_{x \leftarrow y}$	Weight from cell type y to cell type x
$I_{BP}(t)$	CA1 back-projection inhibitory interneuron cells	P_{DG}	Constant excitatory input from dentate gyrus
		P_S	Constant excitatory input from posterior hypothalamus and SUM

follows: Excitatory pyramidal cells

$$\begin{aligned}
 \tau_{E_{CA1}} \frac{dE_{CA1}}{dt} = & -E_{CA1}(t) + (k_e - E_{CA1}(t)) \cdot \\
 & Z_e(-w_{E_{CA1} \leftarrow I_{CA1I}} I_{CA1I}(t) \\
 & -w_{E_{CA1} \leftarrow I_B} I_B(t) \\
 & -w_{E_{CA1} \leftarrow I_{BS}} I_{BS}(t) \\
 & +w_{E_{CA1} \leftarrow E_{CA3}} E_{CA3}(t) \\
 & +P_{EC}(t))
 \end{aligned} \tag{13a}$$

PV-containing basket cells

$$\begin{aligned}
 \tau_{I_B} \frac{dI_B}{dt} = & -I_B(t) + (k_i - I_B(t)) \cdot \\
 & Z_i((w_{I_B \leftarrow E_{CA1}} E_{CA1}(t)) \\
 & -w_{I_B \leftarrow I_S} I_S(t) \\
 & -w_{I_B \leftarrow I_{BS}} I_{BS}(t) \\
 & +w_{I_B \leftarrow E_{CA3}} E_{CA3}(t) \\
 & +P_{EC}(t))
 \end{aligned} \tag{13b}$$

Bistratified cells

$$\begin{aligned}
\tau_{I_{BS}} \frac{dI_{BS}}{dt} &= -I_{BS}(t) + (k_i - I_{BS}(t)) \cdot \\
&\quad Z_i((w_{I_{BS} \leftarrow E_{CA1}} E_{CA1}(t)) \\
&\quad \quad - w_{I_{BS} \leftarrow I_B} I_B(t) \\
&\quad \quad - w_{I_{BS} \leftarrow I_S} I_S(t) \\
&\quad \quad + w_{I_{BS} \leftarrow E_{CA3}} E_{CA3}(t))
\end{aligned} \tag{13c}$$

Back-projection cells

$$\begin{aligned}
\tau_{I_{BP}} \frac{dI_{BP}}{dt} &= -I_{BP}(t) + (k_i - I_{BP}(t)) \cdot \\
&\quad Z_i((w_{I_{BP} \leftarrow E_{CA1}} E_{CA1}(t))
\end{aligned} \tag{13d}$$

Hippocampo-Septal projections

$$\begin{aligned}
\tau_{I_{CA1P}} \frac{dI_{CA1P}}{dt} &= -I_{CA1P}(t) + (k_i - I_{CA1P}(t)) \cdot \\
&\quad Z_i((w_{I_{CA1P} \leftarrow E_{CA1}} E_{CA1}(t))
\end{aligned} \tag{13e}$$

All other inhibitory interneurons in CA1

$$\begin{aligned}
\tau_{I_{CA1I}} \frac{dI_{CA1I}}{dt} &= -I_{CA1I}(t) + (k_i - I_{CA1I}(t)) \cdot \\
&\quad Z_i((-w_{I_{CA1I} \leftarrow I_S} I_S(t) \\
&\quad \quad - w_{I_{CA1I} \leftarrow I_B} I_B(t) \\
&\quad \quad - w_{I_{CA1I} \leftarrow I_{BS}} I_{BS}(t) \\
&\quad \quad + w_{I_{CA1I} \leftarrow E_{CA1}} E_{CA1}(t) \\
&\quad \quad + w_{I_{CA1I} \leftarrow E_{CA3}} E_{CA3}(t) \\
&\quad \quad + P_{EC}(t))
\end{aligned} \tag{13f}$$

From the microcircuit of CA3, the following oscillatory model is derived as follows: Excitatory pyramidal cells

$$\begin{aligned}
\tau_{E_{CA3}} \frac{dE_{CA3}}{dt} = & -E_{CA3}(t) + (k_e - E_{CA3}(t)). \\
& Z_e(w_{E_{CA3} \leftarrow E_{CA3}} E_{CA3}(t) \\
& - w_{E_{CA3} \leftarrow I_{CA3I}} I_{CA3I}(t) \\
& - w_{E_{CA3} \leftarrow I_B} I_B(t) \\
& - w_{E_{CA3} \leftarrow I_{BS}} I_{BS}(t) \\
& - w_{E_{CA3} \leftarrow I_{BP}} I_{BP}(t) \\
& + P_{EC}(t) + P_{DG}(t))
\end{aligned} \tag{14a}$$

PV-containing basket cells

$$\begin{aligned}
\tau_{I_B} \frac{dI_B}{dt} = & -I_B(t) + (k_i - I_B(t)). \\
& Z_i((w_{I_B \leftarrow E_{CA3}} E_{CA3}(t) \\
& - w_{I_B \leftarrow I_{BS}} I_{BS}(t) \\
& - w_{I_B \leftarrow I_S} I_S(t) \\
& - w_{I_B \leftarrow I_{BP}} I_{BP}(t) \\
& + P_{DG}(t))
\end{aligned} \tag{14b}$$

Bistratified cells

$$\begin{aligned}
\tau_{I_{BS}} \frac{dI_{BS}}{dt} = & -I_{BS}(t) + (k_i - I_{BS}(t)). \\
& Z_i((w_{I_{BS} \leftarrow E_{CA3}} E_{CA3}(t) \\
& - w_{I_{BS} \leftarrow I_{BP}} I_{BP}(t))
\end{aligned} \tag{14c}$$

Septo-hippocampal input

$$\begin{aligned}
\tau_S \frac{dI_S}{dt} = & -I_S(t) + (k_i - I_S(t)). \\
& Z_i((-w_{I_S \leftarrow I_{CA3I}} I_{CA3I}(t) \\
& + P_S)
\end{aligned} \tag{14d}$$

All other inhibitory interneurons in CA3

$$\begin{aligned}
\tau_{I_{CA3I}} \frac{dI_{CA3I}}{dt} = & -I_{CA3I}(t) + (k_i - I_{CA3I}(t)). \\
& Z_i((w_{I_{CA3I} \leftarrow E_{CA3}} E_{CA3}(t) \\
& - w_{I_{CA3I} \leftarrow I_{BP}} I_{BP}(t) \\
& - w_{I_{CA3I} \leftarrow I_S} I_S(t)) \\
& + P_{EC}(t) + P_{DG}(t))
\end{aligned} \tag{14e}$$

The common input from septum to both CA1 and CA3 is given as follows.

$$\begin{aligned}
\tau_S \frac{dI_S}{dt} = & -I_S(t) + (k_i - I_S(t)). \\
& Z_i((-w_{I_S \leftarrow I_{CA3P}} I_{CA3P}(t) \\
& - w_{I_S \leftarrow I_{CA1P}} I_{CA1P}(t)) \\
& + P_S(t))
\end{aligned} \tag{15a}$$

The model equations are defined according to the microcircuit given in figure 13. For easier reference, we have also provided the connectivity matrix in tables 4 and 5, which explains CA1 to CA3 projections via the back-projection cells and from CA3 to CA1 via the Schaffer collaterals from CA3 pyramidal cells to CA1. Now that we have the framework, we can consider time constants in the next section in table 7. Symbol definitions are as given in table 6. Parameter values for the variables in the individual model simulations are given in section 4.3 in tables 8 and 9, and parameter values for the variables in the integrated model simulations are given in tables 10 and 11 about which we will be discussing more in the later sections of this chapter.

4.2.3 TIME CONSTANTS OF NEURONAL POPULATIONS

Membrane time constants for each cell type is chosen from literature. Pyramidal cells in CA1 are anatomically observed to have a membrane time constant between $16.5 - 39ms$ from various sources [130], and we consider a slightly minimum value of $16ms$ [135] to have enough time to obtain theta and theta-coupled gamma oscillations. Whereas CA3 pyramidal cells have a membrane time constant between $12 - 61ms$, and we consider $12ms$ [136], to have enough recovery time after an action potential and still obtain theta and theta-coupled gamma oscillations.

Basket cells in CA1 and CA3 are observed to have a membrane time constant of 11 – 13ms, and we have considered 11ms for both CA1 [137] and CA3 [138].

Bistratified cells are modeled with a 18ms time constant for CA3 [138], and since there is lack of evidence of patch-clamp recordings for the time constant of CA1 bistratified cells, we have adopted the same, 18ms, as the membrane time constant for CA1 bistratified cells also.

The membrane time constant for septum is deduced to be 30ms, as there is no proper evidence in literature for the latency of propagation of signals from the medial septum to CA1 pyramidal cells and hence, we retained the same value chosen by Denham et. al [2] the the septal-pacemaker circuit.

The populations of calbindin-containing hippocampo-septal neurons and other inhibitory interneurons are categorized into GABAergic bistratified populations which have a membrane time constant of $18.6 \pm 8.1ms$ in CA1 [139]. Since such data is not available for CA3, we consider 11ms for both of these populations in CA1 and CA3, to obtain oscillations having $\geq 7Hz$ frequency.

Membrane time constant for CA1 back-projection cells is not present in literature and hence, we consider 10ms, a minimum value for an inhibitory interneuron considering the ranges of other inhibitory interneurons.

4.2.4 METHODS OF ANALYSIS

We have used numpy, scipy, scipy FFTpack and matplotlib packages from python 3.6.9 version to simulate our population model of CA1 and CA3. The differential equations are solved using the *scipy.integrate.odeint* function.

One of the important factors to analyze in the simulation results is the frequency of oscillations obtained in each region for each neuron type. The frequency of oscillations of the different populations is dependent on the weights of many projections. Activity dynamics of the model simulated result in two frequencies superposed on one another. The base frequency

Table 7: Time constants of cells in CA1 and CA3 taken as close as possible from literature, and hence is the same for all the models, both individual and integrated models. The time constants are used as given in equations 13, 14 and 15.

Cell type	Time (ms)
τ_{ECA1}	16
τ_{ECA3}	12
τ_{IB}	11
τ_{IBS}	18
τ_{IBP}	10
τ_{ICA1P}	11
τ_{ICA1I}	11
τ_{ISEPT}	30

oscillation acts as a carrier for the second frequency oscillation and the latter is seen in the crest of the former (only on the positive axes in our simulations).

The purpose of analyzing the frequencies of the oscillatory dynamics here is to determine the presence or absence of bifurcation points in the model. In the model proposed by Denham et. al [2], the frequencies seen were the 4-10Hz theta frequency oscillations alone, and the model did exhibit bifurcations which is explained by Denham et. al. To determine if there is another bifurcation that occurs when the model transits from theta frequency oscillating mode to theta-coupled gamma frequency oscillating mode, bifurcation analysis using the AUTO functionality of XPPAUT software was used. However, no such bifurcations could be found. To ascertain this, a parameter scope exploration is performed.

To calculate the frequencies, we have used two methods. One is a simple method implemented, where we calculate the frequencies manually by comparing every point in the neuronal activity with a threshold and increment peaks by one when the points in the activity increase beyond a pre-set threshold. The thresholds for theta and slow gamma frequencies are different and is necessary to avoid counting noisy peaks in the activity if present. This is explained in figure 20.

Whenever the activity dynamics descends, we can note the start of the inter-spike interval. Whenever the activity dynamics ascends beyond the threshold, we can increment the number of peaks by one, and note the beginning of a peak as the end of the inter-spike interval. Since we are dealing with periodic oscillations here, the inter-spike interval for 7-10Hz oscillations is the same between peaks for the whole duration of the simulation, and similarly the inter-spike interval for the 30-50Hz oscillations is also the same between peaks. The number of such inter-spike intervals in the whole simulation duration gives us the frequency of oscillations.

The second method is to use the FFT of the neuronal activity. The FFTs for CA1 pyramidal cells have frequencies in the range of 7-15Hz and 20-60Hz which confirms the frequencies present in the activity as theta and slow-gamma oscillations.

It is worth mentioning that both the methods lead to the same results as the frequency determines the kind of oscillations being generated by the system. However, since FFT is the established standard to determine frequencies, we will be using this going forward.

By selecting certain points including the boundary points of the model for different connection weights and external inputs, and simulating the model for these points, we analyzed the frequency from the results of each simulation.

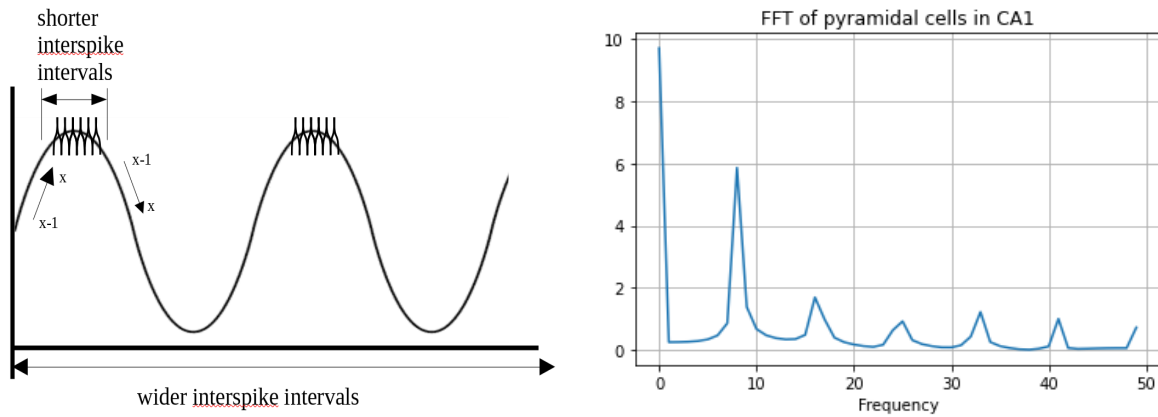


Figure 20: (left) As the activity rises, $(x - 1) < x$, the number of peak count is incremented, and as the activity decreases, $(x - 1) > x$ the inter-spike interval count gets incremented. The same is observed for the secondary oscillations superposed on top of the carrier wave. (right) FFT of CA1 pyramidal cells.

Let the total frequency of oscillations be γ , and the frequency of the carrier wave be θ .

If $\gamma = 0\text{Hz}$, and $\theta = 0\text{Hz}$, the system is in steady state.

If $30\text{Hz} < \gamma < 60\text{Hz}$, the system is oscillating with slow gamma frequency, with no 7Hz theta oscillations.

If $\gamma > 80\text{Hz}$, the system is oscillating with fast gamma frequency, with no 7Hz theta oscillations.

If $4\text{Hz} < \theta < 13\text{Hz}$, the system is oscillating with theta frequency, with no 30-50Hz slow gamma oscillations.

If $4\text{Hz} < \theta < 13\text{Hz}$, and if $30\text{Hz} < \gamma < 60\text{Hz}$, the system is oscillating with theta-coupled slow gamma frequency.

Using the simple technique or FFT to calculate the frequency of the results obtained during each simulation for each value of the parameters under examination, we can determine the type of oscillations present in the resultant activity. The results of these simulations is given and explained in section 4.3.3.

In the simulations of CA1 and CA3 regions, we found many possible connection weights that result in different dynamics. However, increasing the connection weight of bistratified cells to pyramidal cells even further gives rise to theta frequency oscillations and increasing it even further, gives rise to theta-coupled gamma oscillations. This is found to be true in both the individual model and the integrated model. Running through different values of external weights, and varying the connection weight from bistratified to pyramidal cells, the

non-linear dynamical system of CA1 and CA3 ends up in one of the cases of oscillating system as described above. A detailed analysis of the results obtained through this method is discussed in sections 4.3 and 4.4.

4.3 RESULTS

4.3.1 CA1 MODEL WITH CONSTANT EXTERNAL INPUTS

The model equations for the CA1 microcircuit are as explained in section 4.2. It is to be noted that all results in this section have CA3 as a constant external input.

According to the cell-theta-phase relationships recorded by Klausberger et. al [140, 133],

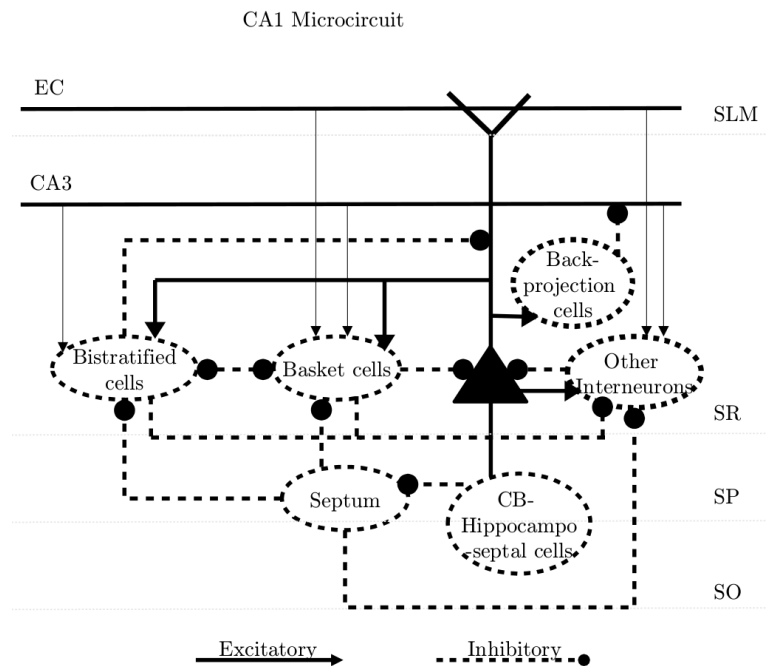


Figure 21: CA1 microcircuit where CA3 and EC are constant inputs.

CA1 pyramidal cells are in-phase with CA1 bistratified cells and are out-of-phase with CA1 basket cells. We start the simulations by establishing parameter values that result in combined theta-coupled gamma oscillations in CA1 pyramidal cells, with the cell-theta-phase relationships as observed by Klausberger et. al. In CA1 region, increasing excitation of inhibitory bistratified cells from pyramidal cells produces slow gamma rhythms coupled with theta oscillation, while decreasing excitation of inhibitory basket cells from pyramidal cells produces theta oscillations. The result is given in figure 22, with values of parameters as given in table

8 and time constants for each cell type in table 7 in the previous section.

When the excitation of basket cells from pyramidal cells is low, inhibition of bistratified cells from basket cells is also low and hence, the oscillations of pyramidal cells and bistratified cells synchronize. As the excitation of basket cells increases, pyramidal cells and basket cells synchronize. However, due to the recurrent inhibition between bistratified and basket cells, these two populations remain out-of-sync. However, by increasing excitation of bistratified cells from pyramidal cells, and decreasing basket cell excitation from pyramidal cells, pyramidal and bistratified cells are synchronized as shown in figure 23.

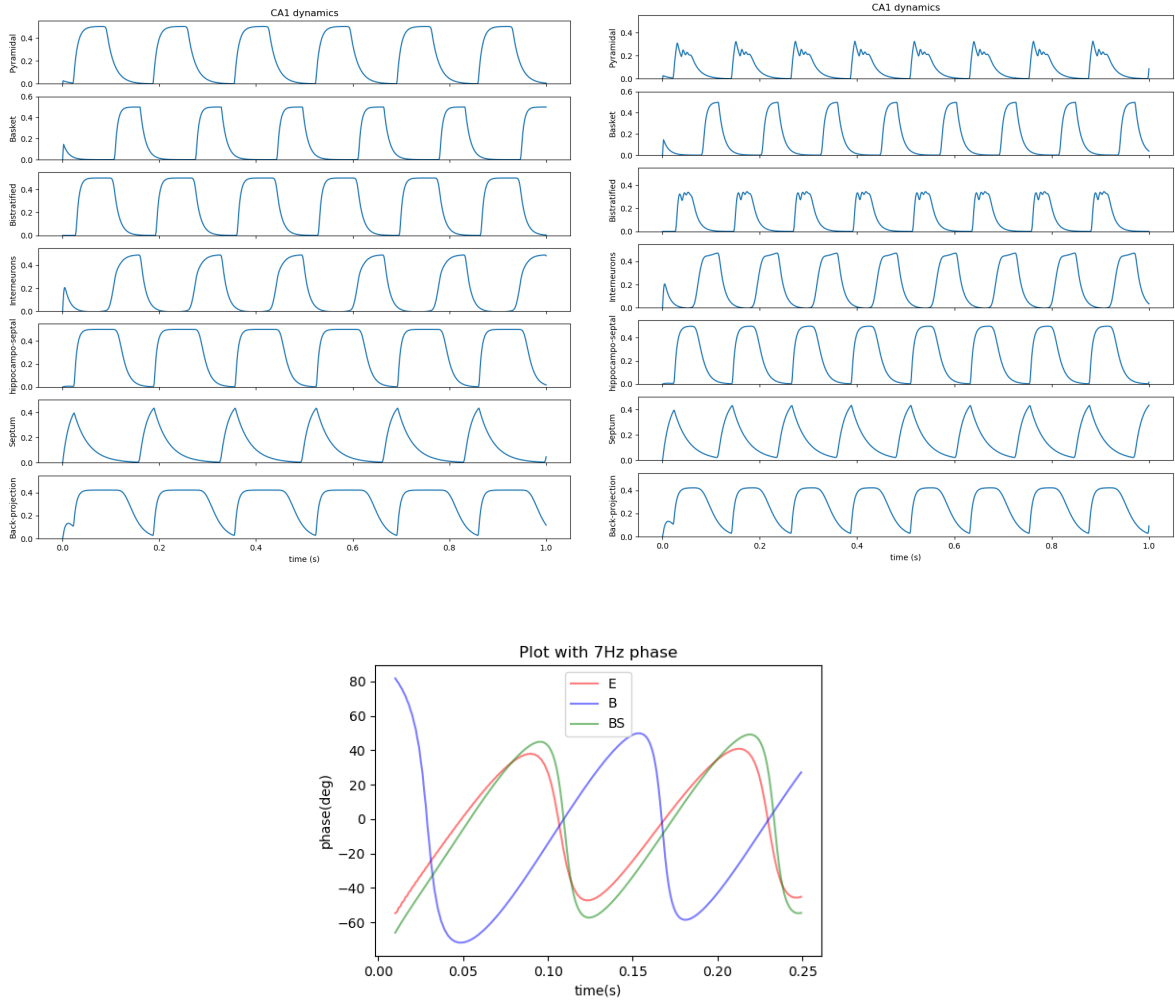
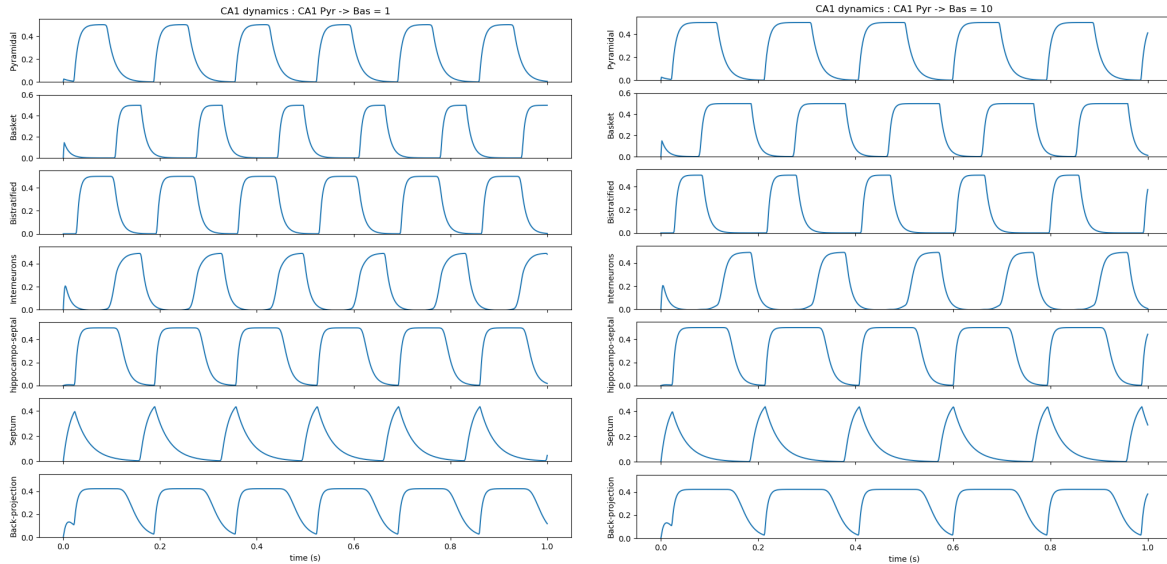


Figure 22: CA1 (top-left) 6Hz theta and (top-right) 24Hz theta-coupled slow gamma oscillations; (bottom) phases of pyramidal, basket and bistratified cells for the theta-coupled gamma oscillatory activity to show the phase synchronization between pyramidal and bistratified cells, and the phase-difference between pyramidal and basket cells.

Table 8: Weights and external input values for CA1. The values of external inputs P_{CA3} , P_{EC} and P_s are excitatory constant inputs to the individual model.

From \ To	PC	BC	BSC	ICAI	ICAP	BP	Septum
PC		1	10	10	50	50	
BC	1		10	5			
BSC	$10(\theta); 20(\gamma)$	10		5			
ICAI	150						
ICAP							150
BP	10						
CA3: Pyr	8	8	8	8			
Septum		100	1	50			
EC	3	3	3				
P_s							8

Septal input to the inhibitory interneurons in CA1 is the main source of theta rhythm propagation. From the simulation results shown in figure 22, the septal theta oscillations are in phase with CA1 pyramidal cells and bistratified cells and that the oscillations of 6Hz frequency when the weight from CA1 bistratified cells to pyramidal cells is low, and 8Hz theta-coupled with three gamma cycles in each theta half cycle when the weight from CA1 bistratified cells to pyramidal cells is increased.



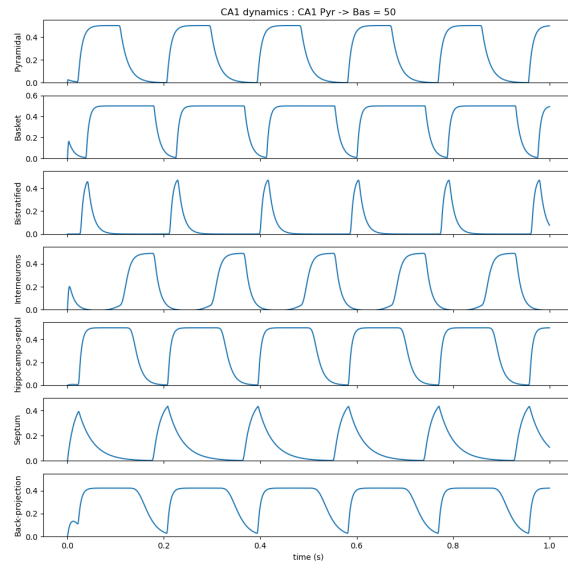


Figure 23: CA1 pyramidal, basket and bistratified cells are in-synch

4.3.2 CA3 MODEL WITH CONSTANT EXTERNAL INPUTS

CA3 region has the recurrent connections formed by the excitatory pyramidal cells which are also known to be intrahippocampal theta oscillators [17]. CA3 pyramidal cells receives its input from the CA3 pyramidal cells via the recurrent collaterals, EC via the perforant path, from DG via the mossy fibers, projection from ms-dBB and inhibitory projections from back-projection cells in CA1 to the interneurons, and the inhibitory interneurons to pyramidal cells in the region. The inhibitory interneurons receive GABAergic excitation from the septum. The CA3 microcircuit along with its different compartments namely, stratum lacunosum-moleculare (SLM), stratum radiatum (SR), stratum lucidum (SL), stratum pyramidale (SP) and stratum oriens (SO) is as shown in figure 24. The basic model from Denham et. al is modified to include excitatory recurrent connections and distinct computational equations for some of the inhibitory interneurons, which are given in the previous section 4.2. All results in this section have the CA1 back-projection cell input as a constant inhibitory external input.

From the simulation results, we can observe oscillations of 7Hz frequency when the weight from CA3 pyramidal cells to basket cells is low, and 8.5Hz theta-coupled with 5 gamma cycles in each theta half cycle or 40Hz slow-gamma oscillations when the weight from CA3 pyramidal to basket cells is increased. The result is given in figure 25, with values of parameters as given in table 9 and time constants for each cell type in table 7.

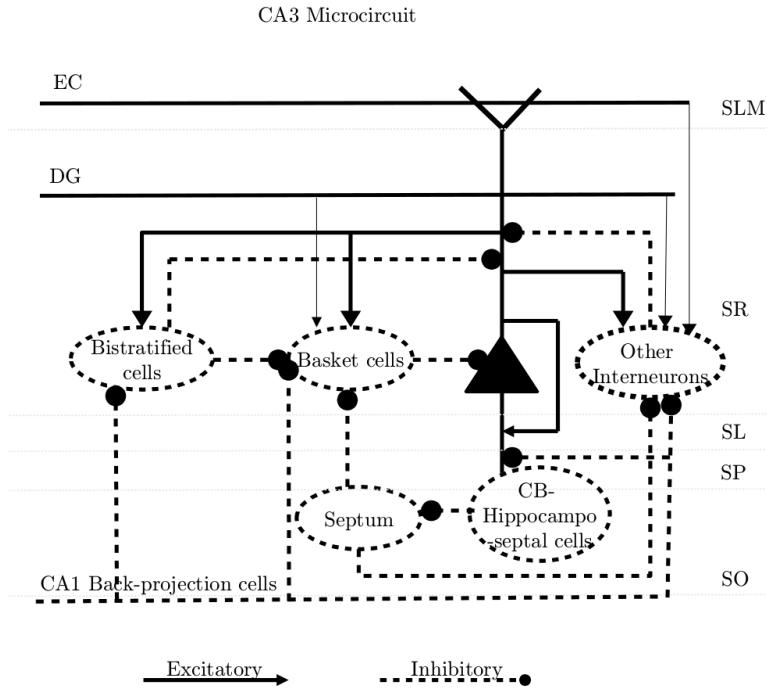


Figure 24: CA3 microcircuit where CA1, EC and DG are constant inputs.

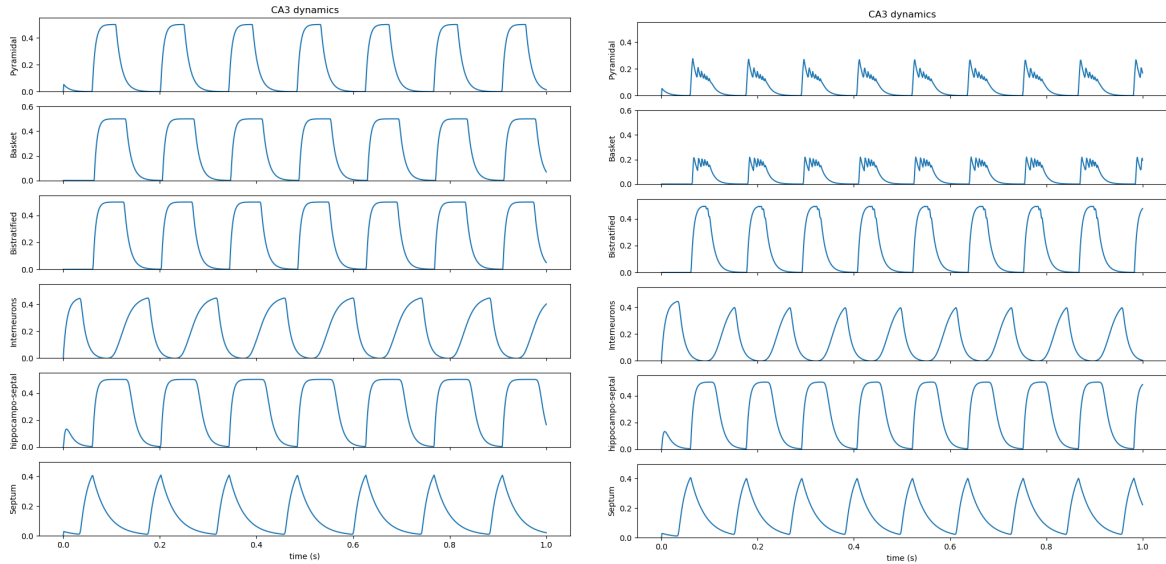


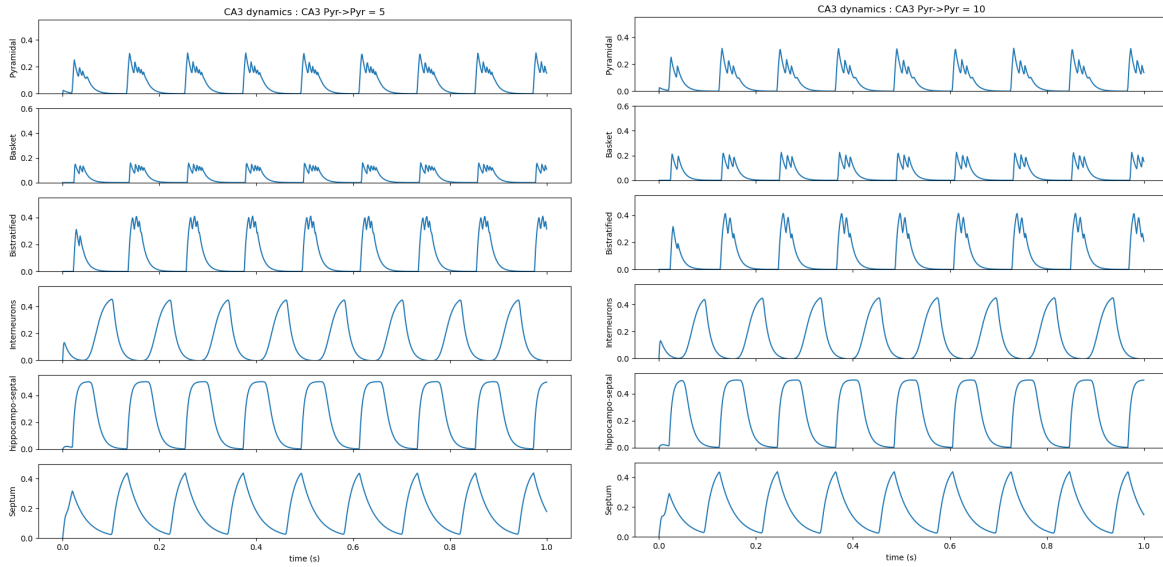
Figure 25: CA3 (left) 7Hz theta and (right) 50Hz theta-coupled slow gamma oscillations.

As the weight of the CA3 recurrent excitation, the frequency of gamma oscillations decreases and disappears, but theta oscillations are sustained for high values of the weight owing to the

Table 9: Weights and external input values for CA3. The values of external inputs P_{EC} , P_{DG} and P_s are excitatory constant inputs to the individual model. P_{CA1} is the constant external inhibitory input coming from CA1 to CA3.

From \ To	PC	BC	BSC	ICAI	ICAP	CA1:BP	Septum
PC	5	100	50		100		
BC	$1(\theta);50(\gamma)$						
BSC	1	5					
ICAI	150						
ICAP							150
DG	1	1		1			
CA1: BP	4	4	4	4			
Septum		50		50			
EC	12			12			
P_s							8

presence of the septal pacemaker circuit. However, too high values results in steady state as shown in figure 26.



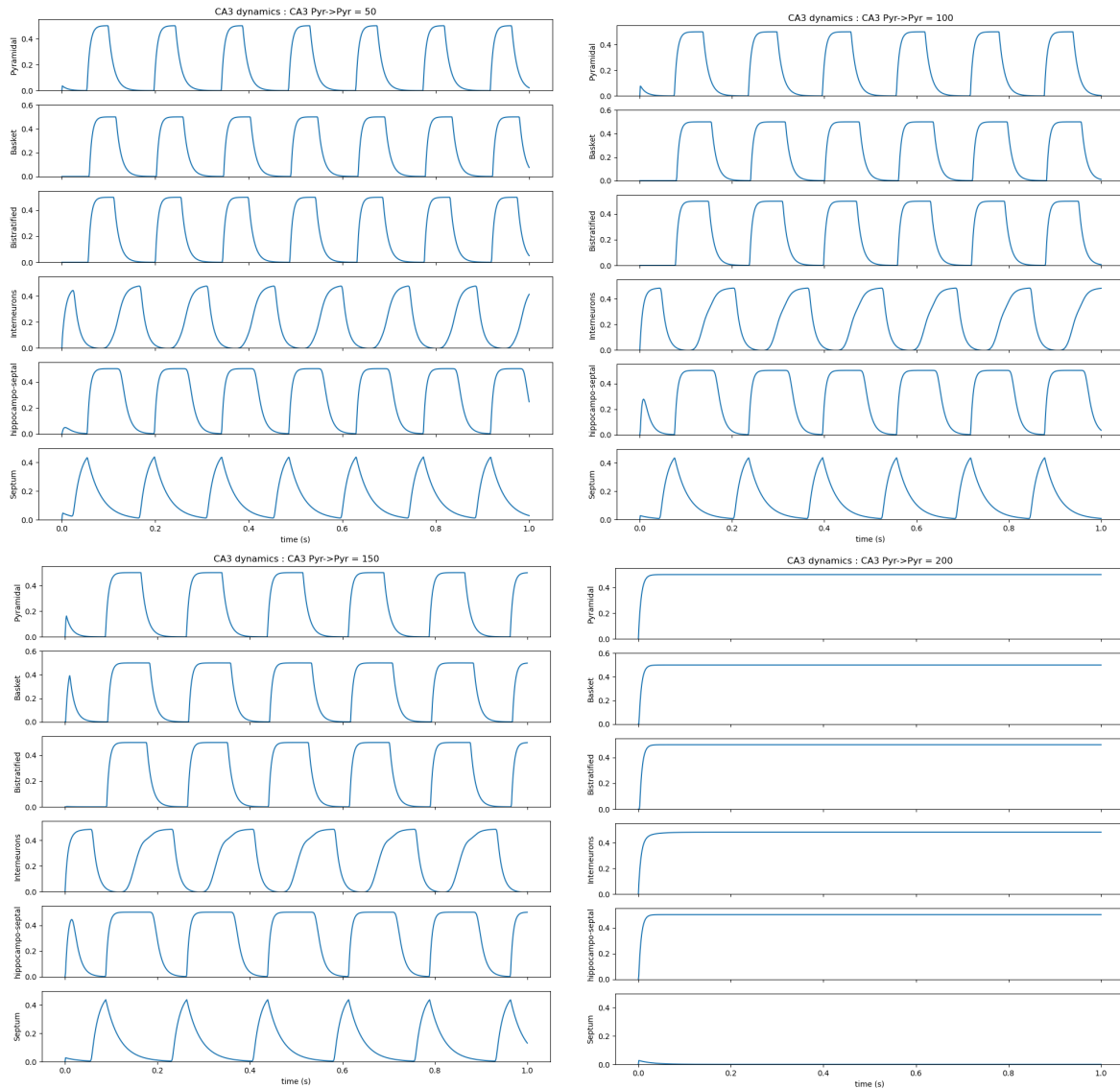


Figure 26: Effects on CA3 neuronal network as recurrent pyramidal excitation increases.

When pyramidal cells get excited, they excite more basket and bistratified cells. Bistratified cells, on excitation, reduce gamma oscillatory activity whereas, basket cells show a subtle increase in gamma oscillatory activity. However, the excited bistratified cells also inhibit basket cell excitation thus reducing gamma oscillatory activity. And hence, pyramidal, basket and bistratified cells exhibit only theta oscillations when the recurrent excitation increases.

Increasing inhibition to pyramidal cells from other inhibitory interneuron population, and increasing inhibition to septum, decreases the frequency of oscillations. Increasing CA1 inhibition introduces slow gamma oscillations in bistratified cells as shown in figure 27.

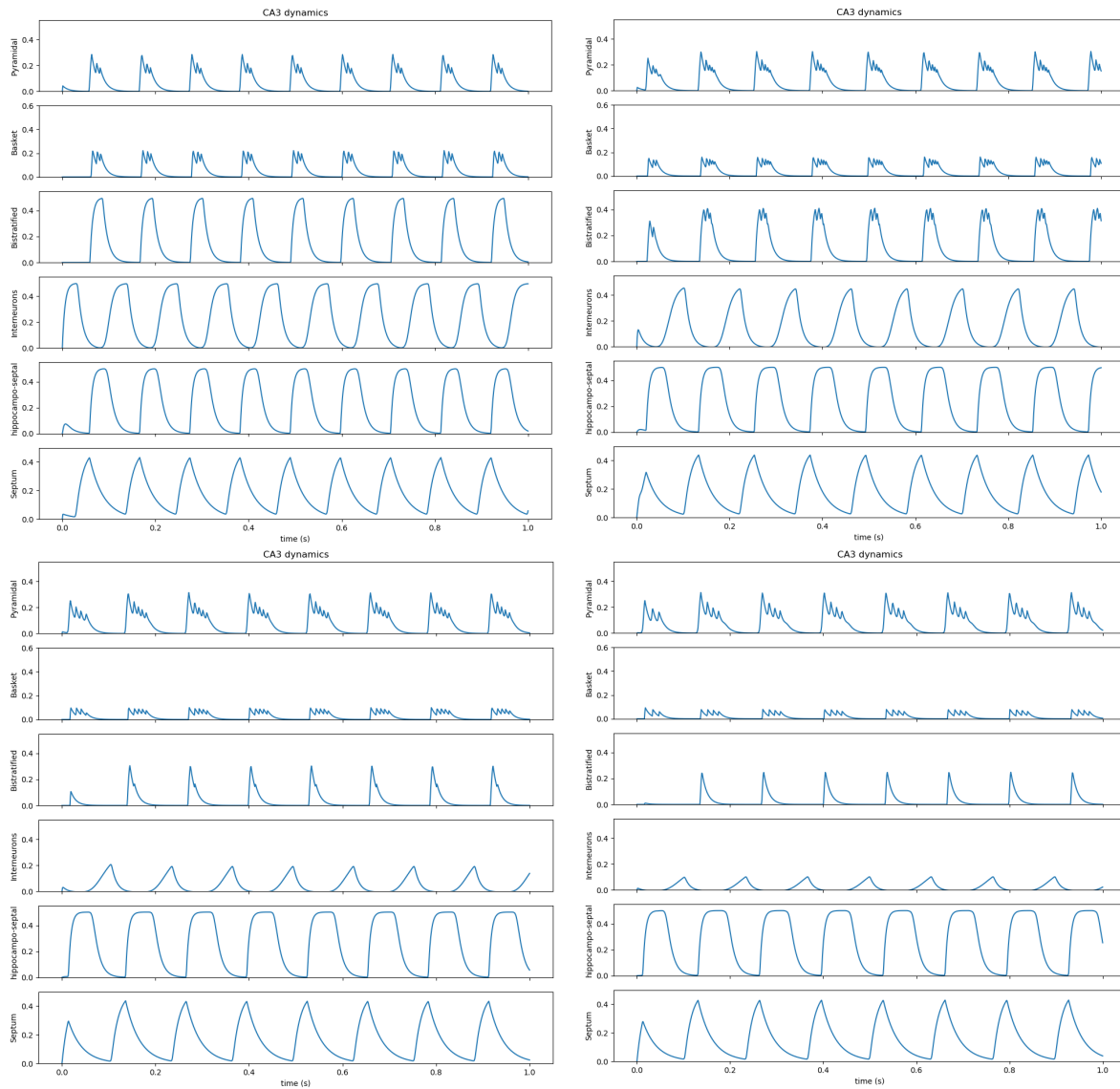


Figure 27: Effects on CA3 neuronal network as recurrent pyramidal excitation increases.

DG input is projected directly to pyramidal and basket cells in CA3, which forms a part of the trisynaptic pathway. As DG input increases, the frequency of oscillations also increases, as expected. However, the slow gamma oscillatory activity disappears in all the cell types.

When DG input increases, frequency of oscillations increases in pyramidal cells. As EC, CA1 and DG inputs increase, pyramidal, basket and bistratified cells converge to a steady state. Theta frequency oscillations are maintained as septal input increases until a certain threshold which is explained in the next section 4.3.3. However, when septal input crosses the threshold, all cell types stop oscillating reaching steady state activity.

4.3.3 CA1-CA3 INTEGRATED MODEL

The CA1 and CA3 regions are integrated to analyze and understand the impacts of the two major pathways, namely, the Schaffer collateral projection from CA3 to CA1 and the back-projection cells from CA1 to CA3 interneurons. Also, this study attempts to reveal the differences between PV-containing basket and bistratified cells found in both the regions. The connection strengths of the integrated microcircuit is given in tables 10 and 11 for CA1 and CA3 respectively. The simulation results is as shown in figure 28.

CA1 results - When the connection strength of CA1 bistratified cells to CA1 pyramidal cells is less than 60, CA1 pyramidal cells display theta oscillations; for connection strength greater than 80, theta-coupled gamma oscillations can be seen; however, when the connection strength increases to greater than 250, *the frequency of theta oscillations increases and slow gamma oscillatory activity decreases from 40 Hz to 20Hz in CA1*, as shown in figure 29. CA1 pyramidal cells are in-phase with CA1 bistratified cells and CA1 basket cells are out-of-phase with CA1 pyramidal cells. This phase synchronization is as observed in [141, 140]. The state of CA3 governs the state of CA1 when they are combined. We also show here that the slow gamma oscillations are propagated to CA1 from the CA3 pyramidal cells. CA1 also sustains oscillations without CA3 which is a different question discussed later.

Slow gamma oscillations in the range of 30-50Hz coupled with theta oscillations are seen in the integrated model by projecting CA3 synapses onto CA1 populations as observed in literature [142]. In our simulations, CA3 pyramidal cells project onto CA1 pyramidal, basket and bistratified cells which oscillate with slow gamma frequency. Although EC input is constant in our model, we can observe from the activity plots in figures 31 and 32 that large values of EC projecting to inhibitory interneurons and pyramidal cells in CA1 and CA3 causes steady state and that only a small range of external input values can sustain the 4-13Hz oscillations coupled with 30-50Hz slow gamma oscillations, in both CA1 and CA3.

When the connection strength between CA3 pyramidal cells to CA1 pyramidal cells increases to greater than 20, the beginning of gamma oscillations in theta oscillations can clearly be seen in CA1 pyramidal and CA1 bistratified cells. Theta-coupled gamma oscillatory activity disappears with the increase in connection strength between CA3 pyramidal cells to CA1 basket cells to greater than 50.

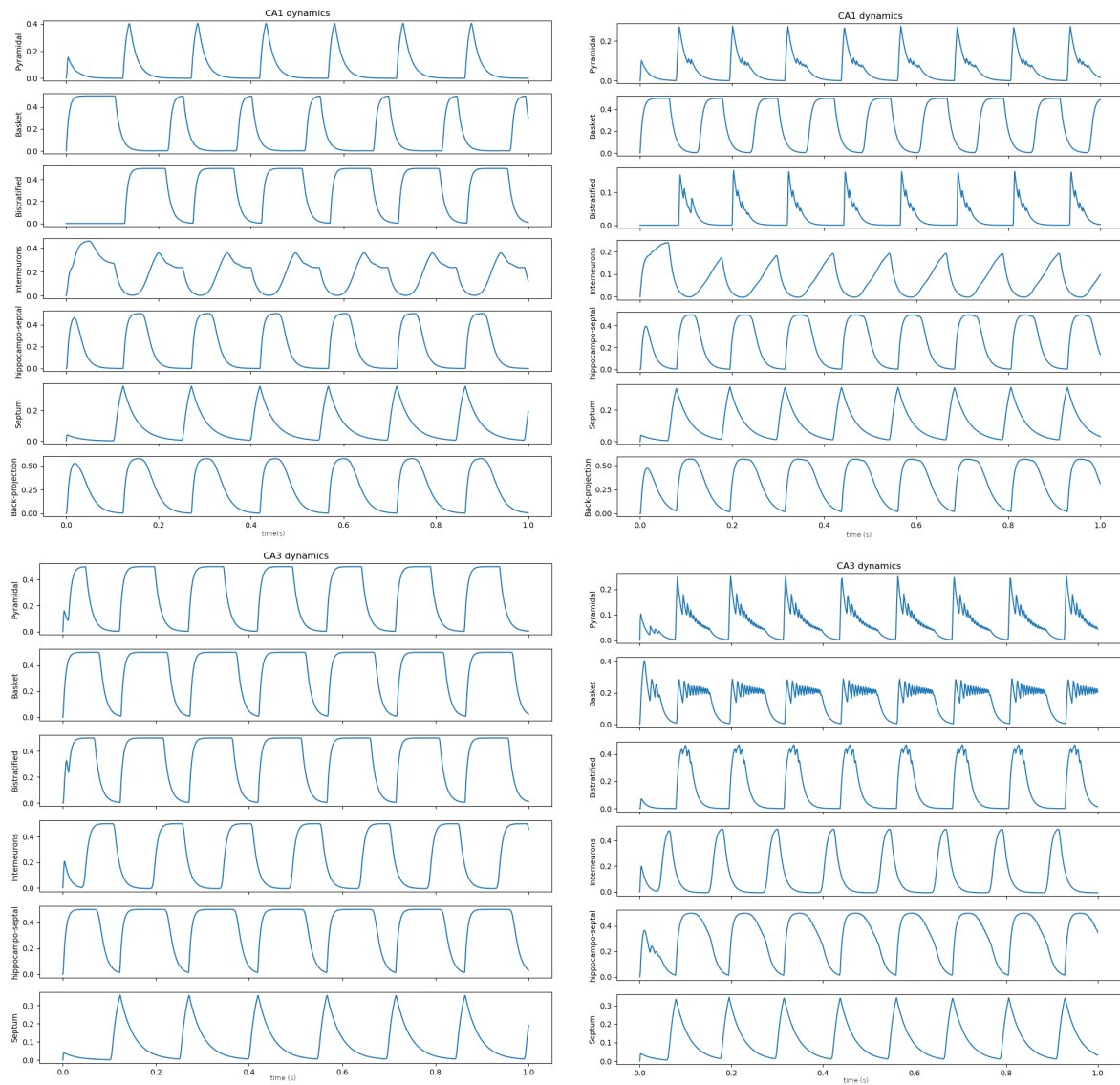
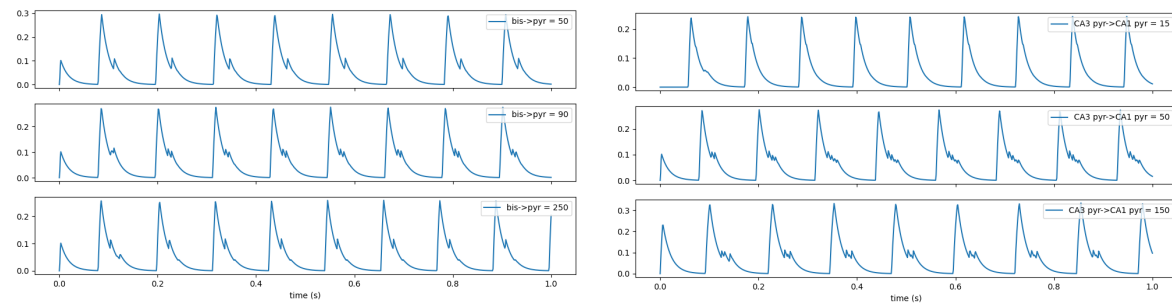


Figure 28: CA1-CA3 theta and theta-coupled gamma oscillations. (top) CA1 (left) 6Hz theta and (right) 32Hz theta-coupled slow gamma oscillations. (bottom) CA3 (left) 7Hz theta and (right) 50Hz theta-coupled slow gamma oscillations.



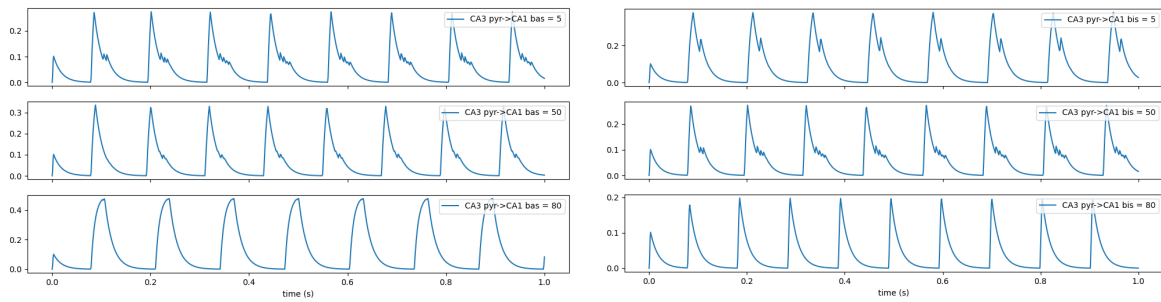


Figure 29: Effect on CA1 pyramidal cells for different connection strength values. (top-left) CA1 bistratified to CA1 pyramidal cell connection strength changes from theta oscillations to theta-coupled gamma oscillations to back again to theta oscillations from 50 to 90 to 250. (top-right) Theta oscillations to theta-coupled gamma oscillations when connection strength from CA3 pyramidal cells to CA1 pyramidal cells increases from 15 to 50 to 150. (bottom-left) Theta-coupled gamma oscillations disappears as connection strength between CA3 pyramidal cells to CA1 basket cells increases from 5 to 50 to 80. (bottom-right) Theta-coupled gamma oscillations disappears as connection strength between CA3 pyramidal cells to CA1 bistratified cells increases from 5 to 50 to 80.

As the connection strength between CA3 pyramidal cells and CA1 bistratified cells increases, theta-coupled gamma oscillations decreases. These results are as shown in figure 29. This implies that as excitation of CA1 pyramidal cells increases, gamma oscillatory activity persists, and as inhibitory activity from CA1 basket and bistratified cells increases, slow-gamma oscillatory activity coupled with theta oscillations decreases.

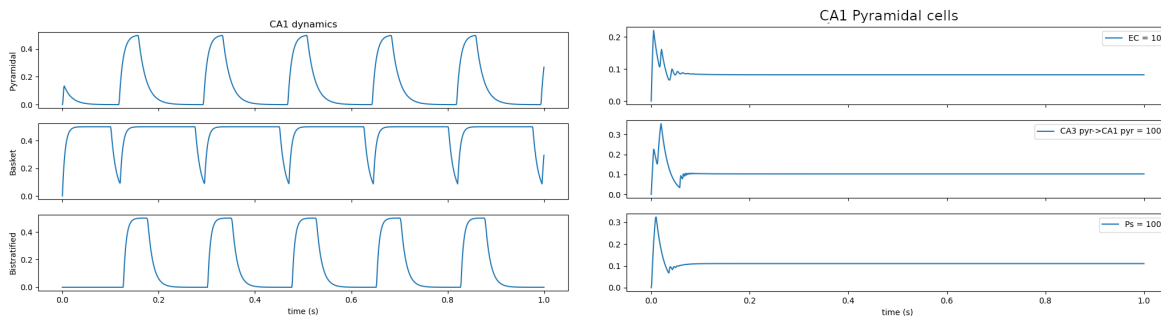


Figure 30: (left) Pyramidal, basket and bistratified cells are in-sync with each other. (right) Larger connection strength from EC, P_s and CA3 to CA1 pyramidal cells results in steady state activity.

Inhibition from septum and inhibition of bistratified cells from basket cells forces CA1 bistratified cells to synchronize with CA1 pyramidal cells; whereas, the phase synchronization of pyramidal cells, basket cells and bistratified cells occurs when the connection strength of pyramidal cells to basket cells increases from 1 to 100, and the connection strength from bistratified to pyramidal cells decreases from 50 to 1. In other words, decreasing the inhibition

Table 10: Weights & external input values for CA1 integrated model. The values of external inputs P_{EC} and P_S are excitatory constant inputs to the integrated model of CA1. Excitatory inputs from CA3 is a continuous input to the neuronal populations in CA1.

From \ To	PC	BC	BSC	ICAI	ICAP	BP	Septum
PC		1	50	10	100	50	
BC	5		50				
BSC	$50(\theta); 100(\gamma)$	10					
ICAI	50						
ICAP							50
BP	1						
CA3: Pyr	50	5	50	5			
Septum		50		50			
EC	4	4		4			
P_S							8

of pyramidal cells synchronizes the activity of pyramidal cells with bistratified and basket cells as shown in figure 30.

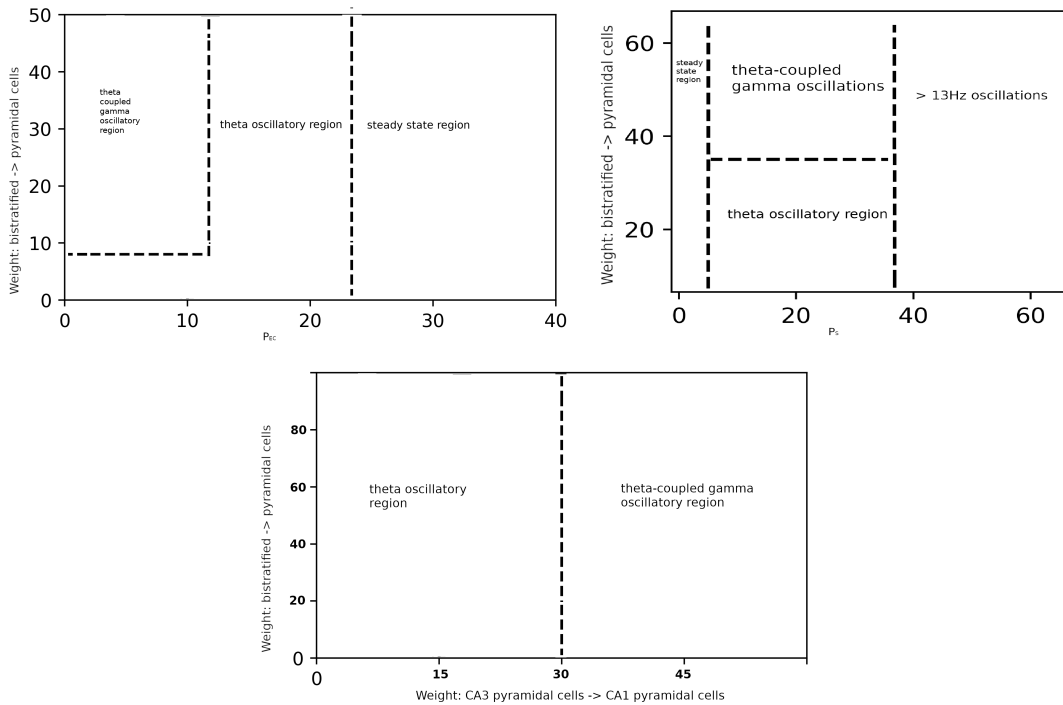


Figure 31: As the connection strength between CA1 bistratified cells and CA1 pyramidal cells changes for different values of EC , P_S and CA3 pyramidal cells to CA1 pyramidal cells, different activity states are observed in CA1 pyramidal cells.

As EC and CA3 inputs are increased, CA1 pyramidal cell activity reaches steady state as

Table 11: Weights & external input values for CA3 integrated model. The values of external inputs P_{EC} , P_{DG} and P_S are excitatory constant inputs to the integrated model of CA3. Inhibitory inputs from CA1 is a continuous input to the neuronal populations in CA3.

From \ To	PC	BC	BSC	ICAI	ICAP	CA1:BP	Septum
PC	10	100	50	10	100		
BC	$10(\theta);50(\gamma)$						
BSC	1	5					
ICAI	50						
ICAP							50
DG	2	2		2			
CA1: BP	1	1	1	50			
Septum		50		50			
EC	12			12			
P_s							8

shown in figure 30. The activity plots for CA1 pyramidal cells with respect to the EC and the external input to septum is as shown in figure 31. From the activity plots obtained from the FFT of the activity dynamics of CA1 in the integrated model, we can see the types of frequencies and states the model oscillates/settles in, and that the theta-coupled gamma oscillations occur for a very narrow range of values of external inputs. *CA3 results* - The inhibition of pyramidal cells or excitation of basket cells in CA3 affects the frequency of oscillations by introducing slow-gamma oscillations in the theta oscillatory network. For connection weights less than 20 from basket cells to pyramidal cells, we get theta oscillations due to the presence of the septal pacemaker circuit. As this connection weight increases to a value greater than 20, we observe 2 small oscillatory peaks in each theta half-cycle which increases to 8 small oscillatory peaks summing to 64Hz slow gamma oscillatory frequency coupled with 8 Hz theta oscillations gradually when the value is further increased to 50.

The activity plots for CA3 pyramidal cells for different values of external inputs is as given in figure 32. A high value of P_S gradually converts 7-13Hz oscillations to fast oscillations with a frequency greater than 70Hz, reaching steady state. This is true even when there is no input from CA1 to CA3 and vice-versa.

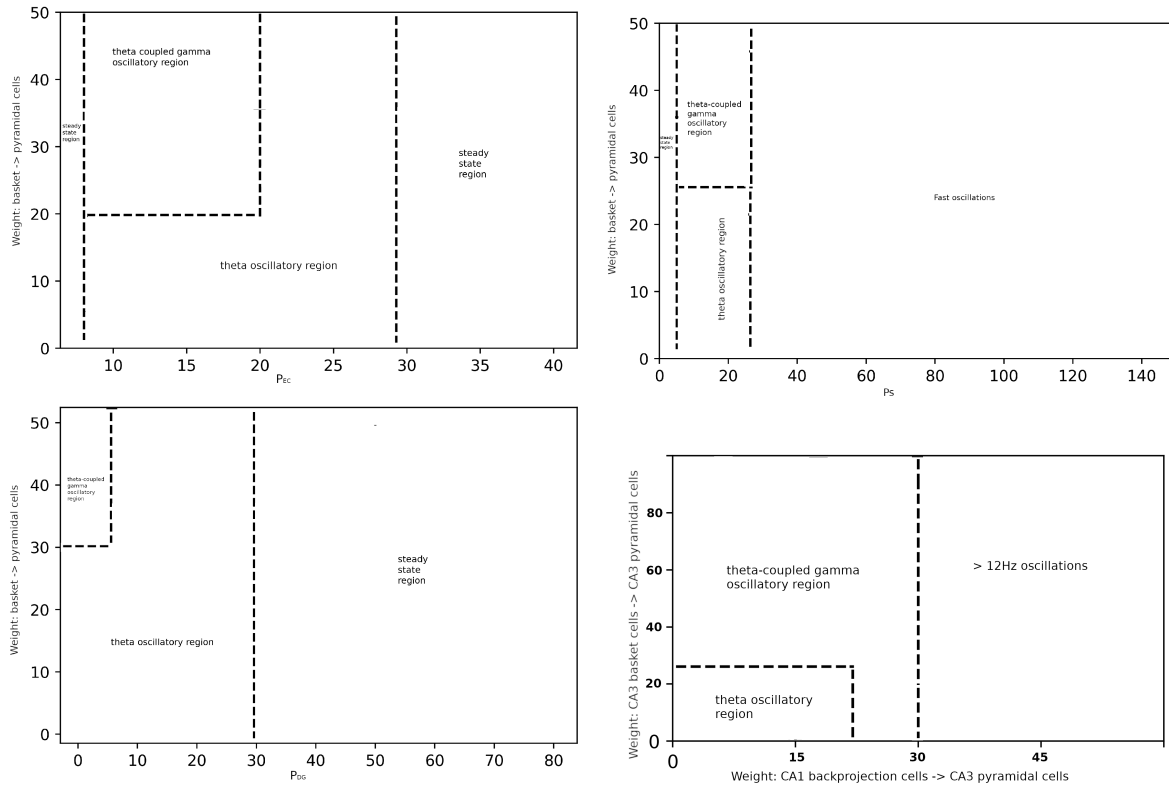


Figure 32: As the connection strength between CA3 basket cells and CA3 pyramidal cells changes for different values of EC, DG, P_s and CA1 backprojection cells to CA3 pyramidal cells, different activity states are observed in CA3 pyramidal cells.

Septo-hippocampal loop - Theta oscillations are produced both due to the recurrent excitation present in the network, and due to the presence of septo-hippocampal feedback loop. The septo-hippocampal input is required to regulate the oscillations generated in the CA3 region. When verifying if the septo-hippocampal loop indeed propagates theta frequency rhythms to the hippocampal CA1 and CA3 regions, we found that the septo-hippocampal loop is necessary to maintain theta frequency oscillations not only in CA1, but also in CA3, as given in table 12. We found oscillations in CA3 even when the septo-hippocampal loop was disrupted in CA3 because of septally-connected interneurons, which are observed to be aligned across the septotemporal axis in CA3 [143], and because of EC input that generate theta frequency oscillations in CA3, which are also propagated to CA1. By removing the septum projections to basket and other inhibitory interneurons, the septal feedback loop is broken, resulting in steady state as shown in figure 33. However, even without the septal loop, CA3 and CA1 display 7.5Hz oscillations due to the presence of an E-I circuit in the model. These are the intrinsic theta oscillators which are responsible for generating the 7Hz hippocampal theta oscillations which are only noticed when the septal loop is absent in the model, as shown in

figure 33. However, we can also observe that when the septal loop is broken in CA1, CA3 still has with 14Hz oscillations but oscillations are absent in CA1, as shown in figure 33.

However, when the septo-hippocampal loop is disrupted in CA3 and inhibition from other inhibitory interneurons to pyramidal cells is decreased, we can observe a transient oscillatory period of different frequencies from fast gamma oscillations to 8Hz oscillations, ending up in steady state. With reference to the table 12, we can also see the corresponding figures in figure 34.

CA1 sustains theta oscillations from the feed-forward excitation of CA3 pyramidal cells without septal input. Disrupting the CA1 septo-hippocampal loop by removing the septal to CA1 interneurons link in the CA1 model, results in producing no oscillations in CA1. However, increasing the weight from CA3 pyramidal cells to CA1 pyramidal cells produces theta-coupled gamma oscillations in both pyramidal and basket cells in CA1 and CA3 in the descending phase as present in literature [31, 141]. This shows that CA1 can oscillate in slow-gamma coupled with theta oscillations frequency without septal input, and these theta-coupled gamma oscillations are propagated from CA3 to CA1.

4.3.4 CONNECTION WEIGHTS ANALYSIS

Calbindin(CB)-containing hippocampo-septal projections complete the feedback loop from hippocampus to the septum, propagating theta oscillations. This input is seen to be significant for both CA1[2] and CA3 to sustain septally propagated theta oscillations. Septal projections to CA1 and CA3 via GABAergic inhibitory interneurons exert high inhibition on pyramidal cells, which in turn drive major feedback projections to PV-containing GABAergic septal population via calbindin-containing hippocampo-septal projections [131]. This is observed both in the individual and integrated model of CA1 and CA3 regions.

In CA3, the CB-containing hippocampo-septal feedback loop combined with excitation of basket cells generates theta-gamma coupling by inhibiting the recurrent excitation of pyramidal cells. By inhibiting CA3 pyramidal cells, it is possible to induce slow gamma oscillations in CA3.

In CA1, the CB-containing hippocampo-septal feedback loop combined with excitation of bistratified cells is required to introduce slow gamma frequency coupling. Without CA3 input to CA1, slow-gamma oscillations disappear. It is known that gamma oscillations are propagated to the hippocampus from EC, and in the absence of EC, CA3 region is known to propagate gamma frequency oscillations [53]. These gamma oscillations propagated to CA1

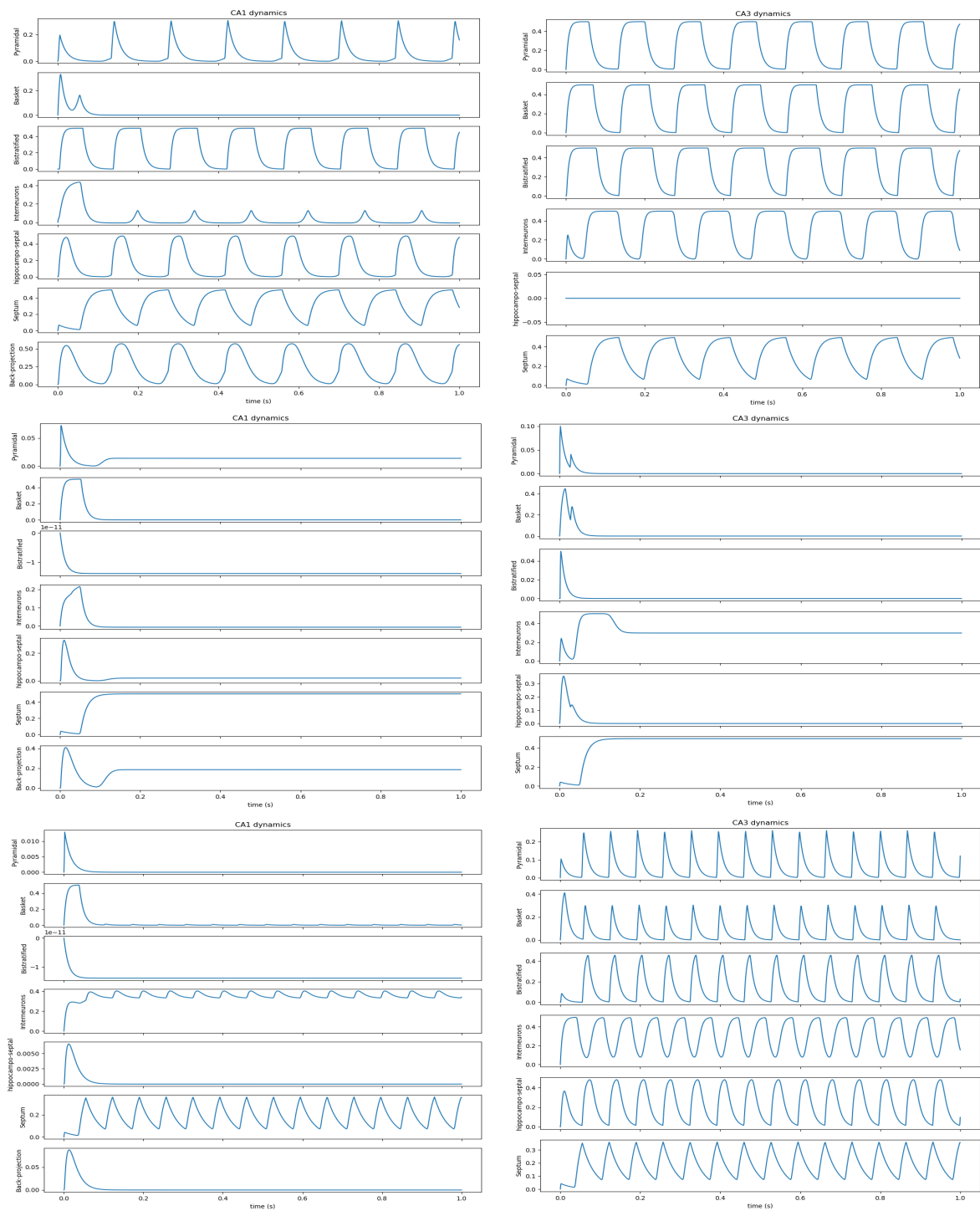


Figure 33: Simulations when (top) the septal loop is broken ; (middle) the septum input is removed from CA3 basket cells and CA3 other inhibitory interneurons; (bottom) septal input is removed from CA1 other inhibitory interneuron population. The left column represents CA1 and right column represents CA3 results.

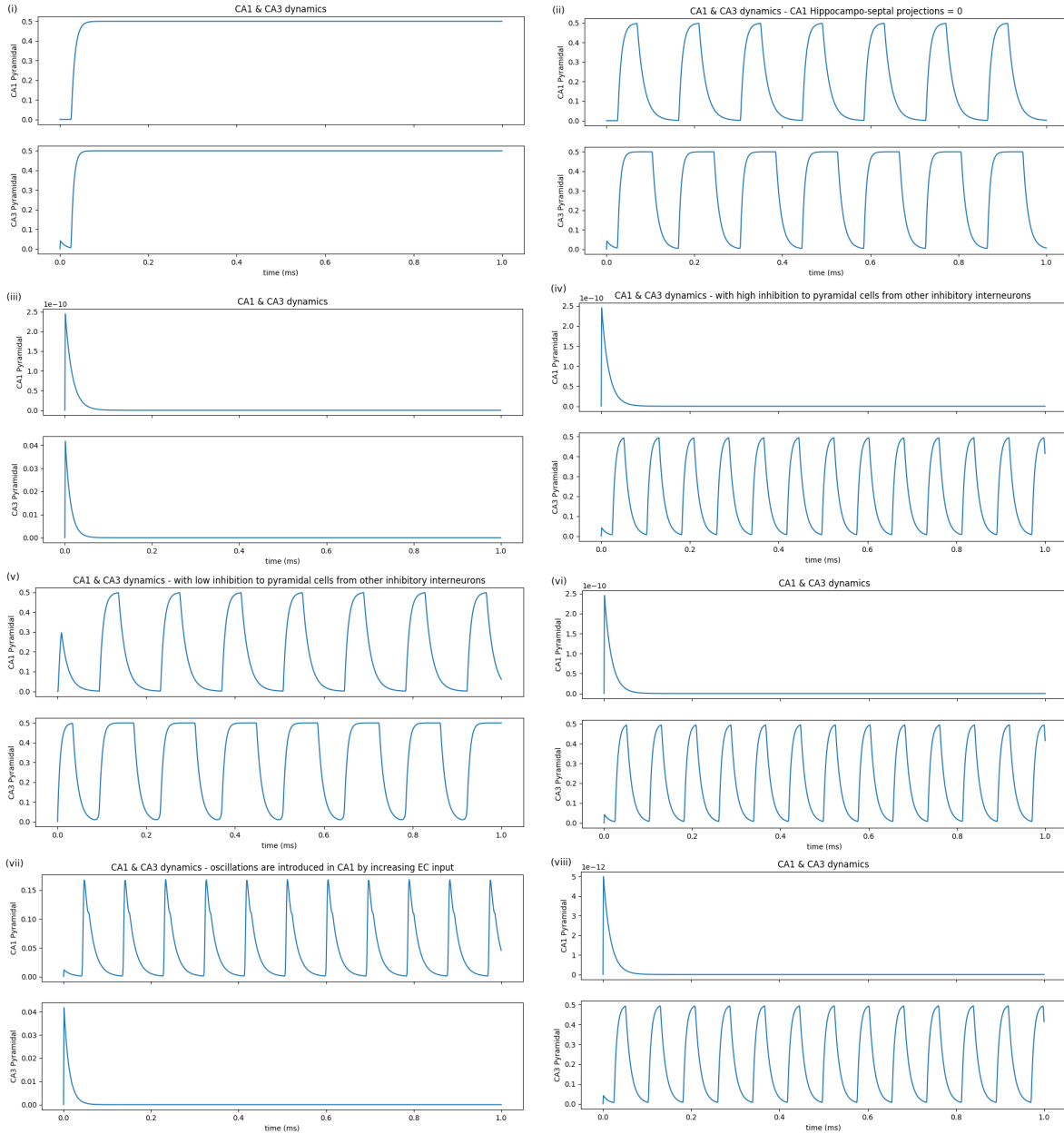


Figure 34: Effect of the septo-hippocampal loop, Schaffer collaterals and CA1 back-projection cells, on CA1 and CA3 regions, which is explained in table 12.

Table 12: Effect of septo-hippocampal loop on CA1 and CA3 as shown in figure 34

	Projection type	Type of oscillation	Reasoning
(i)	Hippocampo-septal projections from CA1 and CA3 = 0	No oscillations	Expected
(ii)	Hippocampo-septal projections from CA1 = 0 or CA3 = 0	Oscillations are observed in both CA1 and CA3	If either one of them = 0, that region would still get oscillatory activity from septum as septum receives activity input from the other region.
(iii)	Septo-hippocampal projections from CA1 and CA3 = 0	No oscillations	Expected
(iv)	Septo-hippocampal projections from CA1 = 0	Oscillations in CA1 are observed when inhibition to pyramidal cells is decreased, but 12Hz oscillations in CA3 is observed	Oscillations occur due to projections from CA3 to CA1
(v)	Septo-hippocampal projections from CA3 = 0	Oscillations in CA1 and CA3 are observed when inhibition to CA3 pyramidal cells is decreased	Oscillations occur in CA3 due to septo-interneuron projections which are propagated to CA1
(vi)	Projections from CA1 back-projection cells to CA3 = 0 and septo-hippocampal projections from CA1 = 0	No oscillations in CA1 pyramidal and basket cells, but 13Hz oscillations in CA3	Now that there are no projections from CA1 to CA3, disrupting septo-hippocampal loop in CA1 disrupts oscillations in the CA1.
(vii)	Projections from CA1 back-projection cells to CA3 = 0 and septo-hippocampal projections from CA3 = 0	No oscillations in CA3 and CA1, but oscillations can be introduced in CA1 by increasing EC input	Now that there are no projections from CA1 to CA3, disrupting septo-hippocampal loop in CA3 disrupts oscillations in CA3, in turn disrupting oscillations in CA1 also.
(viii)	Septo-hippocampal projections from CA1 = 0 and removing CA3 input to CA1	No oscillations in CA1 and 13Hz oscillations in CA3	Expected as Schaffer collateral input from CA3 to CA1 is disrupted and the septo-hippocampal loop is disrupted

from CA3 are due to the fast-spiking PV containing interneurons such as the basket and bistratified cells, which, as also seen in our simulations, when excited more by pyramidal cells, produce gamma frequency oscillations in the half cycles of theta oscillations [144, 54]. Increasing CA1 bistratified cell excitation, increasing CA1 pyramidal cell inhibition, and CA1 basket to CA1 bistratified cells inhibition, contribute to slow gamma oscillations in the CA1 model. Thus, increasing excitatory drive from external EC and CA3 is required for inducing slow gamma oscillations in CA1. Slow gamma oscillations in CA1 are disrupted when there is no CA3 input to CA1 in the integrated model, although there are theta-coupled gamma oscillations in CA3, as seen in experiments [40, 53, 124]. To sustain theta-coupled gamma oscillations, low inhibition is given to CA1 basket cells which in turn inhibits CA1 bistratified cells.

In the simulations, it was difficult to get theta oscillations in CA3 due to the densely-populated excitatory recurrent connections amongst CA3 pyramidal cells, and hence, they require high inhibition from other inhibitory interneurons, low excitation of pyramidal cells from other CA3 pyramidal cells.

4.3.5 OSCILLATORY MODES AND BIFURCATION ANALYSIS

Different oscillatory modes for different ranges of external inputs was noticed while working on the model ranging from low frequency oscillations to fast oscillations to steady state. The parameter ranges for the different kinds of oscillations for both CA1 and CA3 is given in the previous section.

In CA3, for low values of EC and an increasing value of connection weight from pyramidal to basket cells gives rise to intermediary oscillatory states which belong neither to theta frequency nor slow-gamma frequency, which on increasing the connection weight does not converge to a steady state. This is shown in figure 35.

The non-linear behaviour of the model starts off from a steady state, and bifurcates with an unstable homoclinic bifurcation, into an unstable limit cycle with complex conjugate eigen values, which displays Andronov-Hopf bifurcation. For even higher external currents, the system settles in a steady state. When all external inputs are low, the system remains in steady state. As the external inputs start increasing, in combination with connection weights from bistratified cells to pyramidal cells in CA1 and basket cells to pyramidal cells in CA3, the steady state of the system changes to a single limit cycle when theta oscillations appear. When the weights increase even more, this limit cycle changes to encompass another limit

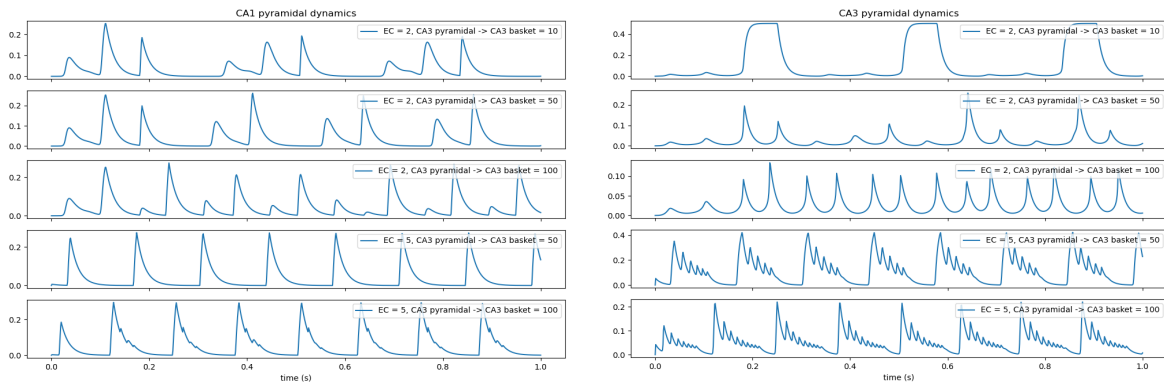


Figure 35: Intermediate states when EC is low and connection weights of CA3 pyramidal to CA3 basket cells increases. (left) CA1 pyramidal cell activity (right) CA3 pyramidal cell activity.

cycle representing theta oscillations encompassing the 30-50Hz gamma subcycles in each theta half cycle, as shown in the phase plot in figure 36.

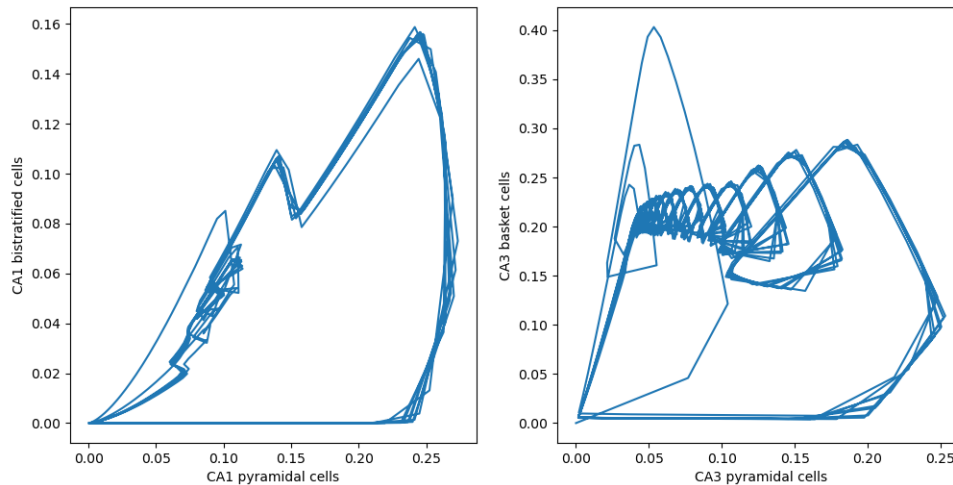


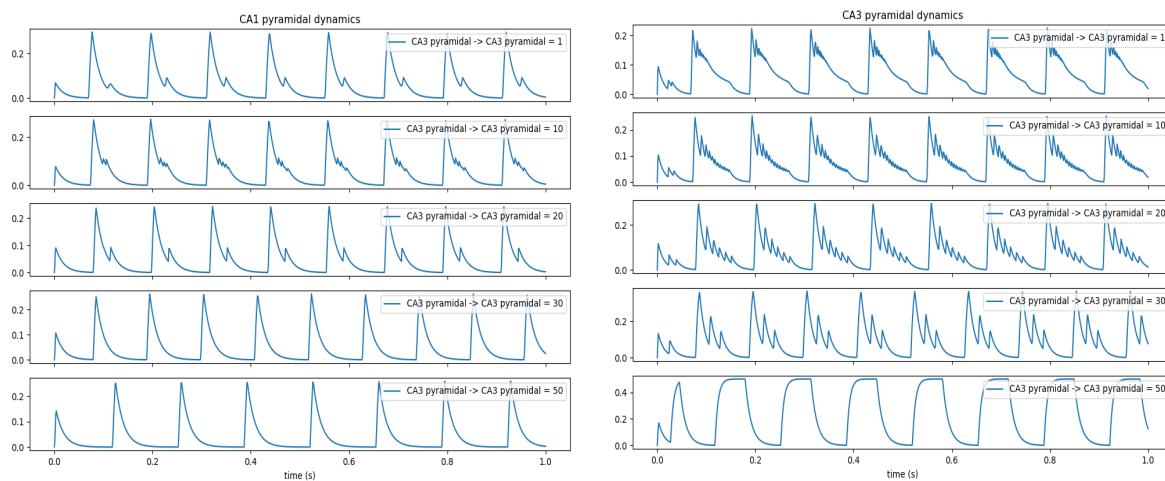
Figure 36: Phase plots of (left) CA1 pyramidal and CA1 bistratified cells; (right) CA3 pyramidal and CA3 basket cells.

The activity mode plots, as shown in figures 31 and 32 captures the change from steady state to oscillatory state and back from oscillatory state to steady state. The intermediate states other than the 7-10Hz oscillatory state such as 7-10Hz oscillations coupled with 30-50Hz oscillations, >13Hz oscillations and fast oscillations are not bifurcations but a gradual change from one type of oscillatory mode to another. All of these oscillatory states happen in

between the two Hopf bifurcation points where an unstable limit cycle is present. To capture all of these activity states shown in figures 31 and 32, we used our custom tool with only a few points for connection weights from bistratified cells to pyramidal cells and a few points for external inputs in both CA1 and CA3 regions. The analysis methods using our custom tools and techniques are as explained in the analysis section in section 4.2.4. It is observed that the range of values for which theta-coupled gamma oscillations is observed is small as compared to the range of values for which the system converges to a steady state or oscillates in other frequencies.

4.3.6 EFFECTS OF CA3 RECURRENT CONNECTIONS ON CA1-CA3 NEURONAL NETWORK

CA3 pyramidal cells synapse onto other pyramidal cells in CA3 region, inhibitory interneurons in CA3 and CA1 region, and also the pyramidal cells in CA1 region. As the connection strength of the recurrent collaterals increases, gamma oscillatory activity decreases in both CA1 and CA3 pyramidal and basket cells. However, if there is no sufficient excitation of basket cells, there is no gamma oscillatory activity even if the excitation of recurrent collaterals in CA3 is high as shown in figure 37. The behaviour of pyramidal, basket and bistratified cells is governed by the recurrent pyramidal excitation from pyramidal cells and the inhibitory input from basket and bistratified cells to pyramidal cells.



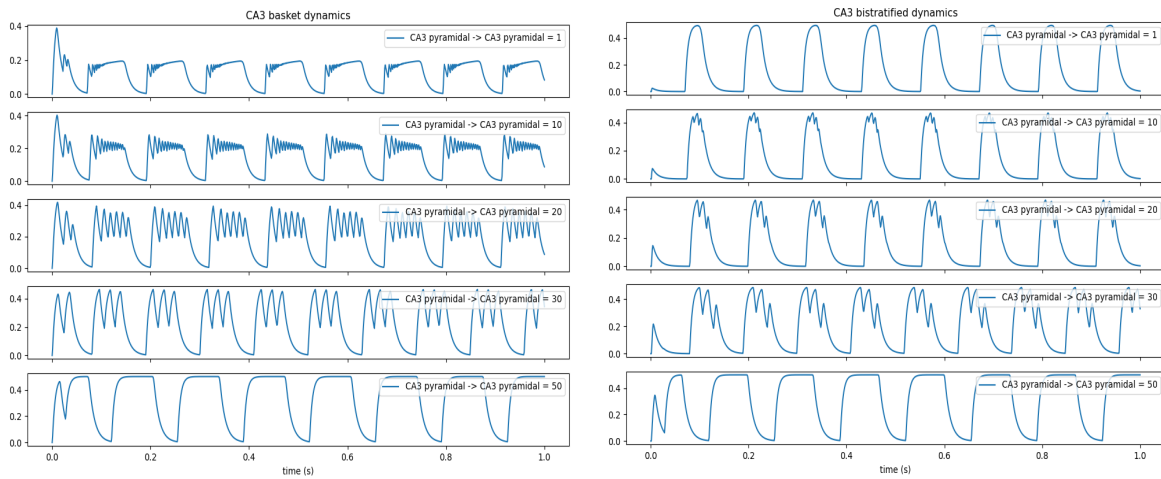


Figure 37: Effects of CA3 recurrent excitation on the activity of CA1 pyramidal cells (top-left), CA3 pyramidal cells (top-right), CA3 basket cells (bottom-left) and CA3 bistratified cells (bottom-right). As the connection strength value increases from 1 to 50, the activity also changes from theta or theta-coupled gamma oscillations to just theta oscillations. As excitation increases, the effects of inhibition lowers, reducing slow gamma oscillations.

4.3.7 EFFECTS OF CA1 BACK-PROJECTION CELLS ON CA1-CA3 NEURONAL CIRCUIT

The CA1 back-projection cells are recently discovered, with limited knowledge about their connections to CA3 and their functionality. From the simulation of these back-projection cells on CA3, an increase in the back-projection cell input to CA3 disrupts the oscillatory state. The back-projection cells synapse on CA3 interneurons driven by the CA1 pyramidal cells to propagate feedback back to CA3 [131]. The CA1 back-projection cells could also be projecting to other inhibitory interneurons in the stratum radiatum in CA3[131]. From this literature, we have projections from CA1 back-projection cells to CA3 pyramidal, basket, bistratified and other inhibitory interneurons in our simulation model.

In the individual CA1 model, when the weight of CA1 pyramidal to back-projection cells is low, amplitude of CA1 back-projection cells is low; but the back-projection cells still oscillate in-sync with pyramidal cells, which is expected as CA1 pyramidal cells are the sole excitatory input to CA1 back-projection cells in our model. However, as the weight increases, amplitude of CA1 back-projection cells increases. In the combined model, when the weight of CA1 pyramidal cells to CA1 back-projection cells is low, it disrupts theta and theta-coupled gamma oscillating frequency. As the excitation of back-projection cells from CA1 pyramidal cells increases to values greater than 10, 8Hz theta oscillations coupled with 52Hz gamma oscillations are seen in CA3 pyramidal & basket cells, and 64Hz gamma oscillations are seen

coupled with 8Hz theta oscillations in CA1 pyramidal & basket cells. This implies, changes to the strength of CA1 back-projection cells affects population of neurons in CA3 and in-turn affects population of neurons in CA1, as shown in figure 38.

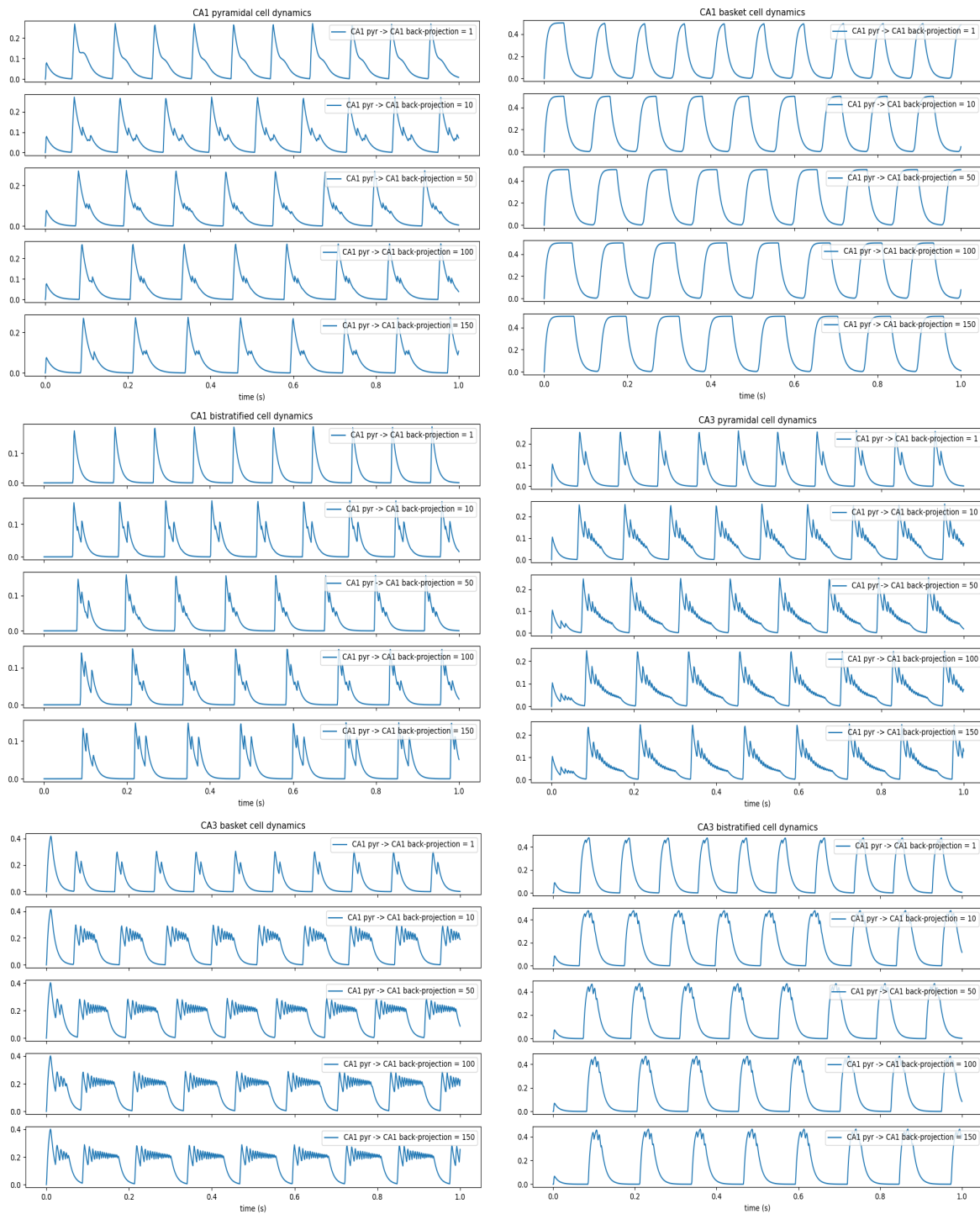


Figure 38: Effects of varying connection weight of CA1 pyramidal cells to CA1 back-projection cells on CA1 pyramidal cells (top-left), CA1 basket cells (top-right) and CA1 bistratified cells (middle-left), and CA3 pyramidal cells (middle-right), CA3 basket cells (bottom-left) and CA3 bistratified cells (bottom-right), where the connection weight is increased gradually from 1 to 150.

The effect of CA1 back-projection cells on CA3 is also analyzed here for the first time in the simulation of the combined model. To ascertain the synaptic targets in CA3 from the CA1 back-projection cells, various simulations were conducted. In the theta-coupled gamma oscillatory mode, when the CA1 back-projection cell synapses were applied to CA3 basket cells, increasing the connection strength to a value greater than 50, reduced the gamma oscillatory activity in CA3 as shown in figure 39.

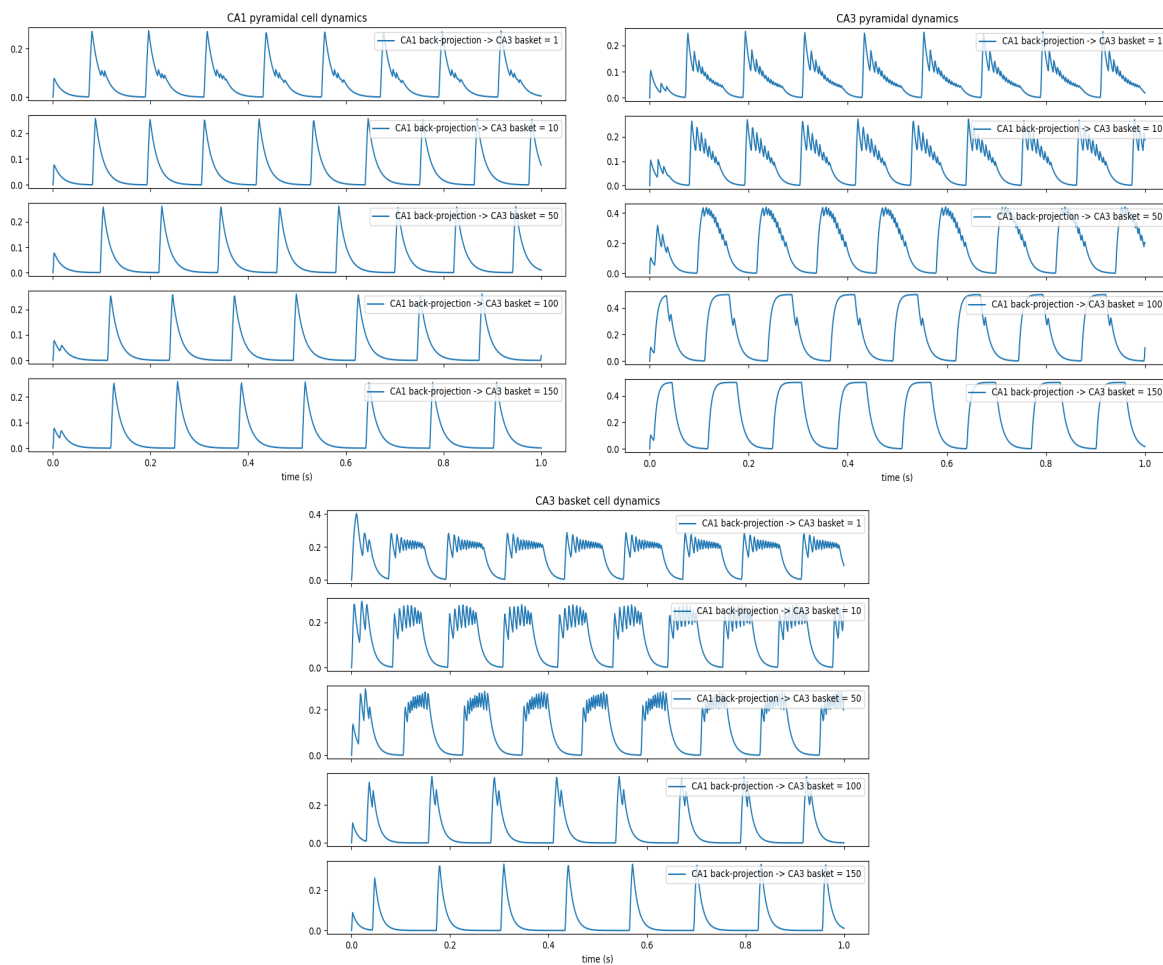


Figure 39: Effects of varying connection weight of CA1 back-projection cells to CA3 basket cells on CA1 pyramidal cells (left), CA3 pyramidal cells (middle) and CA3 basket cells (right).

When the CA1 back-projection cell synapses were applied to CA3 bistratified cells, theta-coupled gamma oscillatory activity remained unaltered, however, the activity of CA3 bistratified cells declined as the inhibitory projection strength increased as shown in figure 40.

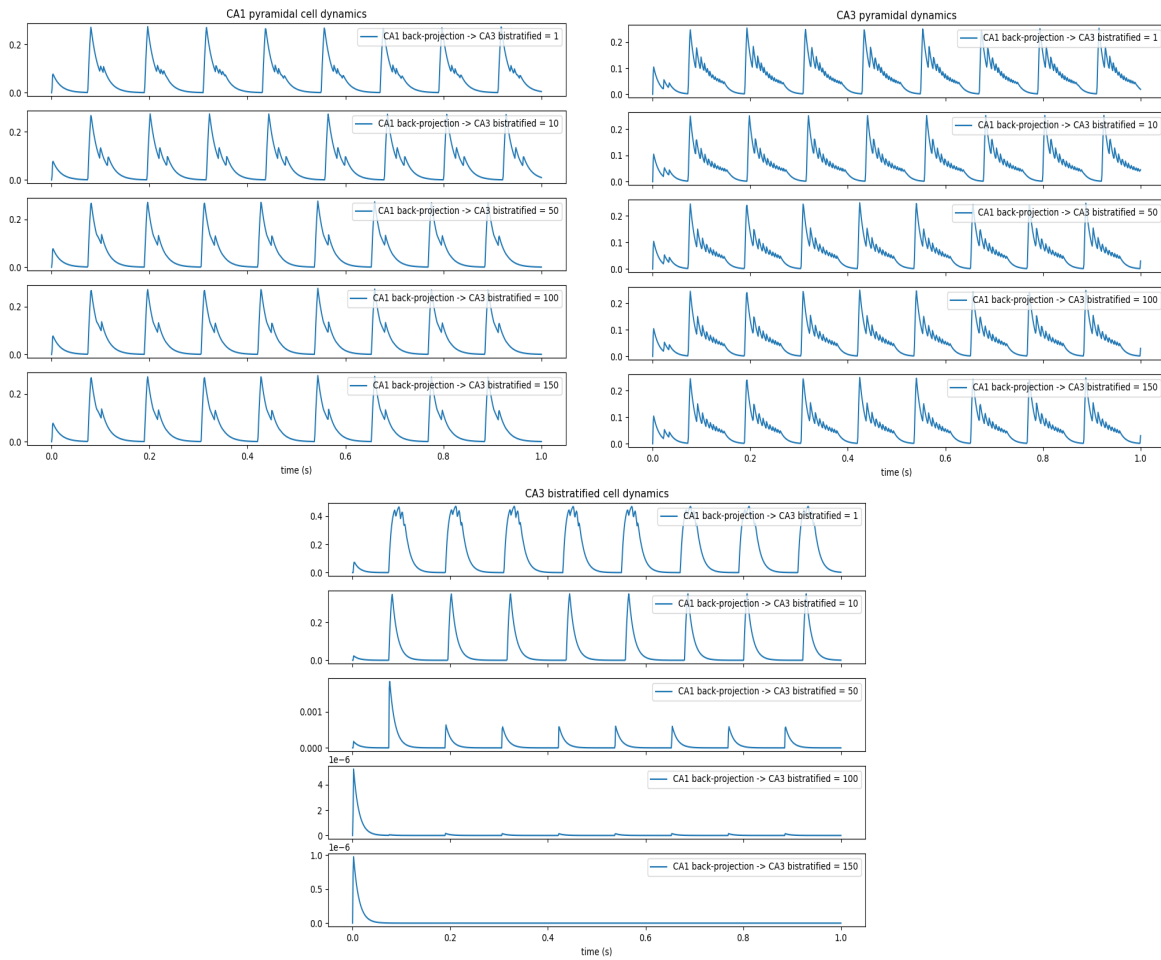


Figure 40: Effects of varying connection weight of CA1 back-projection cells to CA3 bistratified cells on CA1 pyramidal cells (left), CA3 pyramidal cells (middle) and CA3 bistratified cells (right).

When the CA1 back-projection cell synapses were applied to CA3 pyramidal cells, theta-coupled slow-gamma oscillations got reduced to 10-12Hz theta oscillations as shown in figure 41.

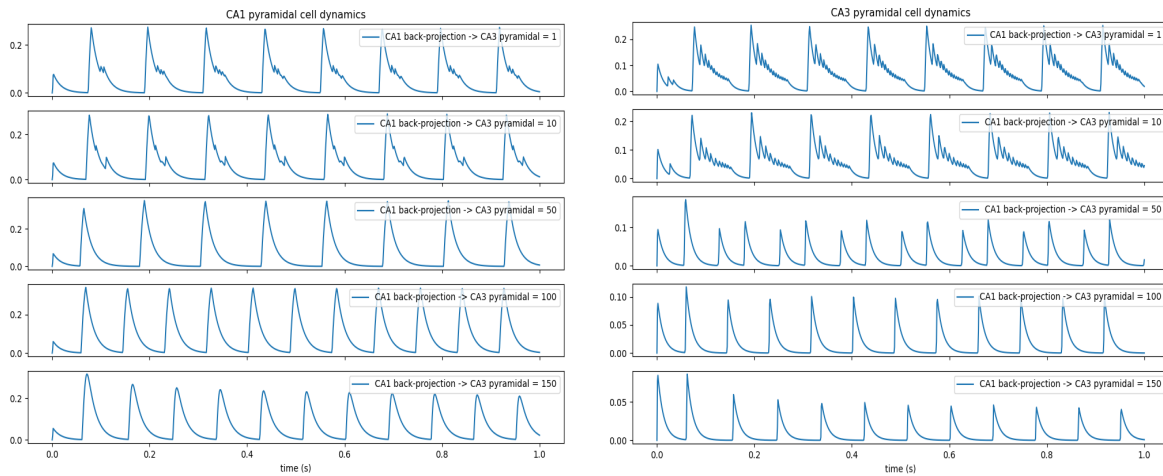
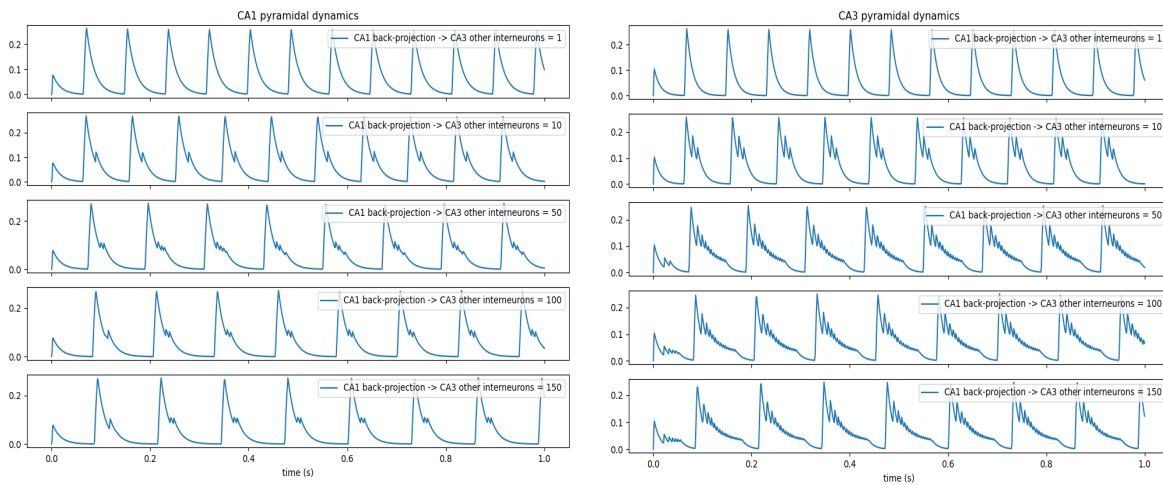


Figure 41: Effects of varying connection weight of CA1 back-projection cells to CA3 pyramidal cells on CA1 pyramidal cells (left) and CA3 pyramidal cells (right).

Lastly, when the CA1 back-projection input was applied to other inhibitory interneurons in CA3, for values less than 10, there were 12Hz oscillations, for values greater than 10, we started to observe smaller peaks of slow gamma oscillations in CA3 pyramidal cells which were sustained for high values of the projection strength as shown in figure 42.



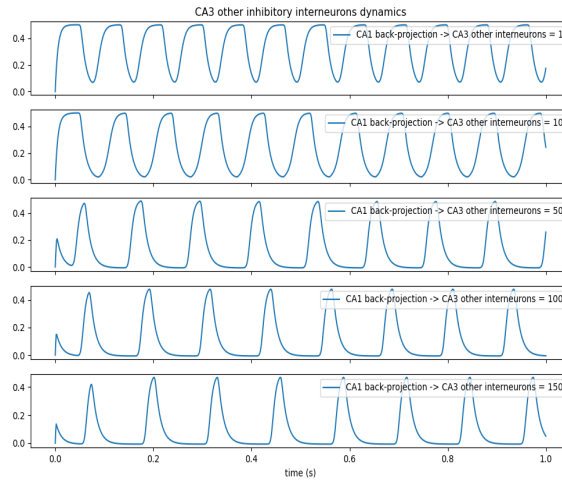


Figure 42: Effects of varying connection weight of CA1 back-projection cells to CA3 other inhibitory interneurons cells on CA1 pyramidal cells (left), CA3 pyramidal cells (middle) and CA3 other inhibitory interneurons (right).

4.3.8 CA1-CA3 PHASE DIFFERENCES

Let's consider the individual CA1 model again, with theta-oscillating sine-wave inputs from CA3 and EC layer III rather than having constant inputs. It is observed by Mizuseki et al [145] that the phase of CA1 pyramidal cells do not synchronize with the phases of either CA3 or EC although the CA1 pyramidal cells receive their inputs from CA3 and EC. The phase of EC layer III is observed to be between -30° and -60° , and the phase of CA3 is observed to be between 60° and 90° . With these phase inputs, the observed phase of CA1 pyramidal cells is 180° . The axonal conduction delays from EC or CA3 to CA1 pyramidal cells alone are not enough to explain the phase-shift or temporal delay observed in CA1 pyramidal cells.

To accommodate these phase differences as seen in literature for EC-CA3-CA1 entorhinal-hippocampal loop [145], instead of having constant inputs from EC and CA3, we generate a sinusoidal input that matches the theta frequency in CA1 pyramidal cells generated by the septal pacemaker circuit, which is 9Hz in our simulations. We simulated the sinusoidal inputs for a specific time duration in the middle of the simulation and have constant EC and CA3 inputs before and after this time duration. The phases of theta oscillation in both CA1 and CA3 is approximately 90° out-of-phase, and EC is out-of-phase with CA1 pyramidal cells [145]. CA3 phase is set to 0° and EC phase is set to 90° . Amplitude of CA3 is 3 and EC is set to 1. Phase of -90° for EC makes the phases of EC, CA3 and CA1 out-of-sync as seen in figure 43. The observed phase of CA1 pyramidal cells from this simulation is about 108° .

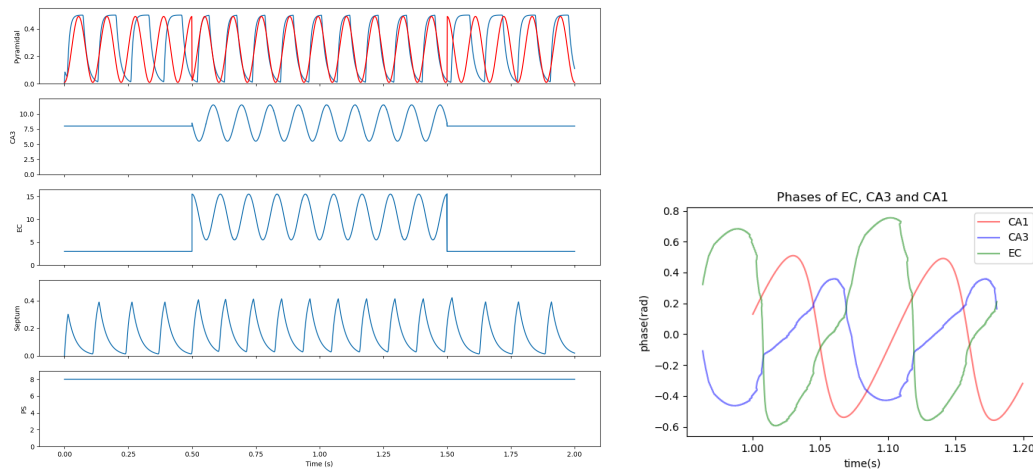


Figure 43: Simulation of CA1 pyramidal cells with CA3 and EC sinusoidal input with CA3 phase = 0° , EC phase = 90° . The sinusoidal waves are generated with a 9Hz frequency. The red line on the CA1 pyramidal activity is a fit to determine the phase of CA1 activity.

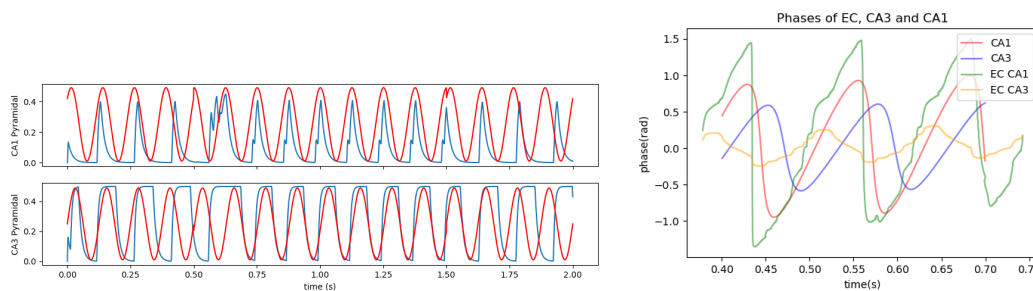


Figure 44: Simulation of CA1 and CA3 pyramidal cells using the integrated CA1-CA3 circuit with EC sinusoidal input with EC layer II input to CA3 having phase = 150° , and EC layer III input to CA1 having phase = 90° . The sinusoidal waves are generated with a 8Hz frequency. The red line on the CA1 pyramidal activity is a fit to determine the phase of CA1 activity.

In both the individual CA1 and integrated CA1-CA3 simulations here, the external input to the septum is kept constant. The phase differences with respect to CA1, CA3 and EC are observed in the integrated model as shown in figure 44. CA1 receives the activity of CA3 as input instead of a constant or a generated sinusoid. EC is a constant input before 0.5 seconds and after 1.5 seconds, and during the middle of the simulation, EC is a sinusoidal input. Different EC sinusoidal inputs with different phases as mentioned in the Misuzeki et al observations [145] are given to CA1 and CA3. The observed phase of CA1 pyramidal cells from this simulation is about 90° , and for CA3 pyramidal cells is about -11.45° . In the individual model, CA3 phase can be controlled by the model as opposed to the integrated model, which results in different phases for CA3 and CA1. We have confirmed that (i) it is possible to obtain phase differences between CA1, CA3 and EC layer II and III; and, (ii)

we can confirm that the phase observed in CA1 pyramidal cells do not result from simple integration of phases of its afferent inputs from CA3 or EC or the medial septum, although we haven't been able to replicate the exact phases observed by Mizuseki et. al through our simulations.

4.4 DISCUSSION

4.4.1 COMPARISON OF CA1 AND CA3 MODELS

Structurally, there are certain major differences between CA1 and CA3 microcircuitry presented in this chapter. The extensive recurrent excitation amongst pyramidal cells is present in CA3 which is sparsely found in CA1; bistratified cells in CA3 do not receive inhibitory input from basket cells; bistratified cells do not receive septal input in CA3. CA1 basket cells receive EC, CA3 and septal input, bistratified cells receives CA3 input. In CA3, basket cells receives DG and septal input, bistratified cells receive no external input except from the hypothesized CA1 back-projection. We observe feed-forward excitation from CA3 to CA1 in Schaffer collaterals and feedback inhibition from CA1 to CA3 through CA1 back-projection cells. CA1 receives external input EC, CA3 and ms-dBB; whereas CA3 receives external input from CA1, EC, DG and ms-dBB. The output from hippocampus is propagated to EC from CA1.

CA3 neurons form conceptual auto-associative memory structures due to the extensive recurrent collaterals network, whereas CA1 neurons form contextual hetero-associative memory structures due to the sparse recurrent collaterals network.

CA1 and CA3 receive septal input from ms-dBB which propagates theta frequency oscillations to the hippocampal structures. CA1 receives slow-gamma oscillations from CA3, whereas CA3 generates slow-gamma oscillations to which the input is propagated from DG. It is also observed that CA1 sustains theta oscillations when the CA1 septal-loop is broken due to the inputs from CA3, which is explained later.

Increasing basket cell excitation from pyramidal cells in both CA1 and CA3 results in theta-coupled gamma oscillations; however, when pyramidal cells are inhibited by bistratified cells in both CA1 and CA3, theta-coupled gamma oscillations are observed. When gamma oscillations couple with theta oscillations, peak amplitude of bistratified cells is observed to reduce to 0.15 while the peak amplitude of basket cells remain stable at 0.45 in CA1, whereas in CA3, the amplitude of basket cells is 0.2 and bistratified cells is 0.4.

Amplitude in this population model refers to the fraction of active neurons at each time step.

Table 13: Comparison of amplitudes (fraction of active neurons in each population) of theta-coupled gamma oscillations between individual models of CA1 & CA3, and the integrated model

Cell type	Individual model	Integrated model
CA1 pyramidal cells	0.3	0.2
CA1 basket cells	0.5	0.45
CA1 bistratified cells	0.3	0.15
CA3 pyramidal cells	0.3	0.2
CA3 basket cells	0.2	0.2
CA3 bistratified cells	0.4	0.4

Amplitude of theta oscillations is bigger than the amplitude of theta-coupled gamma oscillations due to inhibition, which can be overcome by increasing the excitatory input from CA3 pyramidal cells to CA1 pyramidal cells as shown in table 13 in the later section 4.4.

In terms of the various neuronal networks activity, pyramidal-bistratified cells are in-sync in CA1 while pyramidal and bistratified cells are out-of-sync with basket cells in CA1. In CA3, pyramidal-basket-bistratified cells are in-sync with each other. Pyramidal and bistratified cells are in-sync with septal activity in both CA1 and CA3 regions. CA3 basket cells are also in-sync with septal activity.

Frequency of slow-gamma oscillations is noticed to be higher in CA3 than in CA1. Increasing recurrent excitation in CA3 reduces slow-gamma frequency oscillations in CA3 and CA1. Increasing CA3 excitation to CA1 pyramidal cells maintains slow-gamma oscillations in CA1, but increasing CA3 excitation to CA1 basket and bistratified cells reduces theta-coupled gamma oscillations to theta frequency oscillations. However, this is not observed in the individual CA1 model. In the individual model, when CA3 constant input is increased to CA1 pyramidal cells, steady state activity is reached. When CA3 constant input is increased to CA1 basket and bistratified cells, theta coupled gamma oscillations reduces to theta oscillations.

4.4.2 COMPARISON WITH EXPERIMENTS

The simulation results are in accordance with several facts noted in literature. Experimentally in [60], the bursting activity of CA3 pyramidal cells is longer than CA1 pyramidal cells. Our simulations agree with the experimental observations wherein CA3 pyramidal cell oscillatory activity is longer than CA1 pyramidal cells having higher frequency of slow-gamma

oscillations than CA1 pyramidal cells. PV-containing basket cells fire preferentially in the descending phase of theta cycle and are found to produce more oscillations [141, 146]. Basket cells discharge when pyramidal and bistratified cells are inactive in the theta oscillatory mode; when theta-coupled gamma oscillations are noticed, both pyramidal and bistratified cells fire in the descending phase of theta in our CA1 simulations. The phases of CA1 pyramidal, basket and bistratified cells are in sync with the experimental results as found in [145, 24].

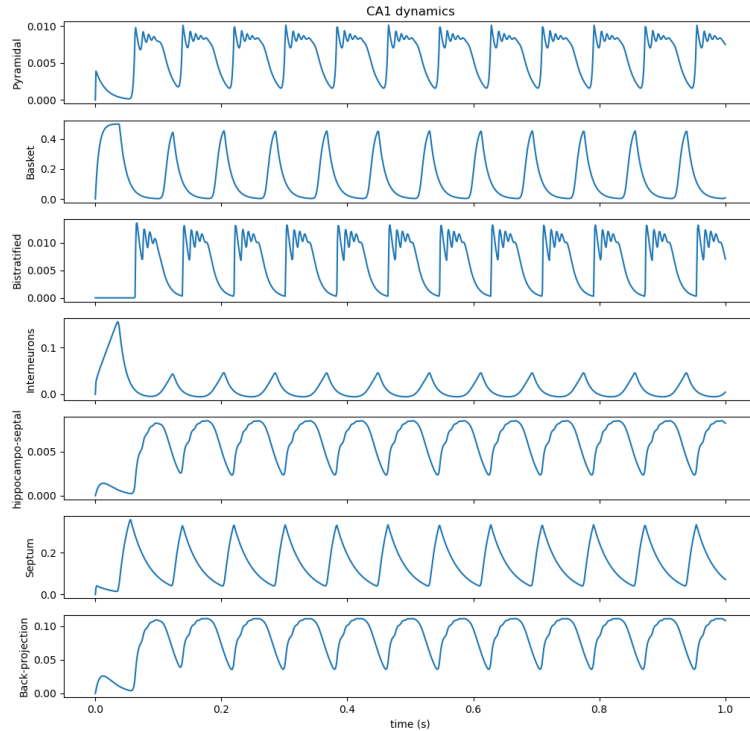


Figure 45: Theta-coupled gamma oscillations in CA1 in the absence of CA3 input.

Klausberger [147] presents arguments that CA1 and CA3 pyramidal cells introduce gamma oscillatory activity in CA1 bistratified cells. In our simulations, we have noticed that, apart from the pyramidal cell excitation, inhibition from basket cells and septum also plays a role in inducing slow-gamma oscillations in bistratified cells.

Goutagny et. al in [143] observed that CA1 theta oscillations are independent of external inputs and it is also noticed to generate theta oscillations from multiple independent theta oscillators in the hippocampus. Accordingly, CA1 theta is independent of septal input and this is true as, when there is no septal and CA3 input to CA1, we still observe 4-10Hz frequency oscillations generated due to the presence of intrinsic oscillators. We can notice this in CA3 as well, as shown in figure 33 in the previous section. In contrast, the simulations

show that for pyramidal cells to oscillate, minimal inhibition is necessary since when there is no inhibition, oscillatory activity from pyramidal cells is absent. The differences between intrinsic hippocampal theta oscillations both in CA1 and CA3, and septally-propagated theta oscillations to the hippocampal CA1 and CA3 still remains an unexplored area, and is not the focus of this research.

In CA3, the average peak amplitude of pyramidal cells is noticed to be broader than other inhibitory interneurons and also, pyramidal cells lead the firing activity before basket cells or bistratified cells fire [148]. Experimentally, it is found that CA3 region generates gamma oscillations independent of other hippocampal regions and that this gamma activity regulates the temporal coordination between CA3 and CA1. This gamma oscillatory activity in CA3 is generated due to the pyramidal and basket cell communication [52] which is propagated to CA1. From the individual model of CA3 and the integrated model, we can see that temporally the activity of CA3 pyramidal cells lead the firing of cells in CA1 and CA3 regions. According to our simulation, if the septo-hippocampal loop is disrupted, then the theta-coupled gamma oscillations do not exist.

When there is no CA3 input to CA1, CA1 is still able to maintain theta and theta-coupled gamma oscillations though the rhythmic pattern changes considerably requiring to increase excitation of CA1 bistratified cells. This is also observed by Theodore et. al [149] and Roman et. al [150] as shown in figure 45.

4.5 CONCLUSION

So far we have developed and analyzed the CA1 and CA3 individual and integrated models, studied the feed-forward and feedback pathways from CA1 to CA3 and vice-versa and their effects on the different cell-types present in these regions. The phase differences of basket and bistratified cells in CA1 and CA3 are clearly shown in our simulation results. We have also studied the cross-frequency coupling of theta-coupled gamma oscillations in both CA1 and CA3 regions, the effects of Schaffer collaterals from CA3 to CA1, and the inhibitory feedback from CA1 to CA3 on theta-coupled gamma oscillations exhibited by CA1 and CA3 pyramidal, basket and bistratified cells, the results of which are validated with the relevant biological references. The effects of external inputs, the parameter space and their bifurcation analysis is also presented here. We have also presented our hypotheses about the possible projections from CA1 back-projection cells to CA3 inhibitory interneurons. Lastly, we have also studied the phases of pyramidal cells in CA1 and CA3 regions, apart from the

phase differences between the excitatory and inhibitory cell-types present in both CA1 and CA3 regions.

The cross-frequency coupling of theta and slow-gamma oscillations in hippocampal CA1 and CA3 regions are studied using the continuous population model. With these results as the baseline, we now move on to the discrete rule-based cellular automata approach to focus on encoding and retrieval of patterns in a cross-frequency coupled oscillatory network of hippocampal CA1 region.

5 CELLULAR AUTOMATA MODEL

As described in the previous sections, the cellular automata approach is a discrete modeling technique that simplifies complex biological processes into simple rules that can be evaluated easily and quickly. Using the discrete modeling technique allows us to analyze the oscillatory behaviour of the model and study encoding and retrieval of patterns. In the cellular automata approach, the logical operation of neurons and their network is simplified as much as possible to derive a “state machine” that mimics the operation of the brain regions.

The main objective of the cellular automata approach here is to reproduce the results from the continuous model for CA1 having theta and theta-coupled gamma oscillations, and then proceed to study encoding and retrieval of patterns in CA1. The model built for CA1 using cellular automata approach follows the microcircuit given in chapter 4.

The cellular automata model implemented here is derived from Pytte et. al model of CA3 [119] and Claverol et. al model of the piriform cortex [3]. We took inspiration from both the models to develop our model which is used here to simulate the CA1 and CA3 regions of the hippocampus to study encoding and retrieval of patterns. The implemented model is message-based and has information about neurons that need to be activated at each time step. Based on this, the neuron’s refractory period, the time step at which the neuron should be returned to its resting state, when the synapses should be fired based on the synaptic delay, how long should the synapses be active based on the synaptic duration are computed. As inputs, the connection weight and the number of projections between populations has to be specified. The properties to be described for a population include the number of neurons in a population, type of neurons in the populations i.e., excitatory or inhibitory, whether it is an external pseudo neuron population, and the learning rate. The architecture and the model design is explained in detail in the next sections.

5.1 ARCHITECTURE OF THE CELLULAR AUTOMATA MODEL

For our use-case of developing the model for neuronal networks, we have kept the design as simple as possible, with both deterministic and non-deterministic stages of simulation. The model has pre-defined inputs that gets processed according to the projection matrix which is essentially a weight matrix, and gives the result as the number of neurons active at any point in time of the simulation. Consequently, the design of such a model involves the interaction between neurons of the same homogeneous population or amongst different heterogeneous

populations which follows non-linear firing dynamics.

The events occurring in this model are at a neuronal level namely, a neuron firing in response to its integrated sum of inputs exceeding the threshold value, a neuron going into refractory period, and a neuron going to an off state. The model begins with stochasticity as the projection matrix of the whole neuronal network is chosen randomly at the beginning of the simulation. However, the model becomes deterministic after this stage as the projection matrix does not change until learning using STDP is introduced. So the plasticity involved in the model purely depends on if the neuron receives enough inputs through its dendrites to exceed the threshold set for the population and generate an action potential.

5.1.1 ELEMENTS IN A CELLULAR AUTOMATA MODEL

The premise of the design of the cellular automata model is as follows. There are multiple neuronal populations; each population has many neurons. The different populations interact with each other depending on the existence of a proven projection, derived from literature.

The different types of neurons can be classified as either excitatory or inhibitory. Excitatory neurons project positive weights, while inhibitory neurons project negative weights. All neurons are at their resting stable state in the beginning, t_0 . When sufficient input is given, i.e., if the input exceeds the threshold, then the neuron fires. An action potential in a cellular automata model implies a spike, and it lasts for a millisecond, which means the neuron fires at t_0 lasting for $t_0 + t_{ap}$ milliseconds. After firing, the neuron is in the refractory period, t_{ref} during which time the neuron cannot fire. The neuron reaches its resting state after the refractory period, which is $t_0 + t_{ap} + t_{ref}$. Biologically, the whole sequence of a neuron firing, entering the refractory period is referred to as an action potential. In a cellular automata model, however, we need to specify the time durations for each of these processes separately. The refractory period differs for every neuron type and is also a characteristic feature defining a neuron.

Many post-synapses form inputs to a neuron. Synapses are activated if the pre-synaptic neuron fires an action potential. The neurons that these synapses project onto get the input after a synaptic delay t_{del} , and the synapse is active for t_{dur} . The afferent neuron gets excited if the integrated sum of inputs exceeds the threshold.

The model has biological parameters such as refractory period τ_{ref} , projection weights k , number of projections from neuronal population A to neuronal population B which is denoted as z , number of neurons in a population N , learning rate, if the neuron is excitatory, inhibitory

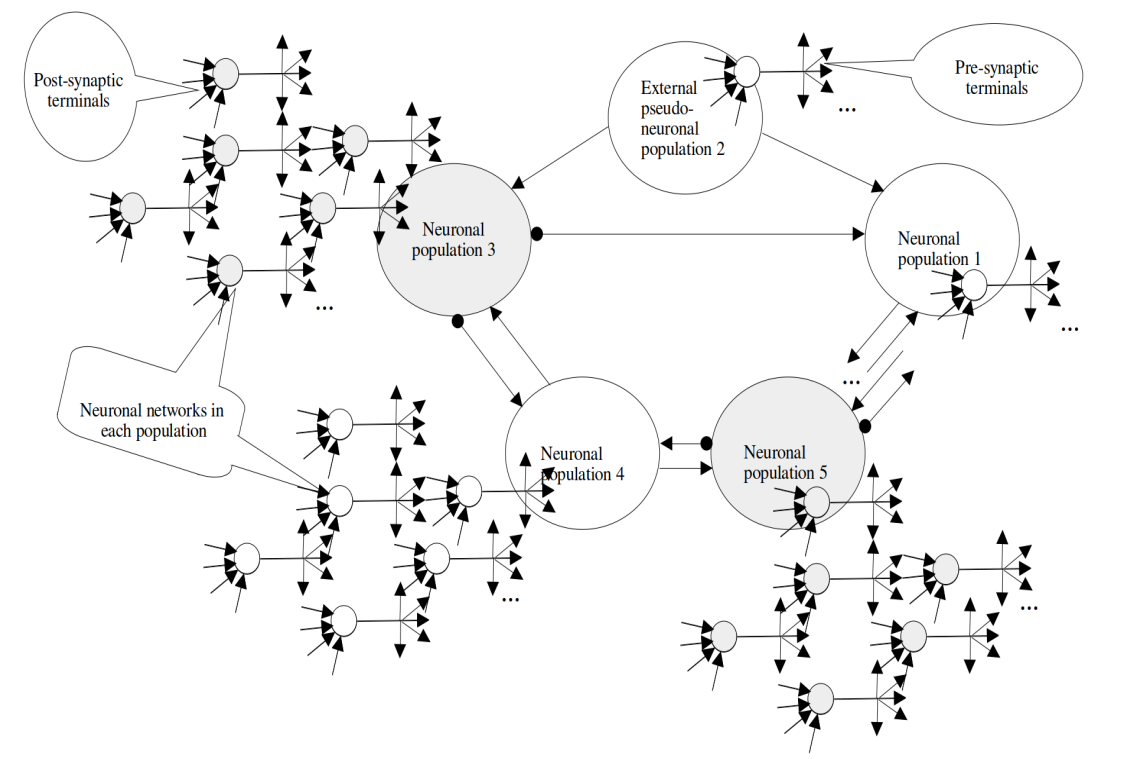


Figure 46: Neuronal network in a cellular automata model, with many excitatory and inhibitory populations (denoted by grey circles and arrows starting with dots), and external pseudo-neuron populations, each having many neurons. Each neuron has a pre-synaptic terminal to propagate signals to other neurons, and post-synaptic terminals to receive signals from other neurons.

or an external pseudo-neuron, the threshold for the neurons in a population, the synaptic delay t_{del} and synaptic duration t_{dur} . The explanation for the working of a neuron in a cellular automata model is as depicted in figures 46 and 47. The threshold of a neuron is the same as the threshold of the population since the populations in the model are all homogeneous.

We have implemented a class of neurons called pseudo-neurons which are external inputs to the populations. The external pseudo-neuron populations are always active, without a refractory period or a synaptic delay. These neurons do not learn but stimulate the actual population to fire and strengthen projections. These neurons can be either excitatory or inhibitory, which means their projection weights are either positive or negative.

5.1.2 STAGES IN A CELLULAR AUTOMATA MODEL

In our cellular automata model, there are two stages, or blocks, where the neuron activation processes take place. Firstly, at each time step, the synaptic block deactivates any

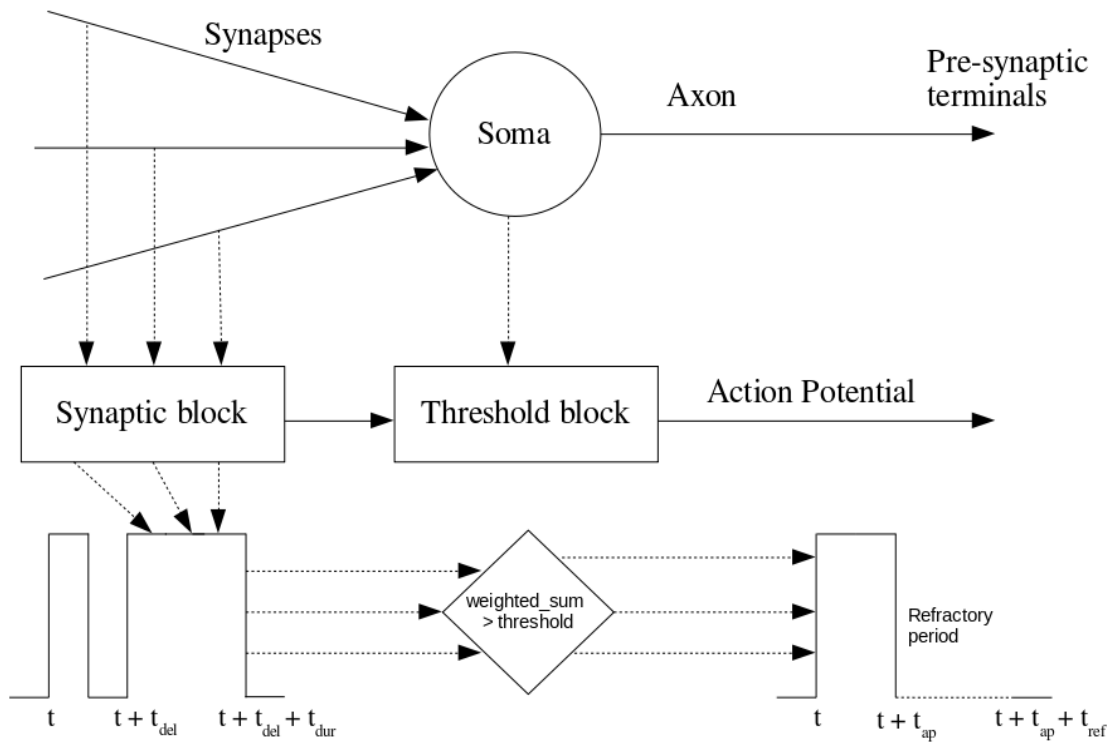


Figure 47: Working of a cellular automata model derived from the work of Claverol et. al [3]. The different stages or blocks of processing messages from neurons align with the working of a biological neuron.

synapses that are not to be active at that time step; sends in a message to the threshold block to activate the input neuron at the current time step; activates synapses that ought to be active after the synaptic delay at that time step.

The second is the threshold block which computes the integrated sum of inputs to fire a neuron, and sets the synapses that ought to be active or not, and sets the refractory period for the neuron to be deactivated after the refractory period. These are as depicted in figure 47.

Projections between populations are weighted. The number of projections between populations is chosen stochastically during the beginning of the simulation. Recurrent neuronal projections are also possible. Random number of external pseudo-neurons are activated at each time step. These random external pseudo-neurons project onto an actual excitatory or inhibitory population. Random neurons from a population are chosen to project onto random neurons chosen from another population that share a known pathway. This is the initial step to build the neuronal network between different populations. The next step would be to choose a random number of external pseudo-neurons to fire at each time step which would

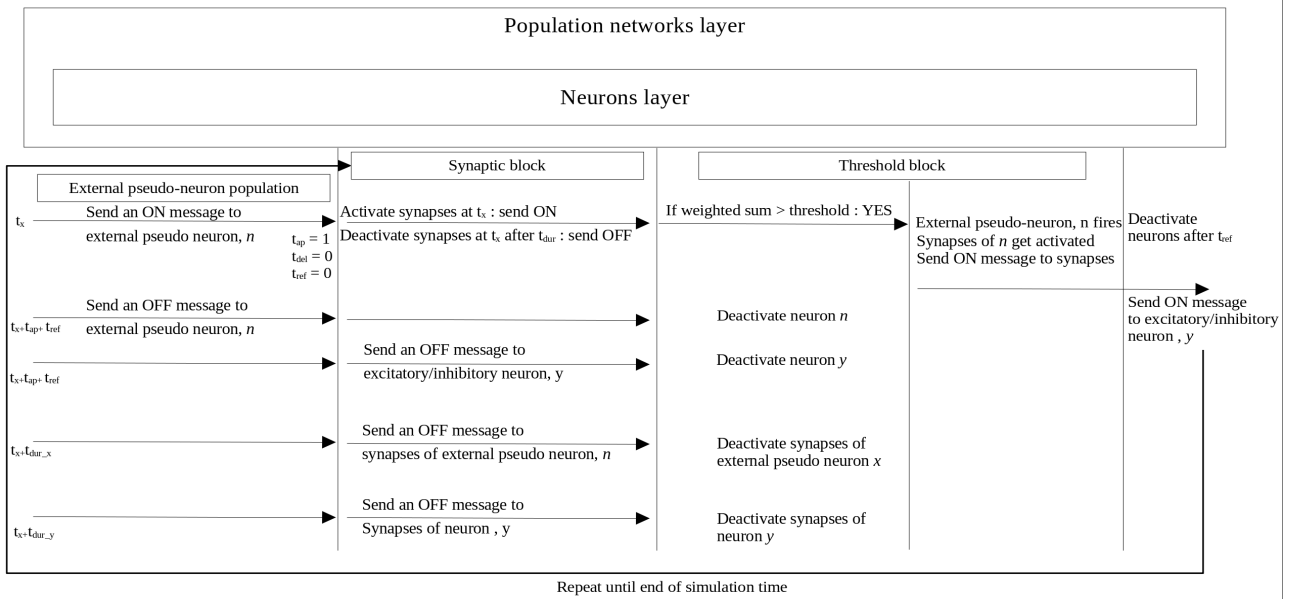


Figure 48: Architecture of the cellular automata model

activate the actual population.

When the inputs from the external pseudo-neuron population arrives at a neuron in an excitatory or inhibitory population, the neuron fires if the integrated sum of inputs is greater than the threshold of the population; otherwise it does not. The fired action potential is for a single millisecond duration, after which the neuron enters its refractory period. The synapses of the fired neuron are activated after the synaptic delay. When these synapses fire, the respective receiving post-synaptic neurons get activated. The activation depends on whether the integrated sum of inputs is greater than the threshold of that population. The cycle continues.

With this architecture, as depicted in the sequence diagram in figure 48, we have obtained the theta-coupled gamma oscillatory activity derived from the septal pacemaker circuit that was previously simulated using the continuous population model as explained in chapter 4. The results of these simulations are given in the next section. With these initial results simulated, we then proceed to store and recall patterns.

5.1.3 INPUTS AND OUTPUTS OF THE MODEL

Inputs to the model are given through JSON files. Each JSON file can either be a neuronal population or a projection between two neuronal populations as shown in table 14. There is currently no restriction on the number of cell-types that can be added to the model, and the number of projections. Since the properties of a neuron are the same as its population, they

are stored as population properties. Each neuron is a row in the weight matrix that represents the synapses a neuron has with other populations in the network. The time durations specified should be less than the simulation time as given in the *time.json* file. The step size in the time file is the difference between consecutive time steps, which in this case is 1ms. The bin size is to plot the activity of neurons in the number of bins specified after the simulation ends. Parameters related to time such as simulation duration, action potential duration, refractory period, synaptic duration, synaptic delay etc., are all in milliseconds.

If *enable_learning* is disabled, then the rest of the values need not be filled and can just be set to zero.

The *networks.dat* file has the names of all the projection files, which indicate the neurons present in the neuronal network, and the population of neurons having connectivity between them. As said before, the projections can be bidirectional and hence, a single entry in the *networks.dat* file represents the two neuronal populations, and the projection file tells the model if there are any projections between the two populations along with the weight of the projections. If the projections between two populations are unidirectional, the *k* and *z* parameters for the non-existent projections will be zero in the projection file. As such, any values that do not apply for a particular model is indicated as zero in the concerned input file.

Other than these parameters, we have introduced a few more boolean parameters to distinguish between populations as propagating either sensory input (*sensory_input*) during learning or cueing input (*cueing_input*) during recall, such as EC and CA3 respectively; and if the populations induce learning inhibition (*learning_inhibition*) by inhibiting other populations to enable learning or if the inhibition from populations aid in recall (*recall_inhibition*), such as basket and bistratified cells respectively.

Unlike the continuous neuronal models where the simulations, the membrane potential variables represent membrane potentials in millivolts (mV), in a discrete model such as the cellular automata model, the parameters simulated represent the fraction of neurons that are active, refractory or inactive at any given time step. The number of neurons active, refractory or inactive is represented in the simulation plots as activity dynamics of the whole population which does not have any unit. Which implies the only parameters having any units in a discrete model such as the cellular automata model are parameters representing time durations. Therefore, a spike in a cellular automata model is an actual spike when the neuron fires an action potential unlike a linear integrate-and-fire neuron because a neuron in a cellular automata model fires an action potential when the integrated sum of weighted inputs exceeds

<pre> <u>ex.json</u> { "ex": 101.0, "type" : 0.0, "N" : 100.0, "k" : 0.0, "threshold" : 15.0, "z" : 0.0, "ap" : 1, "ref" : 16.0, "del" : 15.0, "dur" : 5.0, "enable_learning": 1.0, "learning_rate": 5.0, "unlearning_rate": 10.0, "p_rand_neurons": 20.0, "no_of_patterns": 5, "intersecting_patterns": 1.0 } </pre>	<pre> <u>ex_bas.json</u> { "ex_bas": 214.0, "ksd" : 5.0, "zsd" : 1.0, "kds" : -5.0, "zds" : 5.0 } <u>time.json</u> "time": 1000.0, "step": 1.0, "binsize": 20.0, <u>networks.dat</u> pyramidal ca3 interneurons ca3 septum ps pyramidal hippocamposeptal hippocamposeptal septum septum interneurons yramidal interneurons </pre>
--	--

Table 14: Example of a JSON input file for (left) an excitatory pyramidal neuron population and (right) projection file between excitatory pyramidal and inhibitory basket cell populations. *ex* is name of the neuron and *ex_bas* is the projection between excitatory and basket cell populations. These are also the filenames; *101.0*, *214.0* is any numerical identifier that uniquely identifies the population; *type* can be 0 for excitatory, 1 for inhibitory, 2 for external pseudo-neuron; *N* is the number of neurons; *k* is the weight of any self projections; *z* is the number of self projections; *threshold* is for the integrated sum of inputs to generate an action potential; *ap* is the time duration of a single action potential; *ref* is the refractory period; *del* is the synaptic delay; *dur* is the synaptic duration; *enable_learning* is to enable STDP, the values are 1 for enabling learning and 0 if not; *learning_rate* is the value added to the weights of the selected projections; *unlearning_rate* is the value subtracted from the weights of projections not selected in the pattern; *p_rand_neurons* is the number of neurons in each pattern; *no_of_patterns* is the number of patterns to be selected; *intersecting_patterns* is to select if the patterns are unique or not; *ksd* is the projection weight from source to destination, in this case from pyramidal to basket cells, and vice-versa is *kds*; *zsd* is the number of projections from source to destination, in this case from pyramidal to basket cells and vice-versa is *zds*. The *time.json* file represents the simulation time and is integral in the current implementation. The *networks.dat* file contains the names of the projection files which also represent the neuron types present in the simulation. More about learning rates is explained in section 5.4.

the threshold (which is, biologically, the exact moment when the change in membrane potential exceeds the threshold to fire an action potential in an neuron). Number of such active neurons at a given time step form the activity dynamics of the population.

This is not a new concept as the continuous population model that we have considered in the previous chapter also represents the fraction of neurons active at each time step. Such modeling concepts exist not only in discrete modeling techniques, but also in continuous modeling techniques.

5.2 THETA AND GAMMA OSCILLATIONS IN CA NETWORK MODELS

Once the architecture as described above was implemented, the next step was to design and simulate different models of different regions of the brain, according to the research question we are trying to answer. Here, we experimented with a simple E-I network, with one external pseudo-neuron population which is excitatory, and projections between the external pseudo-neuron population to excitatory population, and E-I projections. This was followed by the implementation of the septal pacemaker circuit to generate theta oscillations, and then theta-coupled gamma oscillations. We then attempted to reproduce the results from the continuous model in chapter 4 in the cellular automata model for the individual model of CA1.

Like in the continuous septal-pacemaker circuit seen in the previous chapter, the external inputs to CA1 are excitatory inputs from EC and CA3, and an inhibitory external pseudo neuron input to the septum coming from the posterior hypothalamus and supramammillary nucleus (SUM).

5.2.1 SIMULATION OF E-I MODEL

In the simple E-I model, there are three populations, excitatory (E), inhibitory (I) and external pseudo-neuron population (Ext), with 100 neurons each as shown in figure 49. The projections are between E-I, I-E, and Ext-E populations. The simulation results here show periodic oscillations as shown in figure 50.

All the populations have 100 neurons each, except the external pseudo-neuron population which projects to the excitatory population which has 10 neurons to maintain the ratio of neurons between the populations. The populations have variable projections between them and these projections are chosen randomly before the beginning of the simulation, although the number of such projections is input through the projection file of the two populations.

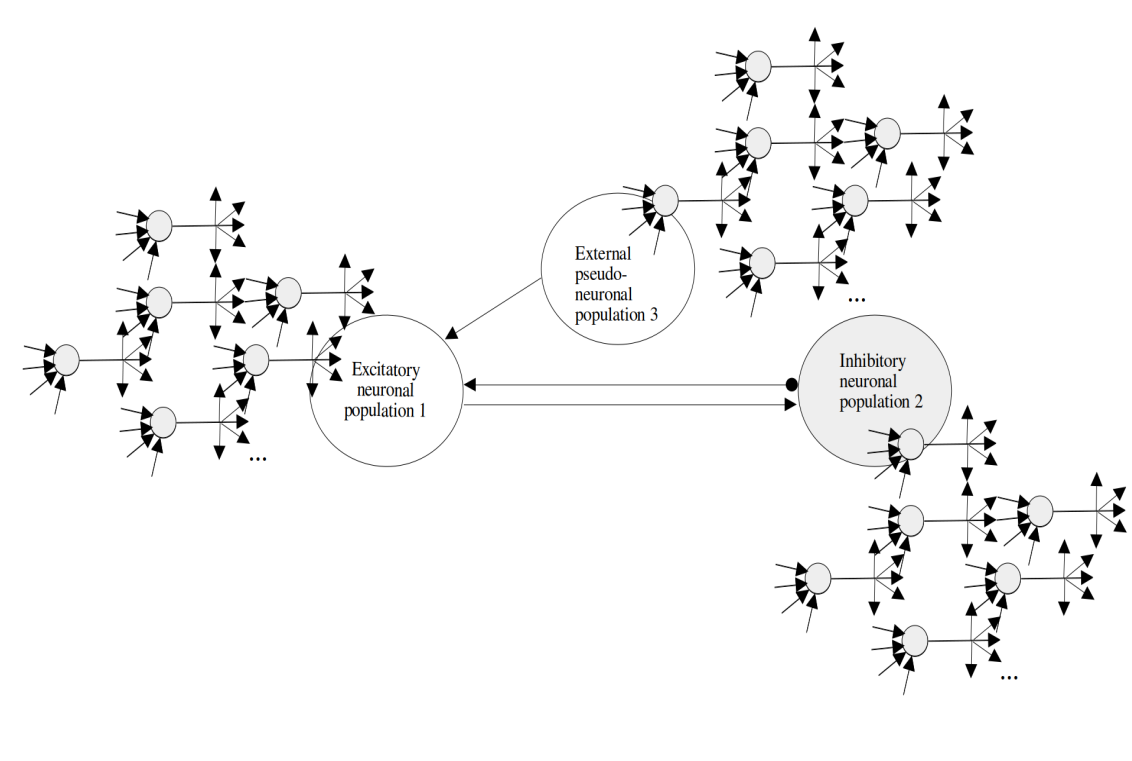


Figure 49: Neuronal network in a cellular automata model, with one excitatory and one inhibitory population (denoted by grey circles and arrows starting with dots), and one external pseudo-neuron population that projects to the excitatory population. The excitatory and inhibitory populations have projections to each other.

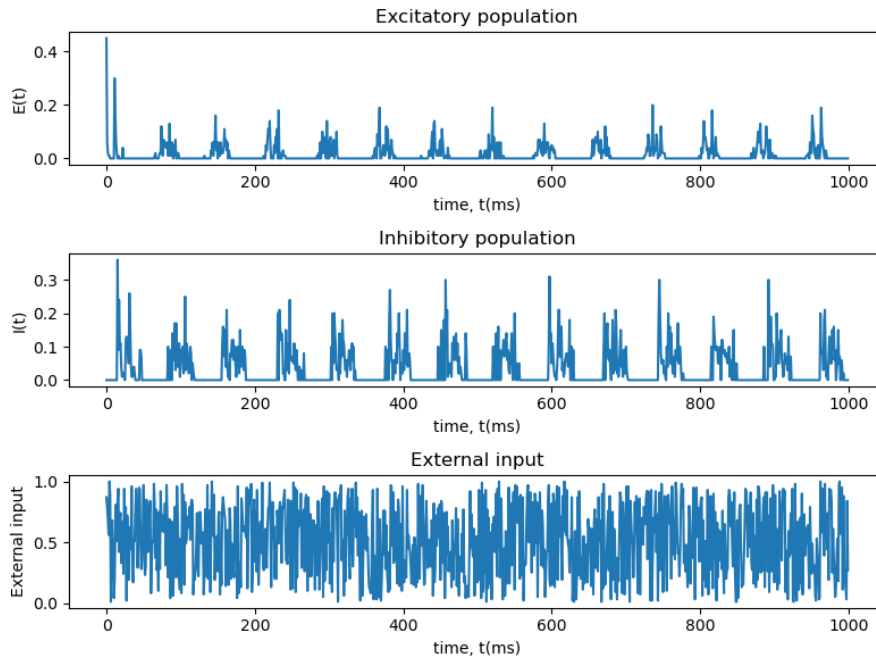


Figure 50: Cellular automata model simulation results for E-I network model

The simulation of E-I model started with just the excitatory and external pseudo-neuron population with each external pseudo-neuron having 10% projections to the excitatory neurons which did result in fast oscillations. Adding the inhibitory interneuron population to the neuronal network without inhibitory feedback to excitatory population resulted in both the excitatory and inhibitory populations in-sync with each other. With 5% inhibitory projections to excitatory population and vice-versa, and increasing inhibitory feedback to excitatory population, we noticed a phase-difference between the two populations.

The results of the E-I model exhibits 14Hz oscillations with a phase-difference between the E-I population activities. The frequency of oscillations are governed by the connection strengths and the number of projections between neuronal populations, along with the refractory period of the neurons. Understanding the influence of excitation and inhibition on populations also plays a role in deciding which parameters of which populations affects the frequency or phase of neuronal activities of a specific population. For example, in this case of E-I model, it is possible to introduce phase shifts between excitatory and inhibitory populations by varying the strength of inhibition; and needless to say, if an excitatory population projects onto an inhibitory population, and if this inhibitory population does not inhibit the excitatory population, then their activities should be synchronized; otherwise, if the inhibition is strong enough to overcome the excitatory connection strength, their activities should

be 180° out of phase; if not, the populations would exhibit a phase-shift in their activities. Here, the excitatory and inhibitory populations have a phase-difference since the inhibition is strong enough to suppress the activity of the excitatory neurons.

The simulation of an E-I model using the cellular automata approach produces results similar to the continuous model as the effects of increasing inhibition or increasing excitation are the same in both the models. The external inputs are constant in the continuous model or are regulated by a system of equations representing the activity of each neuronal population. In the cellular automata model, an external input is represented by an external pseudo-neuron population, a subset of which is active at every time step introducing noisy inputs in the model to achieve variations in activity timings between individual neurons. The product of the number of projections and the strength of each projection between the populations determines the strength of an incoming signal to generate an action potential.

5.2.2 SIMULATION OF CA1 INDIVIDUAL MODEL

Results from the simulation have oscillations of different frequencies superposed together that are fit with a sine wave to emphasize the phase-shifts between the different populations. The frequencies present in the results are plotted with an FFT to ascertain the presence of theta and slow gamma frequency oscillations. Also, from the Hilbert-transformed low-bandpass filtered signal, as shown in figure 53, we can derive and compare the phases of pyramidal, basket and bistratified cells, as shown in figure 52.

The CA1 individual model follows the design of the CA1 microcircuit presented in chapter 4. The simulation results are as shown in figure 51. As depicted in the CA1 microcircuit in the previous chapter, the external inputs come from CA3 and EC to CA1, and P_S to septum.

By balancing the excitation and inhibition of populations, the phase synchronization between pyramidal and bistratified cells, and the out-of-sync behaviour of pyramidal and basket cells, and basket and bistratified cells, that was simulated using the continuous model is also observed in this discrete approach.

When more basket cells receive excitation from pyramidal cells, their phases begin to sync up with pyramidal cells as expected as shown in figure 54. Hence, the number of projections from pyramidal to basket cells is 1/5th of the number of projections from pyramidal to bistratified cells.

Similarly, the projection strength from bistratified to pyramidal cells is 1/5th of the projection strength from basket to pyramidal cells, and there is equal inhibition between basket

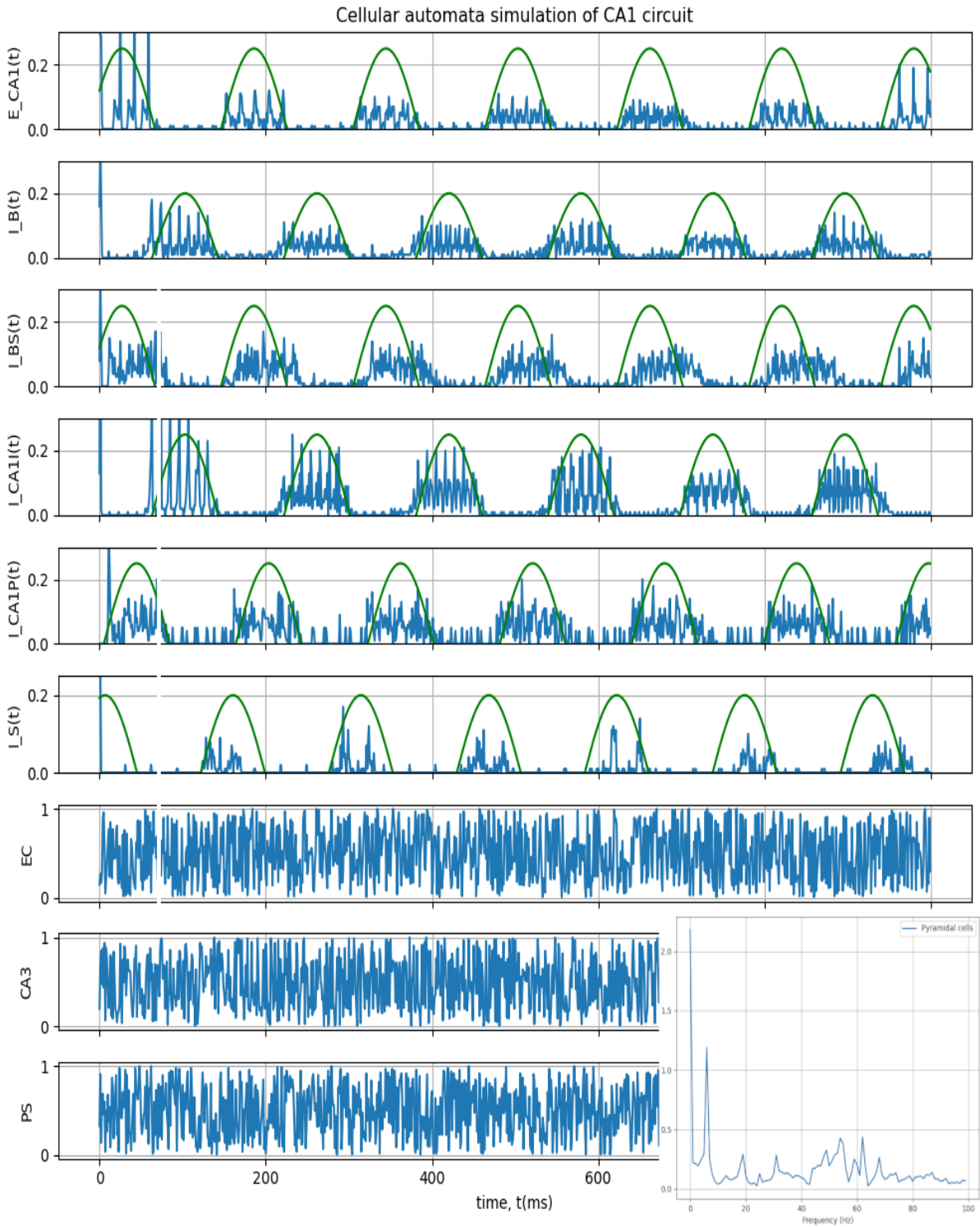


Figure 51: Cellular automata model simulation results for CA1 network model, with the FFT at the bottom showing 7Hz theta frequency and 30-70Hz slow-gamma frequency oscillations. The green line is fit to the actual activity of neurons.

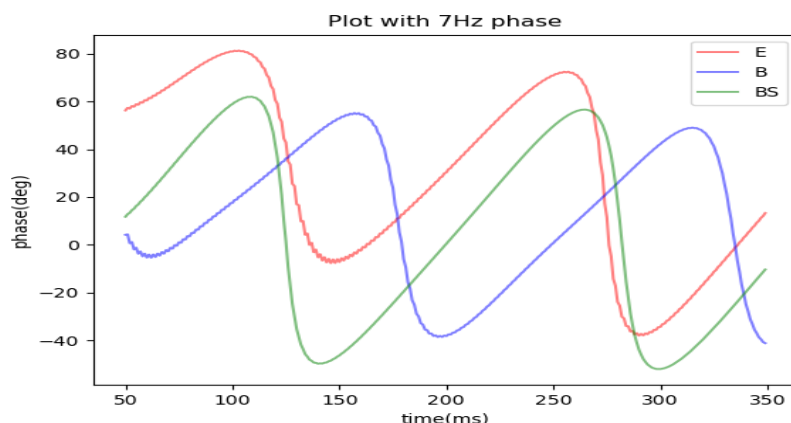


Figure 52: Phases of pyramidal(E), basket(B) and bistratified(BS) populations in cellular automata model simulation results for CA1 network model. The phase-shifts of pyramidal, basket and bistratified populations are comparable to the CA1 theta-coupled gamma oscillatory activity in the continuous model as shown in figure 22.

and bistratified cells, if not the phases of bistratified and basket cells begin to sync up, as shown in figure 54. Without septal input to basket cells, there is no discernible pattern in basket cell activity, as shown in figure 54. With no clear theta frequency oscillations in the basket cell activity, learning and recall does not happen.

When there is less/no inhibition from other inhibitory interneurons (I), there is fast spiking in the pyramidal cell population (E) irrespective of the presence of basket (B) or bistratified cell (BS) populations, due to the interruption in the septal pacemaker circuit. The septal pacemaker circuit gets inhibitory inputs from the septum which are propagated to E from I which helps to maintain theta oscillations. B and BS are not involved in the pacemaker circuit and do not affect theta oscillatory patterns. B and BS affect slow gamma spiking which is coupled with theta oscillations [144, 21].

5.3 LARGE-SCALE SIMULATIONS

One of the purposes of choosing a cellular automata approach is also to simulate large-scale neuronal networks. With 1000 pyramidal neurons, and 100 neurons in each of the other populations, there are totally 1900 neurons in the neuronal network, with 132200 total number of projections. Since all the CA3 external pseudo-neurons are connected to all the pyramidal cells, with a large number of neurons, excitation of pyramidal cells increases and results in fast oscillations. To retain the 7Hz theta oscillations, more inhibition from other

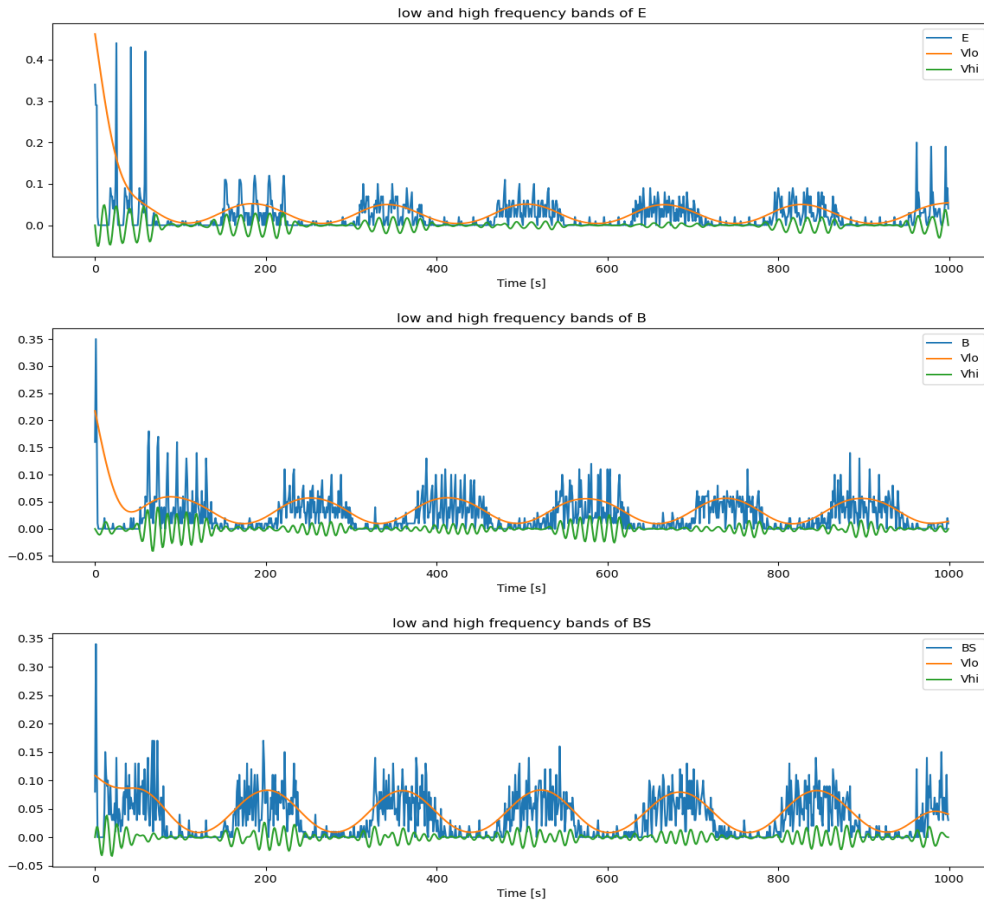


Figure 53: Theta and slow gamma frequency bands in pyramidal, basket and bistratified cell simulation

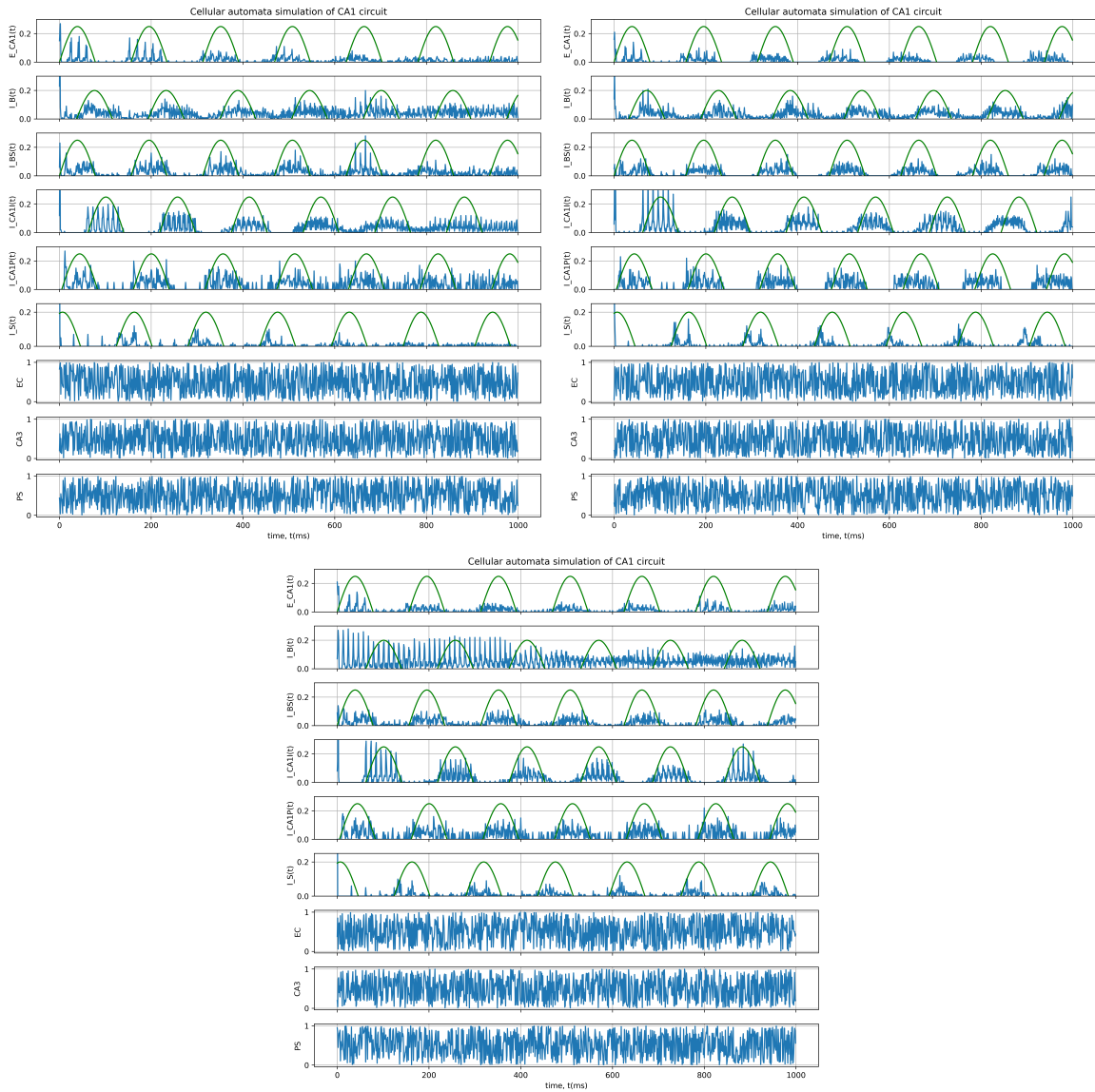


Figure 54: (left) Number of projections from excitatory pyramidal cells to basket cells is increased and hence, pyramidal and basket cell activities have a phase-shift and are not 180° out-of-phase; (right) By increasing basket and bistratified cell excitation from pyramidal cells, and inhibition from both basket and bistratified cells to pyramidal cells, the three populations sync up; (bottom) Removal of septal input to basket cells, we can see that there is no clear pattern in basket cell activity.

inhibitory interneurons is required since the other inhibitory interneuron population forms the septal-pacemaker circuit that propagates 7Hz theta oscillations to CA1 pyramidal cells. Increasing inhibition from basket or bistratified cells to generate 7Hz theta oscillations results in lower or no activity in pyramidal cells.

Without learning, figure 55 shows theta-coupled gamma oscillating model of CA1 with such a big neuronal network. The simulation time for this network without learning took 24mins, while smaller neuronal networks with a 100 neurons in each populations take 6mins to complete the whole simulation including learning and recall.

5.4 MECHANISM OF PATTERN LEARNING AND RECALL IN CELLULAR AUTOMATA MODEL

Following the Hebb rule, if a post-synaptic spike occurs after a pre-synaptic spike, the projection weight between the pre- and post-synaptic neurons is increased leading to Long Term Potentiation (LTP). Following the same principle for the converse statement, when a post-synaptic neuron does not spike after a presynaptic spike, the projection weight between the pre- and post-synaptic neurons is decreased, also called Long Term Depression (LTD), so much that they cannot exceed the threshold to spike.

By decreasing the projection weights between neurons that do not spike in a temporal sequence, we weaken the spiking probability of spurious neurons that are not part of the learning pattern. Hence the patterns intended to be learnt end up having higher projection weights. When these neurons are fired, they tend to have a greater integrated sum of inputs than the threshold, thus firing an action potential, resulting in a recall of a specific learnt pattern. This implies that these neurons are part of learning or recalling particular patterns. This is the spike timing dependent plasticity (STDP) learning rule as explained in table 15.

In the cellular automata model we have developed, the learning rate parameter mentioned in the input JSON file for the neuron defines the weight by which the projection weight has to be incremented according to the LTP mechanism, and the unlearning rate defines the weight by which the projection weight has to be decremented constituting the LTD mechanism. The rates are chosen from a minimum value and increased depending on the recall quality for the five patterns we are trying to learn and recall.

We have simulated 3 cases in our study (i) without LTP or LTD as shown in figure 57 which is without the implementation of any learning rule (ii) without LTD as shown in figure

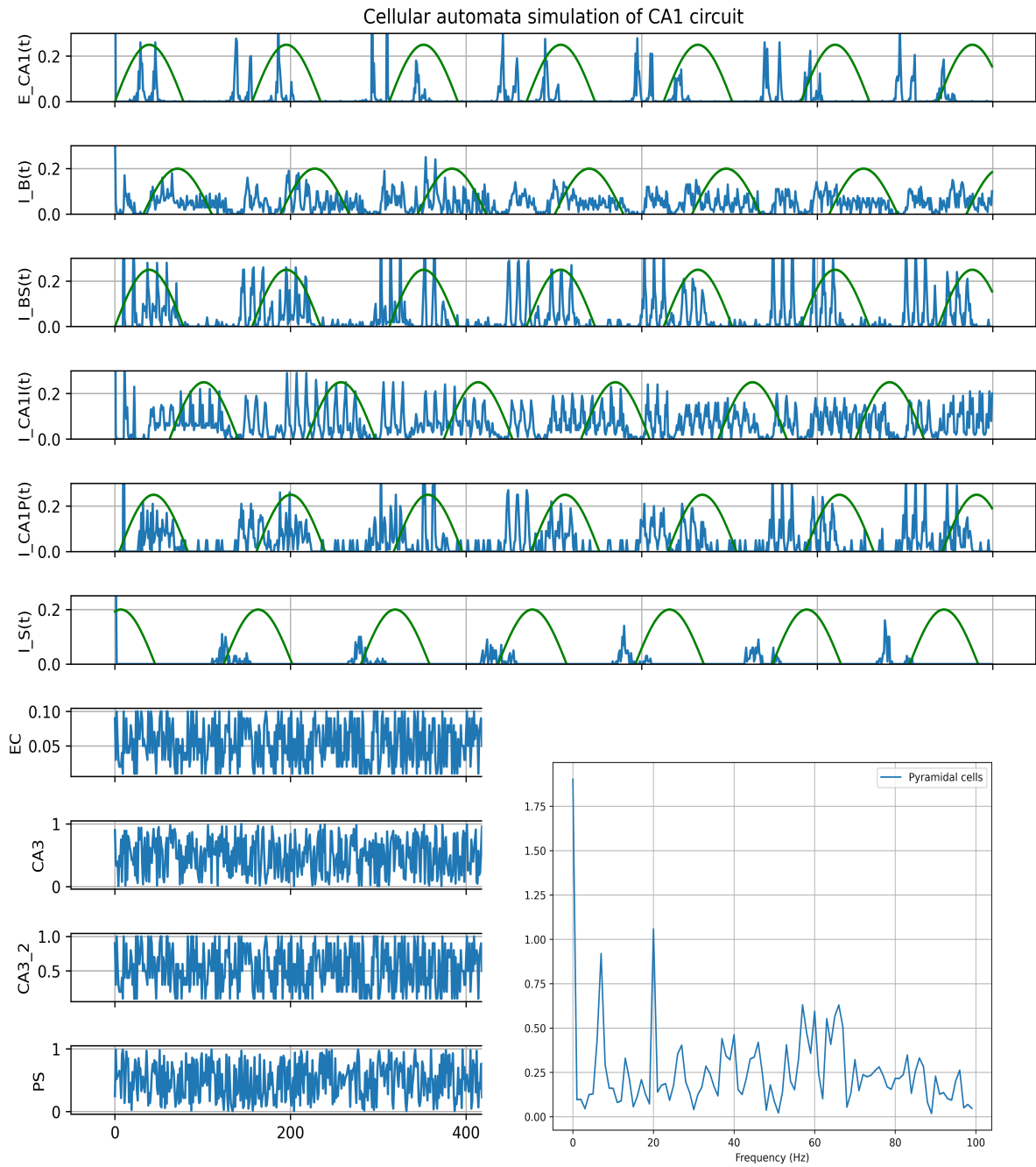


Figure 55: Large-scale simulation results for CA1 network model with the FFT at the bottom showing both theta and slow gamma frequency oscillations. The green line is fit to the actual activity of neurons.

58 which is recall without suppressing noisy neuron activity, and then (iii) with both LTP and LTD, as shown in figure 59 which is with STDP learning rule implemented. This results in very noisy recall in (i) and (ii) cases, and a less noisy recall in case of (iii) because of LTD. The figures are explained later in section 5.5.

Patterns to be learnt are a subset of neurons that are selected randomly during the beginning of the simulation based on the parameters *enable_learning*, *p_rand_neurons* and *no_of_patterns* in the JSON input files for neurons. When learning is enabled for a population of neurons, the model looks for how many patterns to create and how many neurons should each pattern have. Unlike many other artificial neuronal networks simulations, patterns in our simulation model are not a depiction of an image or alphabet or digit, etc.

Let us consider an example to understand what patterns in a cellular automata model mean. When the hippocampus receives sensory stimulus from EC such as a location that is new, a few place cells fire to form new patterns that will be stored later. When the same place cells fire upon receiving the same location information as sensory stimulus, the newly formed patterns get strengthened. As this process repeats, the neurons that fired up for the location information are now learnt due to LTP. Other neurons that would have fired during this learning process will not fire again once the pattern of neurons for a particular location is learnt or encoded due to LTD. The pattern of neurons that we select randomly during the beginning of our cellular automata simulation represents these neurons that need to strengthen the new connections over time. The other projections that exist represents spurious firing while recalling the encoded information which will be suppressed due to LTD over time. During recall, the neurons firing are compared against the patterns learnt to verify if the learnt patterns are indeed recalled.

It is observed in literature [1, 24] that learning and recall occur during different half cycles in a theta cycle, as shown in figure 56. In our simulations, learning takes place when basket cells are active and recall takes place when basket cells are inactive in accordance with literature [151]. Neuronal activity plots in a cellular automata model indicate the number of neurons active in a population at each time step. Based on this information for basket cell population, if the number of basket cells active at each time step exceeds a certain threshold (which is observed from prior simulations that pyramidal and basket cell activities complement each other), then the simulation is in the learning phase of the theta cycle, else, in the recall phase.

We have simulated learning of five patterns. Learning and recall happen throughout the

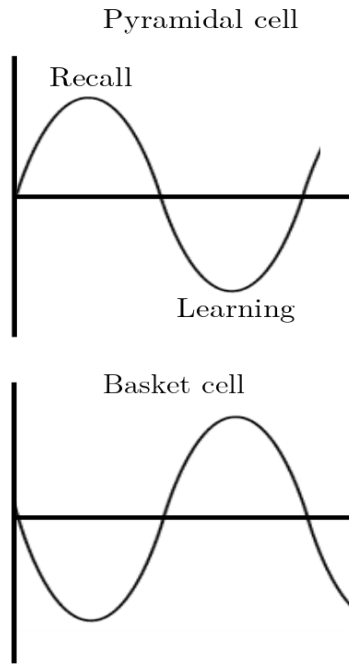


Figure 56: Learning and recall take place at different half cycles of theta wave. When basket cells are active, learning takes place and when basket cells are inactive, pyramidal cells are active and recall takes place.

duration of the simulation of theta cycles. The number of EC and CA3 external pseudo-neurons to fire at each time step is picked randomly from the total number of neurons, and the neurons to fire at each time step, which in our case are the excitatory pyramidal cells are also picked randomly during the beginning of the simulation. The external pseudo-neurons having projections to the five patterns that are learnt are each added as a cue to be recalled, one at every 20ms duration throughout the 1000ms simulation duration. This implies that the time step when both EC and CA3 cells that have projections with pyramidal cells which are in the pattern to be learnt are entirely random.

In our simulations, all the neurons forming a part of the external pseudo-neuron population for CA3 region have projections with all the pyramidal neurons. A fraction of EC input arrives at pyramidal cells with sensory information and all of the CA3 input arrives at pyramidal cells with conceptual information. When EC and CA3 input to pyramidal cells coincide, it induces STDP in pyramidal cells increasing the projection strength leading to encoding new patterns. Due to inhibition from inhibitory interneurons and basket cells, pyramidal cells do not fire an action potential. Pyramidal cells having projections with CA3 neurons that are not receiving EC input are not strengthened to be encoded. During the encoding cycle, basket

cells fire, inhibiting both pyramidal and bistratified neurons. When basket cells are inactive, both pyramidal and bistratified cells fire, recalling the learnt pattern of neurons. Spurious neuron activity during recall occurs due to active EC input to pyramidal cells which are suppressed by bistratified neurons and other inhibitory interneurons.

Basket cells are active when septum is inactive since basket cells receive inhibition from septum, and septum induces theta oscillations through the hippocampo-septal loop. This implies pyramidal cells learn during the trough of the theta cycle when basket cells are active. Hence, encoding and retrieval cycle is theta-aware, regulated by the activity of basket cells. The learning algorithm influenced by basket cell populations is given in table 16.

5.4.1 RECALL QUALITY METRIC CALCULATION

Quality of recall is obtained by calculating the correlation between the recalled pattern and the actual pattern, by taking the normalized dot product of the neurons recalled P and the actual pattern P' learnt, thus calculating the distance between them [24].

$$\text{Recall quality \%} = \frac{P \cdot P'}{(\sum_{i=0}^N P \times \sum_{i=0}^N P')^{1/2}} \quad (16)$$

The recall metric is calculated over a sliding time window equal to 20ms which is approximately equal to the time duration of a single gamma cycle in a single theta cycle. Programmatically, this is implemented by forming a binary vector of length N in which 1s correspond to those neurons that fire in the time window. In our simulations, since we have more than a single pattern to be learnt and recall is associative, we have been able to obtain a correlation or recall quality of 0.7 - 0.8 or 70% - 80%. This implies that the recalled patterns either have spurious activity or certain neurons from the pattern weren't recalled or both. A recall quality of less than 50% denotes that there is a lot of spurious activity and that most of the neurons from the pattern weren't recalled.

5.5 SIMULATIONS INVOLVING LEARNING AND RECALL OF MULTIPLE INTERSECTING PATTERNS

Here, the patterns are not unique and have neurons common to several patterns to be learnt. Learning rate and unlearning rate is as given in the table 17. Since we are simulating neuronal populations in the CA1 region, the primary neuronal population considered is the pyramidal cell population. The excitatory pyramidal cell population receives its main source

- Let M, N be the total number of neurons in the external pseudo-neuron population and the neuron population of interest (in our case, excitatory pyramidal cell population) respectively
- Let x be the number of neurons chosen randomly from the neuron population of interest, ($x < N$)
- Let y be the number of neurons chosen randomly from the external pseudo-neuron population, ($y < M$)
- Let p be the number of patterns to be learnt, with ($x < N$) number of neurons in each pattern (this produces intersecting patterns)
- When a neuron $b \in N$ in the excitatory neuron population receives an "ON" message:
 - Let neuron $a \in M$
 - If $\exists a \rightarrow b$ and both neurons a and b are in the pattern:
 - If integrated sum of inputs to $b > threshold$:
 - If a is "ON":
 - Activate neuron b
 - Activate synapses of neuron b with synaptic delay
 - Increase the projection weight between neurons $a \rightarrow b$ by a learning rate
 - else:
 - Decrease the projection weight between neurons $a \rightarrow b$ by an unlearning rate
 - Let neuron $c \in N$
 - When neuron c , **not** from the pattern in the excitatory neuron population gets an activation message:
 - If $\exists a \rightarrow c$ and either one of the neurons a and c are **not** in the pattern :
 - Decrease the projection weight between neurons $a \rightarrow c$ by an unlearning rate

Table 15: Our implementation of the STDP learning algorithm

- If number of basket cells active at $t_i >$ threshold for active half cycle of theta:
 - For each pyramidal cell p_i having projection from active EC neuron ec_i :
 - If p_i has a projection with active CA3 neuron $ca3_i$: implement STDP learning rule as per table 15
 - return without firing the pyramidal cell p_i
- else call threshold block(t_i, p_i) (recall cycle)

Table 16: Our implementation of the STDP learning algorithm when basket cells are active.

of external input from both EC and CA3. However, it receives input from CA3 while recalling information. Hence, the populations for which learning and recall need to be set in the input JSON files are the pyramidal and external pseudo-neuron CA3 populations. The projections from CA3 to CA1 pyramidal cells are unidirectional in our model. Hence, learning and un-learning rates are set only to the excitatory pyramidal cell population since (i) the projection strength between external pseudo-neuron CA3 and CA1 pyramidal cell population needs to be either strengthened or weakened, and (ii) pyramidal cells are the actual populations that we consider for studying our results (the external inputs are pseudo-neuron populations as mentioned before).

Recall quality of such patterns will not be high as the projection weights increased as per the learning rate represent more than a single pattern. However, due to LTD, only the patterns learnt will be recalled, thus reducing noisy neuronal activity. Parameters for this simulation are given in table 17.

The case where there is no LTP or LTD, spurious neuron activity is 30%. But then, there is no LTP or LTD, therefore no learning takes place, and hence recall of only the neurons present in the pattern is also not possible. The patterns are not learnt here and hence, all the neurons are activated with the same probability. The results are as shown in figure 57.

In the case where there is only LTP but no LTD, there is still 30% spurious neuron activity. There is only learning, but no LTD to decrease the weights of other projections which are not relevant to the pattern, and hence, there will be some spurious neuronal activity. The results are as shown in figure 58.

In the last case where there is both LTP and LTD, only the neurons in the patterns are

activated and very less spurious neurons are active as there is both LTP and LTD. The results are as shown in figure 59.

When the basket cell inhibition is removed from the network, pyramidal and bistrat-

	#Neurons	τ_{ap} (ms)	τ_{ref} (ms)	τ_{del} (ms)	τ_{dur} (ms)	Threshold	L.R	U.R
Pyr	100	1	16	15	5	15	1	5
Bas	100	1	10	5	15	5		
Bis	100	1	10	5	15	5		
Inh. In	100	1	10	5	15	5		
Hipp. Sep	100	1	10	8	50	1		
Septum	100	1	30	8	50	1		
EC	100	1	0	0	5	5		
CA3	100	1	0	0	5	1		
Ps	100	1	0	0	5	1		

	Pyr	Bas	Bis	Inh.In	Hipp. Sep	Septum	EC	CA3	P_s
Pyr		5	5	5	5				
Bas	-1		-1						
Bis	-1	-1							
Inh. In	-10								
Hipp. Sep						-5			
Septum		-5	-1	-20					
EC	5	1		1					
CA3	5	1	1	1					
Ps						1			

	Pyr	Bas	Bis	Inh.In	Hipp. Sep	Septum	EC	CA3	P_s
Pyr		1	5	5	5				
Bas	1		1						
Bis	5	1							
Inh. In	50								
Hipp. Sep						5			
Septum		5	5	5					
EC	50	10		10					
CA3	100	5	1	10					
Ps						8			

Table 17: (top) Parameters of population neurons where $\#Neurons$ are the number of neurons in the population, $L.R$ is the learning rate, $U.R$ is the unlearning rate; (middle) weight matrix; (bottom) projection matrix for intersecting patterns.

ified cell populations are in sync as expected. However, since learning takes place when basket cells are active, learning and recall does not happen in the absence of basket cells and

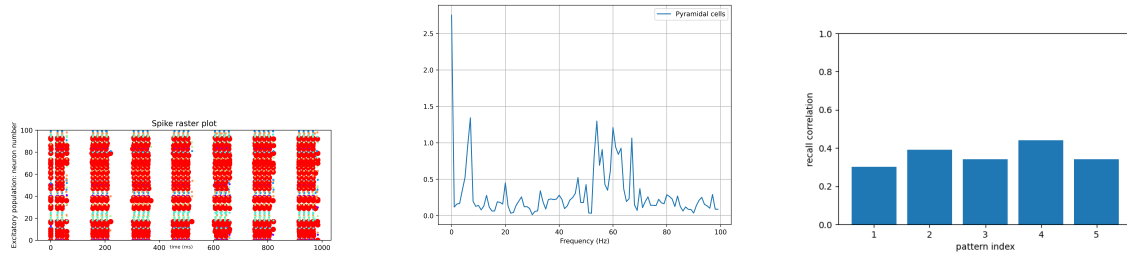
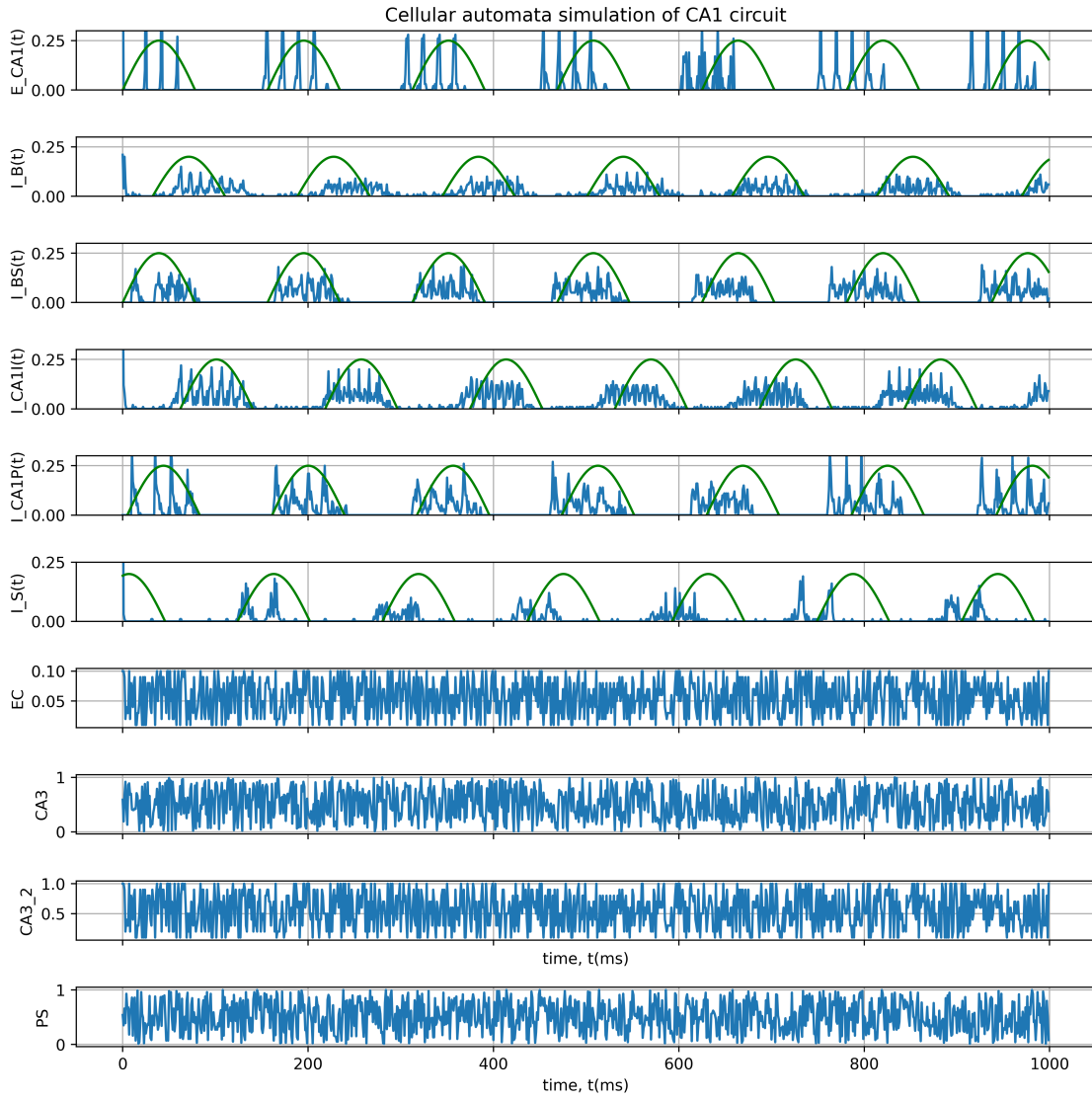


Figure 57: Simulation results for 5 intersecting patterns with no LTP or LTD. (top) shows the neuronal activity of all populations. The bottom row shows the raster plot, FFT and recall quality. Red dots indicate spurious neuron recall, while all other colors indicate activity of neurons in pattern learnt.

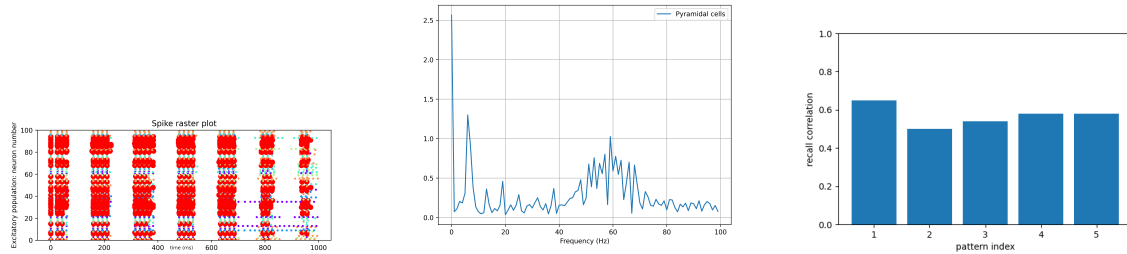
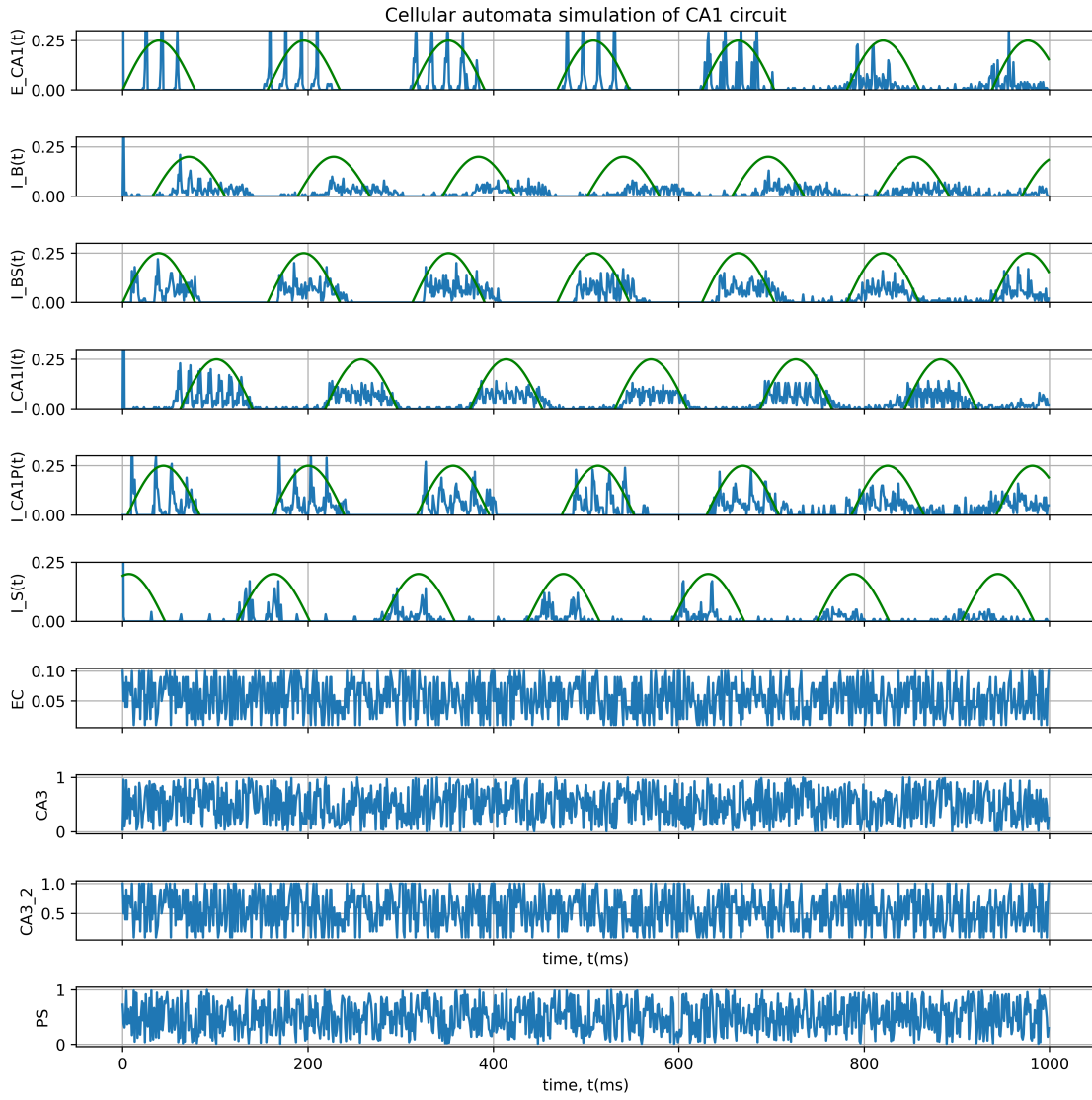


Figure 58: Simulation results for 5 intersecting patterns with no LTD which implies there is no suppression of spurious neuronal activity resulting in noisy recall. (top) shows the neuronal activity of all populations. The bottom row shows the raster plot, FFT and recall quality. Red dots indicate spurious neuron activity, while all other colors indicate activity of neurons in pattern learnt.

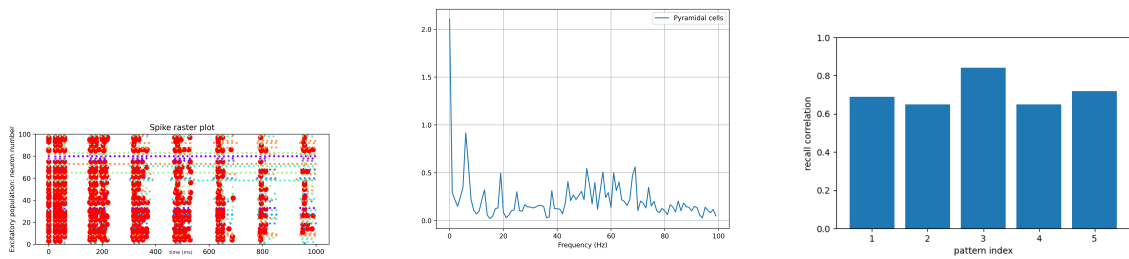
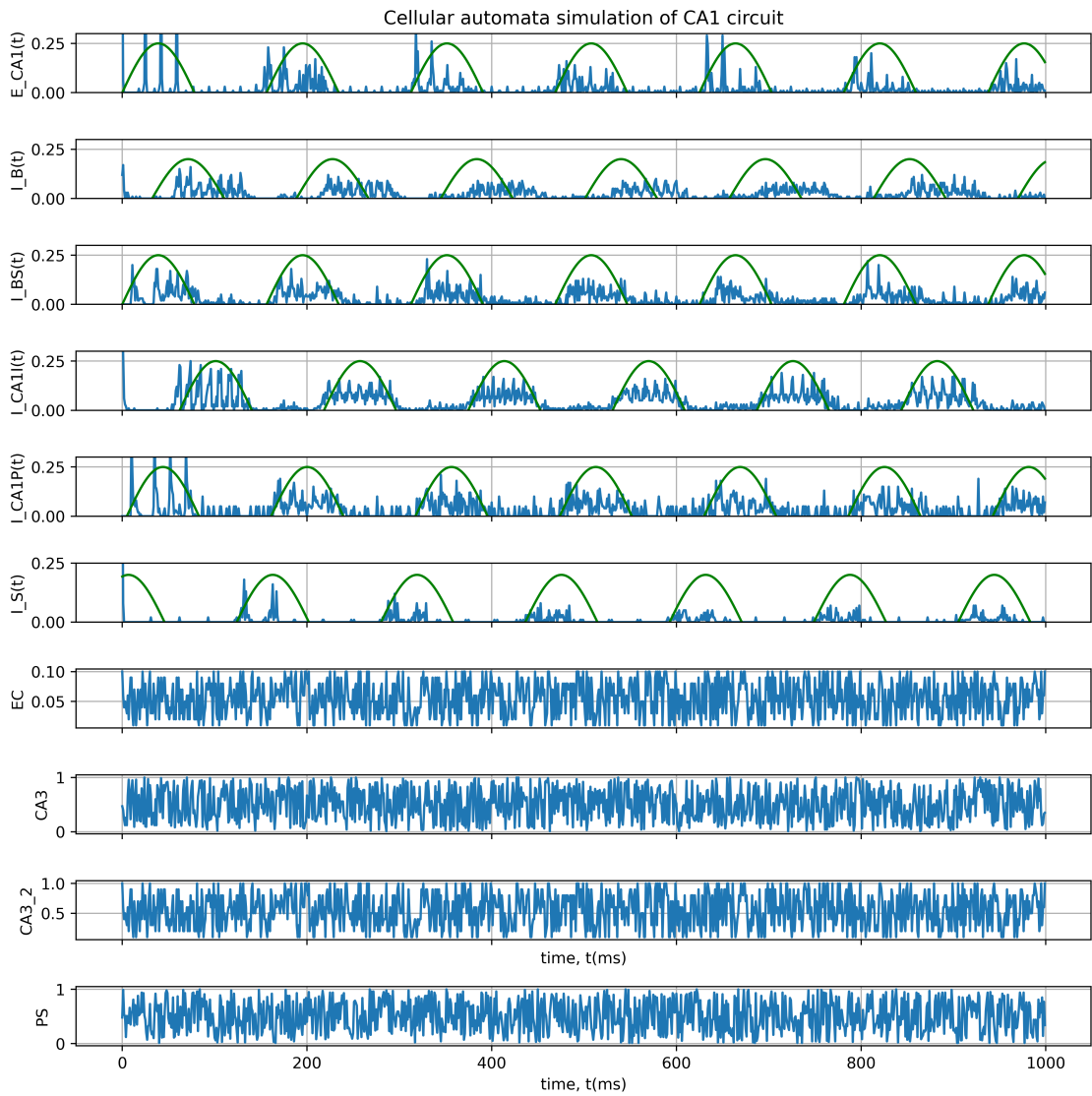


Figure 59: Simulation results for 5 intersecting patterns with LTP and LTD which implies there is learning and hence, we can expect good quality recall with minimal spurious neuronal activity. (top) shows the neuronal activity of all populations. The bottom row shows the raster plot, FFT and recall quality. Red dots indicate spurious neuron recall, while all other colors indicate activity of neurons in pattern learnt.

hence the noisy pyramidal cell activity. When bistratified cell inhibition is removed from the network, pyramidal and basket cell populations are out of sync. However, bistratified cells inhibit spurious neuron activity and since bistratified cells are not present, noisy activity is seen in pyramidal cells. When the inhibition from other inhibitory interneurons is removed from the network, the septal pace-maker circuit is interrupted and hence, a disruption in the theta oscillations is expected as shown in figures 60, 61, 62. However, since basket cells are present, learning and recall takes place with LTP and LTD. This implies there is less noise in the activity of pyramidal cells. However, since there are no theta-coupled gamma oscillations present in the activity as seen in the FFT, the significance of such recall is questionable.

5.6 DISCUSSION

Based on the simulations we have seen to learn and recall patterns using the STDP learning rule, we can now analyze the differences between the continuous and discrete approaches to generate theta-coupled gamma oscillations.

The response functions in the septal-pacemaker circuit are the fraction of neurons firing for an input. They do not directly correspond to the number of projections between populations. In the cellular automata model, we have the parameters for each projection between populations.

Due to continuous external pseudo-neuron input, the model produces a lot of noise. Even without basket and bistratified populations, the activity of the septal-pacemaker circuit results in a noisy 7Hz theta oscillations. As such, it is difficult to identify the frequencies of slow gamma oscillations superposed on theta oscillations without the FFT.

The 7Hz theta oscillations are generated due to the refractory period of pyramidal cells and due to the inhibition from other inhibitory interneurons. Some fraction of pyramidal cells that are not in the refractory period are always active due to the external pseudo-neuron inputs. This activity is inhibited when the inhibitory interneurons are active. In both the continuous and cellular automata models, we can clearly notice that, modifying the inhibition strength from basket and bistratified cells directly affects the slow gamma oscillations, whereas modifying the inhibitory interneuron inhibition strength directly affects theta oscillations.

The learning and recall simulations of the CA1 here are based on the simulations conducted by Cutsuridis et. al [24] with some variations. Physiologically, our model has the septal-pacemaker circuit to generate theta oscillations and basket and bistratified cells to in-

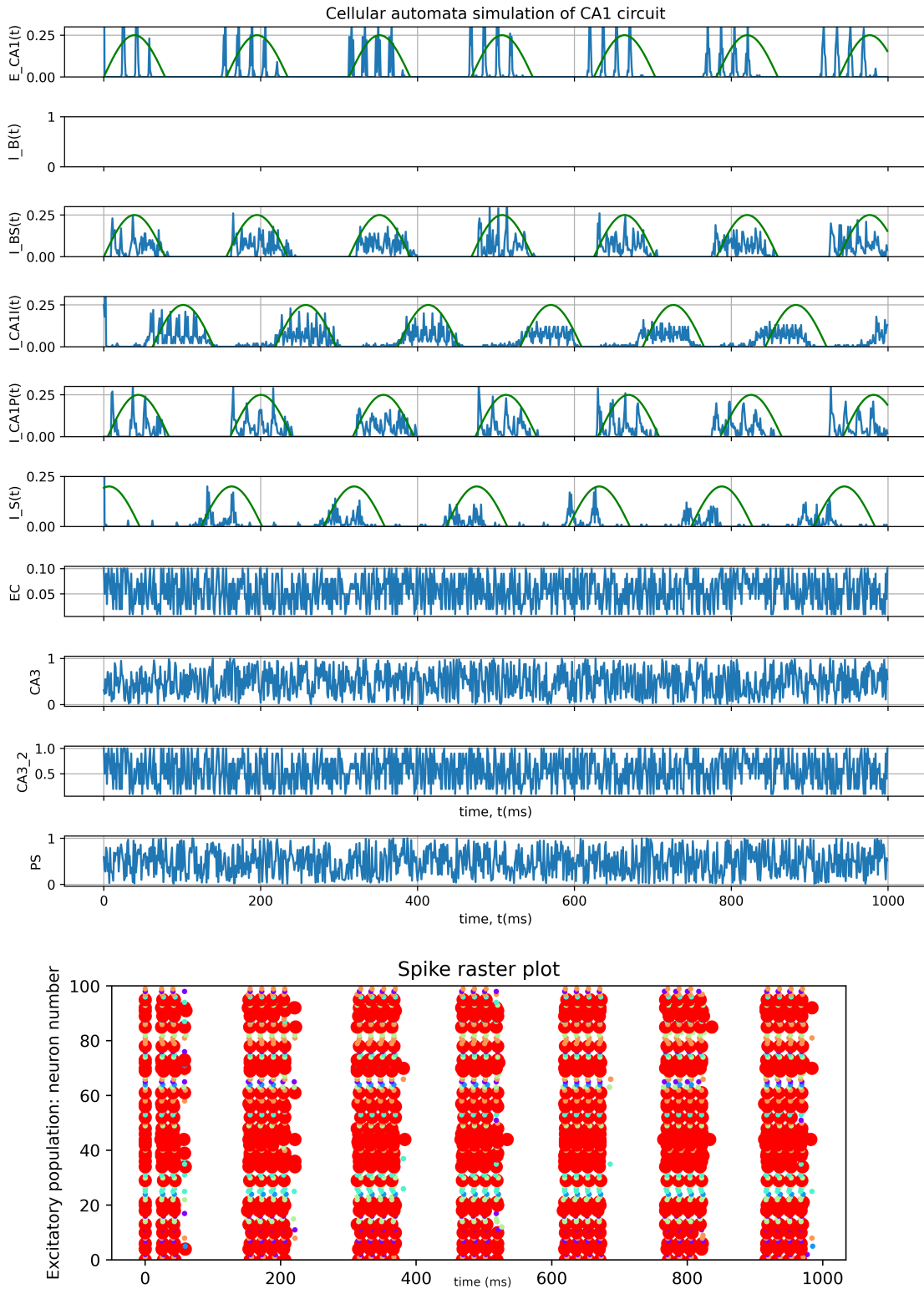


Figure 60: Effect on the population activity of pyramidal cells when basket cell population is completely removed from the network

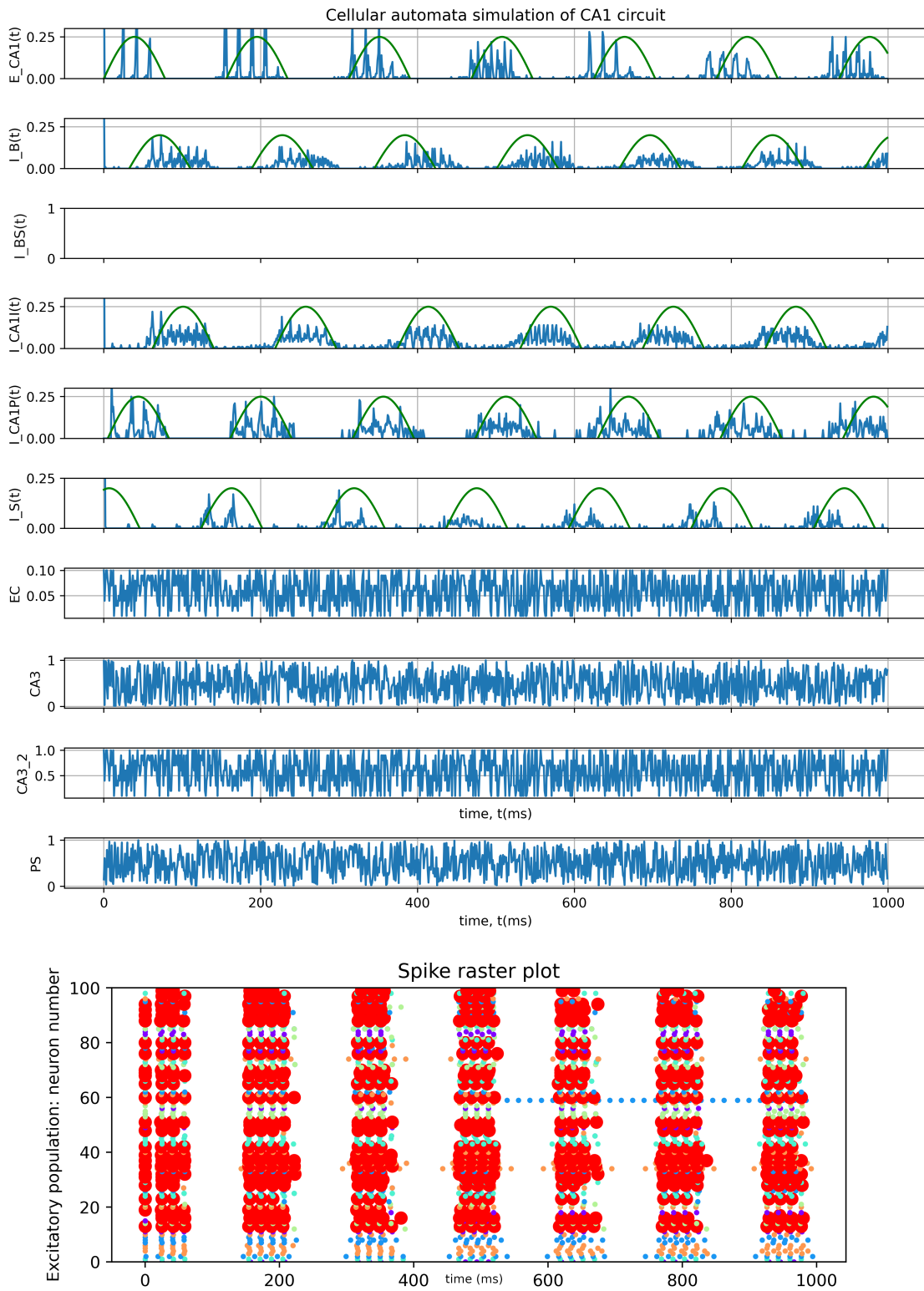


Figure 61: Effect on the population activity when bistratified cell population is completely removed from the network

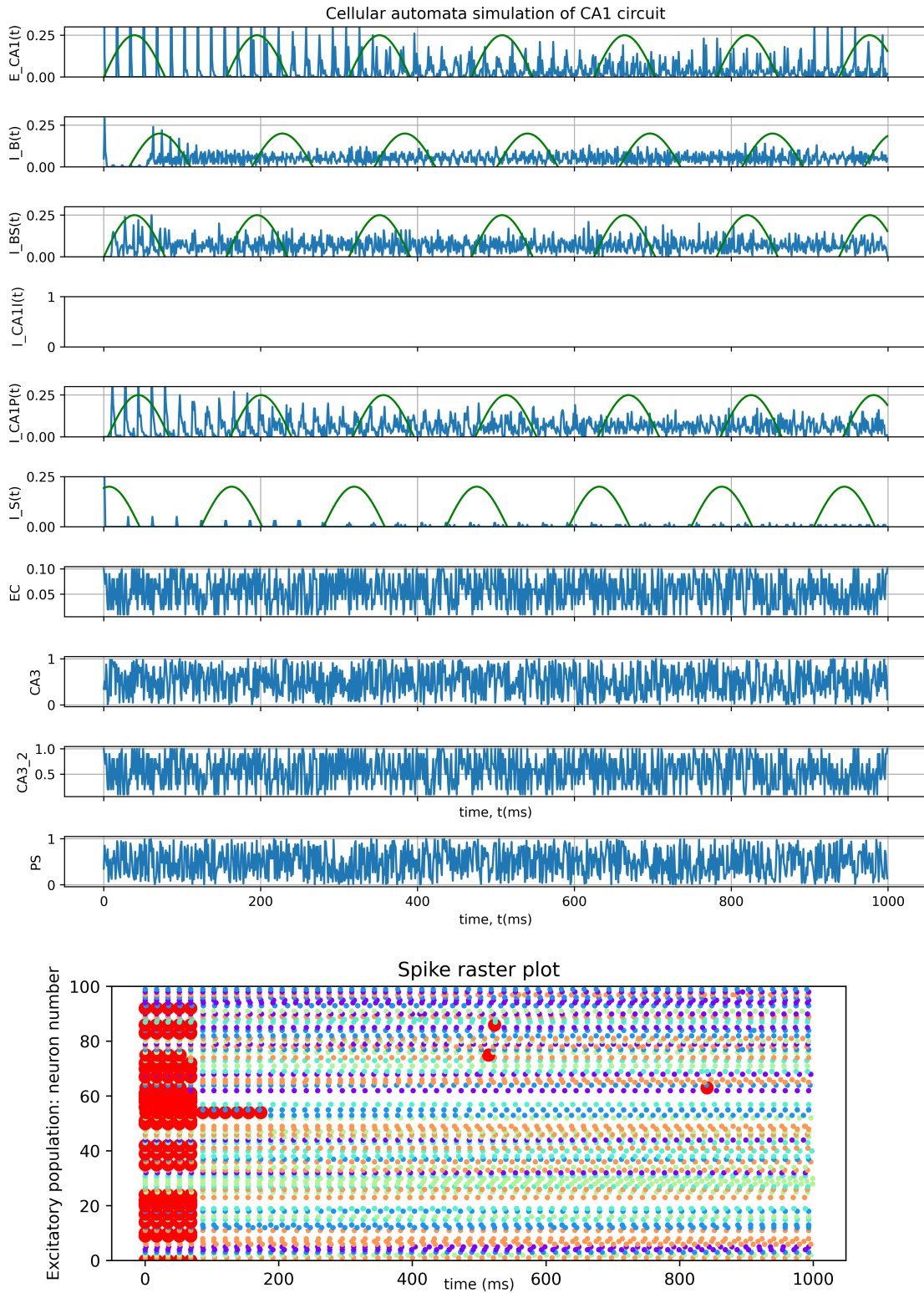


Figure 62: Effect on the population activity when other inhibitory interneuron cell population is completely removed from the network

duce slow gamma oscillations. All other inhibitory interneurons including axo-axonic cells and OLM cells are represented by the inhibitory interneuron population. In the Cutsuridis et. al model, learning occurs during a fixed time window when CA3 and EC firing coincides with basket cell inhibition. In our model, learning occurs on the basis of basket cell activity defining the learning phase of the theta cycle. During recall, average spiking activity over a 20ms window over the last 100ms of the simulation is considered to get the recall quality.

5.7 CONCLUSION

In conclusion, we are able to replicate most of the results we obtained in the continuous theta model using the discrete cellular automata model. We have also implemented learning and recall using the STDP algorithm. The influence of the inhibitory interneuron populations on pyramidal cell population and the effects of the septal pacemaker circuit on the CA1 region are clearly illustrated. We have incorporated biological parameters in the simulations here. Further, due to the flexibility offered by the cellular automata approach to neuronal modeling, we designed the model to accept different inputs representing different regions of the brain or different neuronal populations with different parameters. Hence, it is possible to build different microcircuits of any region of the brain.

6 CONCLUSION AND FUTURE WORK

The reason for building simulation models is to hypothesize how real biology works, to explore newer areas or problematic questions for more justifications. In this sense, it should be plausible to build a newer model that addresses specific concerns, expand any computational model to incorporate newer functionalities and adopt newer research discoveries.

During this doctoral period, we have developed computational models, both continuous and discrete, to understand theta-coupled gamma oscillations in the CA1 and CA3 regions of the hippocampus. Further, we have also simulated encoding and retrieval mechanisms using cellular automata model in the CA1 region. We have listed out our conclusions from our simulations in the next section, and have also listed out the possible future work that can be undertaken.

6.1 MAIN CONTRIBUTIONS

1. We have proposed the first integrated CA1-CA3 model to study the effects of Schaffer collaterals and CA1 back-projection cells on CA1 and CA3 regions of the hippocampus.
2. We have hypothesized the effects of CA1 back-projection cells on CA1 and CA3 based on our simulations. Since there is not much literature available here to validate our results, our simulation results opens doors to future biological confirmations.
3. The results simulated in our model and the effects of varying different parameters in our model are also observed in literature thus validating our results. Specific results are given below.
4. We have developed a discrete rule-based computational model using the cellular automata approach to study neuronal networks from a single-neuron level and from a population level, and also to study encoding and retrieval mechanisms.
5. We have also made our model theta-aware using the activity of basket cells in CA1 so that encoding patterns takes place during the encoding cycle of theta automatically instead of hard-coding specific neurons to fire at a specific time-step.

Trying to understand encoding and retrieval of patterns during cross-frequency coupled theta and slow gamma oscillations from both a single-neuron and population neuronal network level is the motive of our research. To understand the cross-frequency coupling between

theta and slow gamma oscillations in a population neuronal network level in both CA1 and CA3 regions of the hippocampus, we have used the septal-pacemaker circuit as a base to build an integrated CA1-CA3 model. The CA1 and CA3 regions are involved in learning and recall of patterns which has to be studied at a single-neuron level. To achieve this, we developed a simple rule-based cellular automata model. The thus developed cellular automata model not only reproduces the behaviour of the continuous population model, but also uses the activity of inhibitory basket cells to determine when CA1 pyramidal cells should learn and recall in the theta cycle. These contributions are explained briefly along with a few more results from our simulations in this chapter.

6.2 OSCILLATIONS

1. We have used a continuous population model to explore phasic relationships between different inhibitory cell types and pyramidal cells in CA1 and CA3 regions of the hippocampus during theta frequency oscillations. It was possible to match the Klausberger et. al [141, 133] data for CA1 with pyramidal cells in-sync with bistratified cells and out-of-sync with basket cells.
2. The phase shifts seen in CA1 with respect to pyramidal and basket cell populations are not seen in CA3 due to the missing septal input to bistratified cells and unidirectional inhibition from bistratified to basket cells in CA3, as expected.
3. It was possible to match the data observed from Mizuseki et. al [145] that CA3 and CA1 pyramidal cells are phase-shifted; and that the phase observed in CA1 pyramidal cells are not a result of a simple integration of phases from CA3, EC or the medial septum.
4. We have used basket and bistratified cells to superpose slow-gamma frequency oscillations in theta frequency oscillations in both CA1 and CA3 as seen in literature [20, 144, 147].
5. It was possible to observe the propagation of slow-gamma oscillations through the Schaffer collaterals with our CA1-CA3 model which is the first integrated model proposed to observe cross-frequency coupling in CA1-CA3 regions of the hippocampus.
6. We could observe that there is no bifurcation while transiting from theta to theta-coupled gamma oscillations in both CA1 and CA3 regions. The transition is gradual and is not a sudden change in firing activity.

7. The effects of external inputs on CA1 and CA3 regions is explained in both the continuous and discrete models.
 - (a) The continuous population model of CA1 and CA3 exhibits different oscillatory states depending on the external inputs. High values of EC or DG inputs result in steady states, whereas high values of septum or posterior-hypothalamus inputs results in fast oscillations.
 - (b) Increasing CA1 back-projection input to CA3 pyramidal cells results in oscillations with frequencies greater than 12Hz.
8. Results simulated using the continuous population model are also obtained using the discrete cellular automata approach.
 - (a) Theta oscillations are generated by implementing the hippocampo-septal loop. Since in our model all the CA3 neurons are connected to pyramidal cells, it is easy to produce oscillations of frequency greater than 50Hz. To reduce the frequency to 7-10H theta oscillations, an increased inhibition from the inhibitory interneurons is input to pyramidal cells.
 - (b) We were able to reproduce the phasic differences between the different cell types as per Klausberger et. al data [141, 133] as simulated in the continuous population model.
 - (c) Disruptions to the septal-pacemaker circuit causes oscillations of frequency greater than 50Hz in pyramidal cells due to the E-I loops between pyramidal and basket and bistratified cells.

6.3 ENCODING AND RETRIEVAL OF MEMORIES

1. The cellular automata model is a deterministic message-based approach to build complex models using simple rules. The library is a public git repository at: https://github.com/Esash382/Cellular_Automata_New. The cellular automata library written in C++ can be used to design models of different regions of the brain using the JSON input files.
2. Encoding and retrieval of patterns using spike-timing dependent plasticity (STDP) algorithms were implemented.

3. Using a rule-based approach such as the cellular automata, we have simulated the CA1 cell-types that exhibit the complementary phasic nature of learning and recall where learning and recall take place in the opposite phases of a theta cycle.
4. Learning during basket cell activity and recalling during bistratified cell activity is reproduced in the CA1 model simulations making the model oscillations-aware. This differs from the Cutsuridis et. al (2010) simulation model and is more realistic by generating theta frequency oscillations through the hippocampo-septal loop and detecting the encoding and recall phases through the presence/absence of basket cell activity automatically.
5. Without basket cells, encoding and retrieval cycle is disrupted as the model is not theta oscillations-aware without basket cell activity.

We have now simulation models that

1. integrates both hippocampal CA1 and CA3 regions and analyzes the effects in the context of cross-frequency coupling of theta and slow gamma oscillations.
2. reproduces the results found in literature for the encoding and retrieval of information in theta sub-cycles [20] which is regulated by the activity of inhibitory basket cells [141, 140].

6.4 FUTURE WORK

With the current design of the continuous and/or discrete model, taking inspiration from the E-I, CA1, CA3 neuronal network, neurons from different regions of the brain can be modeled. Each population is a homogeneous cluster of neurons that propagates signals to neurons from other populations. Hence, adding more cell types or removing cell types or projections can be studied easily. Removal of neurons or projections, also called lesions can be studied using the continuous or discrete simulations.

In the discrete cellular automata approach, removal of neurons can be done by removing the concerned projections from the *networks.dat* file in which case, the simulations will be unaware of the removed neuron types. To reduce the number of projections between two populations, the z parameter between the concerned populations can be reduced in the projection file of the two populations. This enables us to easily study the effects of removal/absence of projections. Examples of studies that can be undertaken by removal of neurons or projections include:

1. Decreased neuronal density in CA1 region and altered mossy fiber pathways to CA3 is observed in Alzheimer's [152, 153].
2. CA1 and CA3 regions of the hippocampus receive dopaminergic inputs from the perforant path projecting from EC. The direct perforant path carries sensory information to both CA1 and CA3 which is necessary for proper convergence to information stored in memory. Improper convergence leads to delusions responsible for causing paranoid schizophrenia as discussed in [154, 155].

Similarly, addition/growth of newer projections on neuronal populations can also be easily studied by adding more cell types for the CA1 and CA3 regions of the hippocampus. This simply involves adding the respective neuron definition file and the projection files defining its projections with other cell types as inputs to the model. By adding the projection file to *networks.dat* file, we tell the model to include the two populations as part of the neuronal network that is being built. To study increased connectivity between two populations, again the z parameter between the concerned populations can be increased in the projection file of the two populations. For example, many more inhibitory interneurons present in CA1 and CA3 can be included to provide a complete framework of the CA1 and CA3 regions to in turn study the effects of these interneurons on the activity dynamics, encoding and retrieval mechanisms in the hippocampus.

Currently, the activation function is an integrated sum of inputs. Newer implementations will be required for different activation functions. Other brain regions can also be implemented in a similar way having populations of homogeneous neurons having projections with one another. The main difference between the different types of neurons are the characteristics defining each neuron type, which are the definitions given in the neuron definition file. The whole model is basically neurons talking to each other, and hence as long as the definition of neurons, parameters defining the talking mechanism, and the mechanism for processing inputs is defined, any model having similar rules can be modeled using the cellular automata approach.

Both the continuous and discrete models are a good foundation to build upon for more in-depth research to answer the effects of excitatory and inhibitory signals and oscillations on the different regions on the brain. The models developed here are a step closer towards building a biologically realistic model of the regions of the brain, as the primary reason for building computational models for simulation is also to hypothesize and not just reproduce how the real biology works. We propose the following future work that can be undertaken to

enhance the biological plausibility of the model in the cellular automata approach.

1. When an action potential fires and neurotransmitter is released from the synaptic vesicle, the post-synaptic neurons are in the vicinity of the pre-synaptic neuron for associative LTP to occur [67]. The randomness of choosing the post-synaptic neuron can be reduced if the distance between the neurons is also taken into account in the cellular automata model.
2. A neuron has many dendritic compartments, each of which are post-synaptic sites for signals from other neurons from different regions of the brain. Implementing the dendritic compartments would also modularize and segregate the signals coming from different populations to a neuron making the cellular automata approach more distinct and expandable to include various other parameters of the brain. Such an implementation would be a realistic approach to modeling a neuron that can include dendritic parameters such as the capacity, length, resistance, etc [118].
3. Continuing from the previous point, population models of neurons using a cellular automata approach composed of multiple dendritic compartments need to be implemented to study distance-related propagation delays of action potentials and dendritic integration and interaction of synaptic inputs. For example, CA3 and EC inputs to CA1 pyramidal cells arrive at SR and SLM regions, and the strength of the inputs decrease as they propagate towards the soma of the cell. The projection strengths are either constants or get incremented/decremented by a constant value in our simulations until recall, whereas in reality, the projection strengths decrease over the distance traveled which can also be a scope for further implementation.

In this research, the goal was to study the cross-frequency coupling of theta and slow gamma oscillations in CA1 and CA3 regions of the hippocampus while encoding and retrieving information. To do this, we built the continuous population model to study and understand the cross-frequency coupling in both CA1 and CA3 regions of the hippocampus. By establishing the results from the continuous population model as a baseline, we built the cellular automata model for encoding and retrieval of patterns while the model is oscillating with both theta and slow gamma frequency oscillations. The cellular automata model thus lies in the middle between simple biologically implausible models to complex biologically plausible models, and can be seen as a building block along the way to a fully functional biologically realistic neuronal model.

REFERENCES

- [1] Michael E Hasselmo, Clara Bodelón, and Bradley P Wyble. A proposed function for hippocampal theta rhythm: separate phases of encoding and retrieval enhance reversal of prior learning. *Neural computation*, 14(4):793–817, 2002.
- [2] Michael J Denham and Roman M Borisyuk. A model of theta rhythm production in the septal-hippocampal system and its modulation by ascending brain stem pathways. *Hippocampus*, 10(6):698–716, 2000.
- [3] Enric T Claverol, Andrew D Brown, and John E Chad. A large-scale simulation of the piriform cortex by a cell automaton-based network model. *IEEE transactions on biomedical engineering*, 49(9):921–935, 2002.
- [4] G Bard Ermentrout and Carson C Chow. Modeling neural oscillations. *Physiology & behavior*, 77(4):629–633, 2002.
- [5] Chiping Wu, Marjan Nassiri Asl, Jesse Gillis, Frances K Skinner, and Liang Zhang. An in vitro model of hippocampal sharp waves: regional initiation and intracellular correlates. *Journal of neurophysiology*, 94(1):741–753, 2005.
- [6] Klaus M Stiefel and G Bard Ermentrout. Neurons as oscillators. *Journal of neurophysiology*, 116(6):2950–2960, 2016.
- [7] Stefano Taverna, Ema Ilijic, and D James Surmeier. Recurrent collateral connections of striatal medium spiny neurons are disrupted in models of parkinson’s disease. *Journal of Neuroscience*, 28(21):5504–5512, 2008.
- [8] Shun-Ichi Amari. Characteristics of sparsely encoded associative memory. *Neural networks*, 2(6):451–457, 1989.
- [9] Shun-Ichi Amari and Kenjiro Maginu. Statistical neurodynamics of associative memory. *Neural Networks*, 1(1):63–73, 1988.
- [10] Donald Olding Hebb. *The organization of behavior: A neuropsychological approach*. John Wiley & Sons, 1949.
- [11] Terrence J Sejnowski and Gerald Tesauro. The hebb rule for synaptic plasticity: algorithms and implementations. *Neural models of plasticity: Experimental and theoretical approaches*, pages 94–103, 1989.
- [12] Alessandro Treves and Edmund T Rolls. Computational analysis of the role of the hippocampus in memory. *Hippocampus*, 4(3):374–391, 1994.
- [13] Howard Eichenbaum, Paul Dudchenko, Emma Wood, Matthew Shapiro, and Heikki Tanila. The hippocampus, memory, and place cells: is it spatial memory or a memory space? *Neuron*, 23:209–226, 1999.
- [14] John O’keefe and Lynn Nadel. *The hippocampus as a cognitive map*. Oxford: Clarendon Press, 1978.
- [15] LL Voronin. Long-term potentiation in the hippocampus. *Neuroscience*, 10(4):1051–1069, 1983.
- [16] Tim VP Bliss, Graham L Collingridge, et al. A synaptic model of memory: long-term potentiation in the hippocampus. *Nature*, 361(6407):31–39, 1993.
- [17] György Buzsáki. Theta oscillations in the hippocampus. *Neuron*, 33(3):325–340, 2002.
- [18] Jerome M Siegel. The rem sleep-memory consolidation hypothesis. *Science*, 294(5544):1058–1063, 2001.

- [19] Nikolai Axmacher, Florian Mormann, Guillen Fernández, Christian E Elger, and Juergen Fell. Memory formation by neuronal synchronization. *Brain research reviews*, 52(1):170–182, 2006.
- [20] John E Lisman and Marco AP Idiart. Storage of 7 ± 2 short-term memories in oscillatory subcycles. *Science*, 267(5203):1512–1515, 1995.
- [21] Ole Jensen and John E Lisman. Theta/gamma networks with slow nmda channels learn sequences and encode episodic memory: role of nmda channels in recall. *Learning & Memory*, 3(2-3):264–278, 1996.
- [22] Bruce P Graham, Vassilis Cutsuridis, and Russell Hunter. Associative memory models of hippocampal areas ca1 and ca3. *Hippocampal Microcircuits: A Computational Modeler's Resource Book*, pages 459–494, 2010.
- [23] César Rennó-Costa, John E Lisman, and Paul FMJ Verschure. A signature of attractor dynamics in the ca3 region of the hippocampus. *PLoS computational biology*, 10(5):e1003641, 2014.
- [24] Vassilis Cutsuridis, Stuart Cobb, and Bruce P Graham. Encoding and retrieval in a model of the hippocampal ca1 microcircuit. *Hippocampus*, 20(3):423–446, 2010.
- [25] Gyorgy Buzsáki. *Rhythms of the Brain*. Oxford university press, 2006.
- [26] Sirel Karakaş and Robert J Barry. A brief historical perspective on the advent of brain oscillations in the biological and psychological disciplines. *Neuroscience & Biobehavioral Reviews*, 75:335–347, 2017.
- [27] György Buzsáki and Andreas Draguhn. Neuronal oscillations in cortical networks. *science*, 304(5679):1926–1929, 2004.
- [28] Lawrence M Ward. Synchronous neural oscillations and cognitive processes. *Trends in cognitive sciences*, 7(12):553–559, 2003.
- [29] György Buzsáki and James J Chrobak. Temporal structure in spatially organized neuronal ensembles: a role for interneuronal networks. *Current opinion in neurobiology*, 5(4):504–510, 1995.
- [30] Abdelrahman Rayan, José R Donoso, Marta Mendez-Couz, Laura Dolón, Sen Cheng, and Denise Manahan-Vaughan. Learning shifts the preferred theta phase of gamma oscillations in ca1. *Hippocampus*, 2022.
- [31] Damien Lapray, Balint Lasztozci, Michael Lagler, Tim James Viney, Linda Katona, Ornella Valenti, Katja Hartwich, Zsolt Borhegyi, Peter Somogyi, and Thomas Klausberger. Behavior-dependent specialization of identified hippocampal interneurons. *Nature neuroscience*, 15(9):1265–1271, 2012.
- [32] J Allan Hobson and Edward F Pace-Schott. The cognitive neuroscience of sleep: neuronal systems, consciousness and learning. *Nature Reviews Neuroscience*, 3(9):679–693, 2002.
- [33] György Buzsáki and Edvard I Moser. Memory, navigation and theta rhythm in the hippocampal-entorhinal system. *Nature neuroscience*, 16(2):130–138, 2013.
- [34] Jochen Baumeister, T Barthel, Kurt-Reiner Geiss, and M Weiss. Influence of phosphatidylserine on cognitive performance and cortical activity after induced stress. *Nutritional neuroscience*, 11(3):103–110, 2008.
- [35] Mette S Olufsen, Miles A Whittington, Marcelo Camperi, and Nancy Kopell. New roles for the gamma rhythm: population tuning and preprocessing for the beta rhythm. *Journal of computational neuroscience*, 14(1):33–54, 2003.
- [36] Ole Jensen and Laura L Colgin. Cross-frequency coupling between neuronal oscillations. *Trends in cognitive sciences*, 11(7):267–269, 2007.
- [37] Ryan T Canolty, Erik Edwards, Sarang S Dalal, Maryam Soltani, Srikantan S Nagarajan, Heidi E Kirsch, Mitchel S Berger, Nicholas M Barbaro, and Robert T Knight. High gamma power is phase-locked to theta oscillations in human neocortex. *science*, 313(5793):1626–1628, 2006.

- [38] Ole Jensen, Bart Gips, Til Ole Bergmann, and Mathilde Bonnefond. Temporal coding organized by coupled alpha and gamma oscillations prioritize visual processing. *Trends in neurosciences*, 37(7):357–369, 2014.
- [39] Benjamin J Griffiths, George Parish, Frederic Roux, Sebastian Michelmann, Mircea Van Der Plas, Luca D Kolibius, Ramesh Chelvarajah, David T Rollings, Vijay Sawlani, Hajo Hamer, et al. Directional coupling of slow and fast hippocampal gamma with neocortical alpha/beta oscillations in human episodic memory. *Proceedings of the National Academy of Sciences*, 116(43):21834–21842, 2019.
- [40] Jozsef Csicsvari, Brian Jamieson, Kensall D Wise, and György Buzsáki. Mechanisms of gamma oscillations in the hippocampus of the behaving rat. *Neuron*, 37(2):311–322, 2003.
- [41] Adriano BL Tort, Robert W Komorowski, Joseph R Manns, Nancy J Kopell, and Howard Eichenbaum. Theta–gamma coupling increases during the learning of item–context associations. *Proceedings of the National Academy of Sciences*, 106(49):20942–20947, 2009.
- [42] Gergo Orbán, Tamás Kiss, Máté Lengyel, and Péter Érdi. Hippocampal rhythm generation: gamma-related theta-frequency resonance in ca3 interneurons. *Biological Cybernetics*, 84:123–132, 2001.
- [43] Ole Jensen and John E Lisman. Hippocampal ca3 region predicts memory sequences: accounting for the phase precession of place cells. *Learning & Memory*, 3(2-3):279–287, 1996.
- [44] Emrah Düzel, Will D Penny, and Neil Burgess. Brain oscillations and memory. *Current opinion in neurobiology*, 20(2):143–149, 2010.
- [45] Sean M Montgomery, Anton Sirota, and György Buzsáki. Theta and gamma coordination of hippocampal networks during waking and rapid eye movement sleep. *Journal of Neuroscience*, 28(26):6731–6741, 2008.
- [46] Federico Stella and Alessandro Treves. Associative memory storage and retrieval: involvement of theta oscillations in hippocampal information processing. *Neural plasticity*, 2011, 2011.
- [47] Linton C Freeman et al. Centrality in social networks: Conceptual clarification. *Social network: critical concepts in sociology*. Londres: Routledge, 1:238–263, 2002.
- [48] Riko Jacob, Dirk Koschützki, Katharina Anna Lehmann, Leon Peeters, and Dagmar Tenfelde-Podehl. Algorithms for centrality indices. *Network analysis: Methodological foundations*, pages 62–82, 2005.
- [49] Britta Ruhnau. Eigenvector-centrality—a node-centrality? *Social networks*, 22(4):357–365, 2000.
- [50] William Beecher Scoville and Brenda Milner. Loss of recent memory after bilateral hippocampal lesions. *Journal of neurology, neurosurgery, and psychiatry*, 20(1):11, 1957.
- [51] Howard Eichenbaum. Hippocampus: cognitive processes and neural representations that underlie declarative memory. *Neuron*, 44(1):109–120, 2004.
- [52] Sean M Montgomery and György Buzsáki. Gamma oscillations dynamically couple hippocampal ca3 and ca1 regions during memory task performance. *Proceedings of the National Academy of Sciences*, 104(36):14495–14500, 2007.
- [53] Anatol Bragin, Gábor Jandó, Zoltán Nádasdy, Jammille Hetke, Kensall Wise, and Gy Buzsáki. Gamma (40–100 hz) oscillation in the hippocampus of the behaving rat. *Journal of neuroscience*, 15(1):47–60, 1995.
- [54] Laura Lee Colgin and Edvard I Moser. Gamma oscillations in the hippocampus. *Physiology*, 25(5):319–329, 2010.
- [55] David M Smith and Sheri JY Mizumori. Hippocampal place cells, context, and episodic memory. *Hippocampus*, 16(9):716–729, 2006.

- [56] David J Foster and Matthew A Wilson. Reverse replay of behavioural sequences in hippocampal place cells during the awake state. *Nature*, 440(7084):680–683, 2006.
- [57] Laura Lee Colgin. Five decades of hippocampal place cells and eeg rhythms in behaving rats. *Journal of Neuroscience*, 40(1):54–60, 2020.
- [58] Inah Lee and Raymond P Kesner. Encoding versus retrieval of spatial memory: double dissociation between the dentate gyrus and the perforant path inputs into ca3 in the dorsal hippocampus. *Hippocampus*, 14(1):66–76, 2004.
- [59] Steve Kunec, Michael E Hasselmo, and Nancy Kopell. Encoding and retrieval in the ca3 region of the hippocampus: a model of theta-phase separation. *Journal of neurophysiology*, 94(1):70–82, 2005.
- [60] Kenji Mizuseki, Sebastien Royer, Kamran Diba, and György Buzsáki. Activity dynamics and behavioral correlates of ca3 and ca1 hippocampal pyramidal neurons. *Hippocampus*, 22(8):1659–1680, 2012.
- [61] Vincent Douchamps, Ali Jeewajee, Pam Blundell, Neil Burgess, and Colin Lever. Evidence for encoding versus retrieval scheduling in the hippocampus by theta phase and acetylcholine. *Journal of Neuroscience*, 33(20):8689–8704, 2013.
- [62] Edmund T Rolls and Raymond P Kesner. A computational theory of hippocampal function, and empirical tests of the theory. *Progress in neurobiology*, 79(1):1–48, 2006.
- [63] Edmund T Rolls. A theory of hippocampal function in memory. *Hippocampus*, 6(6):601–620, 1996.
- [64] György Buzsáki. Memory consolidation during sleep: a neurophysiological perspective. *Journal of sleep research*, 7(S1):17–23, 1998.
- [65] Tim VP Bliss, Graham L Collingridge, Richard GM Morris, and Klaus G Reymann. Long-term potentiation in the hippocampus: discovery, mechanisms and function. *Neuroforum*, 24(3):A103–A120, 2018.
- [66] Thomas H Brown, Edward W Kairiss, and Claude L Keenan. Hebbian synapses: biophysical mechanisms and algorithms. *Annual review of neuroscience*, 13(1):475–511, 1990.
- [67] German Barrionuevo and Thomas H Brown. Associative long-term potentiation in hippocampal slices. *Proceedings of the National Academy of Sciences*, 80(23):7347–7351, 1983.
- [68] John J Hopfield. Neural networks and physical systems with emergent collective computational abilities. *Proceedings of the national academy of sciences*, 79(8):2554–2558, 1982.
- [69] Amos J Storkey and Romain Valabregue. The basins of attraction of a new hopfield learning rule. *Neural Networks*, 12(6):869–876, 1999.
- [70] Terrence J Sejnowski and Gerald Tesauero. Building network learning algorithms from hebbian synapses. *Brain Organization and Memory: Cells, Systems, and Circuits*, pages 338–355, 1989.
- [71] Michael E Hasselmo, Bradley P Wyble, and Gene V Wallenstein. Encoding and retrieval of episodic memories: role of cholinergic and gabaergic modulation in the hippocampus. *Hippocampus*, 6(6):693–708, 1996.
- [72] Klaus Oberauer, Timothy Jones, and Stephan Lewandowsky. The hebb repetition effect in simple and complex memory span. *Memory & cognition*, 43(6):852–865, 2015.
- [73] MPA Page and D Norris. A model linking immediate serial recall, the hebb repetition effect and the learning of phonological word forms. *Philosophical Transactions of the Royal Society B: Biological Sciences*, 364(1536):3737–3753, 2009.
- [74] György Buzsáki. Theta rhythm of navigation: link between path integration and landmark navigation, episodic and semantic memory. *Hippocampus*, 15(7):827–840, 2005.

- [75] Leslie M Kay, Jennifer Beshel, Jorge Brea, Claire Martin, Daniel Rojas-Líbano, and Nancy Kopell. Olfactory oscillations: the what, how and what for. *Trends in neurosciences*, 32(4):207–214, 2009.
- [76] Joshua Berke. Participation of striatal neurons in large-scale oscillatory networks. *The basal ganglia VIII*, pages 25–35, 2005.
- [77] Jose L Cantero, Mercedes Atienza, Robert Stickgold, Michael J Kahana, Joseph R Madsen, and Bernat Kocsis. Sleep-dependent θ oscillations in the human hippocampus and neocortex. *Journal of Neuroscience*, 23(34):10897–10903, 2003.
- [78] Ze’ev R Abrams, Ajithkumar Warriar, Dirk Trauner, and Xiang Zhang. A signal processing analysis of purkinje cells in vitro. *Frontiers in Neural Circuits*, page 13, 2010.
- [79] Juan P Gambini, Ricardo A Velluti, and Marisa Pedemonte. Hippocampal theta rhythm synchronizes visual neurons in sleep and waking. *Brain research*, 926(1):137–141, 2002.
- [80] Wei-Xing Pan and Neil McNaughton. The supramammillary area: its organization, functions and relationship to the hippocampus. *Progress in neurobiology*, 74(3):127–166, 2004.
- [81] Michael C Ashby and John TR Isaac. Maturation of a recurrent excitatory neocortical circuit by experience-dependent unsilencing of newly formed dendritic spines. *Neuron*, 70(3):510–521, 2011.
- [82] Fu-Sun Lo. Both fast and slow relay cells in lateral geniculate nucleus of rabbits receive recurrent inhibition. *Brain research*, 271(2):335–338, 1983.
- [83] WR Levick, BG Cleland, and MW Dubin. Lateral geniculate neurons of cat: retinal inputs and physiology. *Invest Ophthalmol*, 11(5):302–311, 1972.
- [84] DR Curtis and RW Ryall. The acetylcholine receptors of rensaw cells. *Experimental brain research*, 2(1):66–80, 1966.
- [85] Philip B Bradley. *Introduction to neuropharmacology*. Butterworth-Heinemann, 2014.
- [86] Ann B Butler and William Hodos. *Comparative vertebrate neuroanatomy: evolution and adaptation*. John Wiley & Sons, 2005.
- [87] Marina R Picciotto, Michael J Higley, and Yann S Mineur. Acetylcholine as a neuromodulator: cholinergic signaling shapes nervous system function and behavior. *Neuron*, 76(1):116–129, 2012.
- [88] Michael E Hasselmo. The role of acetylcholine in learning and memory. *Current opinion in neurobiology*, 16(6):710–715, 2006.
- [89] Michael E Hasselmo and Martin Sarter. Modes and models of forebrain cholinergic neuromodulation of cognition. *Neuropsychopharmacology*, 36(1):52–73, 2011.
- [90] Robert P Vertes. Major diencephalic inputs to the hippocampus: supramammillary nucleus and nucleus reuniens. circuitry and function. *Progress in brain research*, 219:121–144, 2015.
- [91] Per Andersen, Richard Morris, David Amaral, Tim Bliss, and John O’Keefe. *The hippocampus book*. Oxford university press, 2006.
- [92] Hiroshi T Ito and Erin M Schuman. Functional division of hippocampal area ca1 via modulatory gating of entorhinal cortical inputs. *Hippocampus*, 22(2):372–387, 2012.
- [93] Attila Sik, Aarne Ylinen, Markku Penttonen, and Gyorgy Buzsaki. Inhibitory ca1-ca3-hilar region feedback in the hippocampus. *Science*, 265(5179):1722–1724, 1994.
- [94] John O’Keefe and Michael L Recce. Phase relationship between hippocampal place units and the eeg theta rhythm. *Hippocampus*, 3(3):317–330, 1993.
- [95] Hiroki Sayama. *Introduction to the modeling and analysis of complex systems*. Open SUNY Textbooks, 2015.

- [96] Alan L Hodgkin, Andrew F Huxley, and Bernard Katz. Measurement of current-voltage relations in the membrane of the giant axon of loligo. *The Journal of physiology*, 116(4):424, 1952.
- [97] Alan L Hodgkin and Andrew F Huxley. A quantitative description of membrane current and its application to conduction and excitation in nerve. *The Journal of physiology*, 117(4):500, 1952.
- [98] Hugh R Wilson and Jack D Cowan. Excitatory and inhibitory interactions in localized populations of model neurons. *Biophysical journal*, 12(1):1–24, 1972.
- [99] Eugene M Izhikevich. Which model to use for cortical spiking neurons? *IEEE transactions on neural networks*, 15(5):1063–1070, 2004.
- [100] CAS Batista, RL Viana, FAS Ferrari, SR Lopes, AM Batista, and JCP Coninck. Control of bursting synchronization in networks of hodgkin-huxley-type neurons with chemical synapses. *Physical Review E*, 87(4):042713, 2013.
- [101] Denis Noble. Applications of hodgkin-huxley equations to excitable tissues. *Physiological Reviews*, 46(1):1–50, 1966.
- [102] Denis Noble. Cardiac action and pacemaker potentials based on the hodgkin-huxley equations. *Nature*, 188(4749):495–497, 1960.
- [103] Denis Noble, Alan Garny, and Penelope J Noble. How the hodgkin–huxley equations inspired the cardiac physiome project. *The Journal of physiology*, 590(11):2613–2628, 2012.
- [104] Melissa G Johnson and Sylvain Chartier. Spike neural models, part i: The hodgkin-huxley model. *The quantitative methods for psychology*, 13(2):105–19, 2017.
- [105] William A Catterall, Indira M Raman, Hugh PC Robinson, Terrence J Sejnowski, and Ole Paulsen. The hodgkin-huxley heritage: from channels to circuits. *Journal of Neuroscience*, 32(41):14064–14073, 2012.
- [106] Claude Meunier and Idan Segev. Playing the devil’s advocate: is the hodgkin–huxley model useful? *Trends in neurosciences*, 25(11):558–563, 2002.
- [107] Shuaiby M Shuaiby, Mohsen A Hassan, and Moumen El-Melegy. Modeling and simulation of the action potential in human cardiac tissues using finite element method. *Journal of Communications and Computer Engineering*, 2(3):21–27, 2012.
- [108] Rose Taj Faghih. *The FitzHugh-Nagumo model dynamics with an application to the hypothalamic pituitary adrenal axis*. PhD thesis, Massachusetts Institute of Technology, 2010.
- [109] Szabolcs Káli and Peter Dayan. The involvement of recurrent connections in area ca3 in establishing the properties of place fields: a model. *Journal of Neuroscience*, 20(19):7463–7477, 2000.
- [110] David Sterratt, Bruce Graham, Andrew Gillies, and David Willshaw. *Principles of computational modelling in neuroscience*. Cambridge University Press, 2011.
- [111] Duane Q Nykamp and Daniel Tranchina. A population density approach that facilitates large-scale modeling of neural networks: Analysis and an application to orientation tuning. *Journal of computational neuroscience*, 8:19–50, 2000.
- [112] Eugene M Izhikevich. *Dynamical systems in neuroscience*. MIT press, 2007.
- [113] Nicolas Fourcaud-Trocmé. Integrate and fire models, deterministic. In *Encyclopedia of Computational Neuroscience*, pages 1683–1689. Springer, 2022.
- [114] Eugene M Izhikevich. Resonate-and-fire neurons. *Neural networks*, 14(6-7):883–894, 2001.
- [115] G Bard Ermentrout and Nancy Kopell. Parabolic bursting in an excitable system coupled with a slow oscillation. *SIAM journal on applied mathematics*, 46(2):233–253, 1986.

- [116] D Hansel and G Mato. Existence and stability of persistent states in large neuronal networks. *Physical Review Letters*, 86(18):4175, 2001.
- [117] Nicolas Fourcaud-Trocmé, David Hansel, Carl Van Vreeswijk, and Nicolas Brunel. How spike generation mechanisms determine the neuronal response to fluctuating inputs. *Journal of neuroscience*, 23(37):11628–11640, 2003.
- [118] Wulfram Gerstner, Werner M Kistler, Richard Naud, and Liam Paninski. *Neuronal dynamics: From single neurons to networks and models of cognition*. Cambridge University Press, 2014.
- [119] E Pytte, G Grinstein, and RD Traub. Cellular automaton models of the ca3 region of the hippocampus. *Network: Computation in Neural Systems*, 2(2):149–167, 1991.
- [120] Raymond L Beurle. Properties of a mass of cells capable of regenerating pulses. *Philosophical Transactions of the Royal Society of London. Series B, Biological Sciences*, pages 55–94, 1956.
- [121] John S Griffith. On the stability of brain-like structures. *Biophysical journal*, 3(4):299–308, 1963.
- [122] Tanya Kostova, Renuka Ravindran, and Maria Schonbek. Fitzhugh–nagumo revisited: Types of bifurcations, periodical forcing and stability regions by a lyapunov functional. *International journal of bifurcation and chaos*, 14(03):913–925, 2004.
- [123] John Lisman and György Buzsáki. A neural coding scheme formed by the combined function of gamma and theta oscillations. *Schizophrenia bulletin*, 34(5):974–980, 2008.
- [124] Mariano A Belluscio, Kenji Mizuseki, Robert Schmidt, Richard Kempster, and György Buzsáki. Cross-frequency phase–phase coupling between theta and gamma oscillations in the hippocampus. *Journal of Neuroscience*, 32(2):423–435, 2012.
- [125] Oswald Steward and Sheila A Scoville. Cells of origin of entorhinal cortical afferents to the hippocampus and fascia dentata of the rat. *Journal of Comparative Neurology*, 169(3):347–370, 1976.
- [126] Thomas van Groen, Pasi Miettinen, and Inga Kadish. The entorhinal cortex of the mouse: organization of the projection to the hippocampal formation. *Hippocampus*, 13(1):133–149, 2003.
- [127] Menno P Witter, Thanh P Doan, Bente Jacobsen, Eirik S Nilssen, and Shinya Ohara. Architecture of the entorhinal cortex a review of entorhinal anatomy in rodents with some comparative notes. *Frontiers in systems neuroscience*, 11:46, 2017.
- [128] Arnau Sans-Dublanç, Adrià Razzauti, Srinidhi Desikan, Marta Pascual, Jaime de la Rocha, Hannah Monyer, and Carlos Sindreu. Septal gabaergic inputs to ca1 govern contextual memory retrieval. *bioRxiv*, page 824748, 2019.
- [129] Menno P Witter. Intrinsic and extrinsic wiring of ca3: indications for connectional heterogeneity. *Learning & memory*, 14(11):705–713, 2007.
- [130] Diek W Wheeler, Charise M White, Christopher L Rees, Alexander O Komendantov, David J Hamilton, and Giorgio A Ascoli. Hippocampome.org: a knowledge base of neuron types in the rodent hippocampus. *Elife*, 4:e09960, 2015.
- [131] Tamas F Freund and György Buzsáki. Interneurons of the hippocampus. *Hippocampus*, 6(4):347–470, 1996.
- [132] Marianne J Bezaire, Ivan Raikov, Kelly Burk, Dhruvil Vyas, and Ivan Soltesz. Interneuronal mechanisms of hippocampal theta oscillations in a full-scale model of the rodent ca1 circuit. *Elife*, 5:e18566, 2016.
- [133] Thomas Klausberger and Peter Somogyi. Neuronal diversity and temporal dynamics: the unity of hippocampal circuit operations. *Science*, 321(5885):53–57, 2008.

- [134] Michele Migliore. On the integration of subthreshold inputs from perforant path and schaffer collaterals in hippocampal ca1 pyramidal neurons. *Journal of computational neuroscience*, 14(2):185–192, 2003.
- [135] Rita Zemankovics, Szabolcs Káli, Ole Paulsen, Tamás F Freund, and Norbert Hájos. Differences in subthreshold resonance of hippocampal pyramidal cells and interneurons: the role of h-current and passive membrane characteristics. *The Journal of physiology*, 588(12):2109–2132, 2010.
- [136] David K Bilkey and Philip A Schwartzkroin. Variation in electrophysiology and morphology of hippocampal ca3 pyramidal cells. *Brain research*, 514(1):77–83, 1990.
- [137] Ludovic Tricoire, Kenneth A Pelkey, Brian E Erkkila, Brian W Jeffries, Xiaoqing Yuan, and Chris J McBain. A blueprint for the spatiotemporal origins of mouse hippocampal interneuron diversity. *Journal of Neuroscience*, 31(30):10948–10970, 2011.
- [138] Tengis Gloveli, Tamar Dugladze, Sikha Saha, Hannah Monyer, Uwe Heinemann, Roger D Traub, Miles A Whittington, and Eberhard H Buhl. Differential involvement of oriens/pyramidal interneurons in hippocampal network oscillations in vitro. *The Journal of physiology*, 562(1):131–147, 2005.
- [139] Eberhard H Buhl, Tibor Szilágyi, Katalin Halasy, and Peter Somogyi. Physiological properties of anatomically identified basket and bistratified cells in the ca1 area of the rat hippocampus in vitro. *Hippocampus*, 6(3):294–305, 1996.
- [140] Thomas Klausberger, László F Márton, Agnes Baude, J David B Roberts, Peter J Magill, and Peter Somogyi. Spike timing of dendrite-targeting bistratified cells during hippocampal network oscillations in vivo. *Nature neuroscience*, 7(1):41, 2004.
- [141] Thomas Klausberger, Peter J Magill, László F Márton, J David B Roberts, Philip M Cobden, György Buzsáki, and Peter Somogyi. Brain-state-and cell-type-specific firing of hippocampal interneurons in vivo. *Nature*, 421(6925):844, 2003.
- [142] Laura Lee Colgin. Theta–gamma coupling in the entorhinal–hippocampal system. *Current opinion in neurobiology*, 31:45–50, 2015.
- [143] Romain Goutagny, Jesse Jackson, and Sylvain Williams. Self-generated theta oscillations in the hippocampus. *Nature neuroscience*, 12(12):1491, 2009.
- [144] György Buzsáki and Xiao-Jing Wang. Mechanisms of gamma oscillations. *Annual review of neuroscience*, 35:203–225, 2012.
- [145] Kenji Mizuseki, Anton Sirota, Eva Pastalkova, and György Buzsáki. Theta oscillations provide temporal windows for local circuit computation in the entorhinal-hippocampal loop. *Neuron*, 64(2):267–280, 2009.
- [146] Ivan E Mysin, Valentina F Kitchigina, and Yakov B Kazanovich. Phase relations of theta oscillations in a computer model of the hippocampal ca1 field: Key role of schaffer collaterals. *Neural Networks*, 116:119–138, 2019.
- [147] Thomas Klausberger. Gabaergic interneurons targeting dendrites of pyramidal cells in the ca1 area of the hippocampus. *European Journal of Neuroscience*, 30(6):947–957, 2009.
- [148] Roger D Traub, Andrea Bibbig, André Fisahn, Fiona EN LeBeau, Miles A Whittington, and Eberhard H Buhl. A model of gamma-frequency network oscillations induced in the rat ca3 region by carbachol in vitro. *European Journal of Neuroscience*, 12(11):4093–4106, 2000.
- [149] Theodore C Dumas, Michael R Uttaro, Carolina Barriga, Tiffany Brinkley, Maryam Halavi, Susan N Wright, Michele Ferrante, Rebekah C Evans, Sarah L Hawes, and Erin M Sanders. Removal of area ca3 from hippocampal slices induces postsynaptic plasticity at schaffer collateral synapses that normalizes ca1 pyramidal cell discharge. *Neuroscience letters*, 678:55–61, 2018.

- [150] Roman A Sandler, Dustin Fetterhoff, Robert E Hampson, Sam A Deadwyler, and Vasilis Z Marmarelis. Cannabinoids disrupt memory encoding by functionally isolating hippocampal ca1 from ca3. *PLoS computational biology*, 13(7):e1005624, 2017.
- [151] Peter Somogyi and Thomas Klausberger. Defined types of cortical interneurone structure space and spike timing in the hippocampus. *The Journal of physiology*, 562(1):9–26, 2005.
- [152] Silvia Viana da Silva, Pei Zhang, Matthias Georg Haberl, Virginie Labrousse, Noëlle Grosjean, Christophe Blanchet, Andreas Frick, and Christophe Mulle. Hippocampal mossy fibers synapses in ca3 pyramidal cells are altered at an early stage in a mouse model of alzheimer’s disease. *Journal of Neuroscience*, 39(21):4193–4205, 2019.
- [153] Manuela Padurariu, Alin Ciobica, Ioannis Mavroudis, Dimitrios Fotiou, and Stavros Baloyannis. Hippocampal neuronal loss in the ca1 and ca3 areas of alzheimer’s disease patients. *Psychiatria Danubina*, 24(2.):152–158, 2012.
- [154] EE Kriekhaus, John W Donahoe, and Maria A Morgan. Paranoid schizophrenia may be caused by dopamine hyperactivity of ca1 hippocampus. *Biological psychiatry*, 31(6):560–570, 1992.
- [155] Nonna A Otmakhova and John E Lisman. Dopamine selectively inhibits the direct cortical pathway to the ca1 hippocampal region. *Journal of Neuroscience*, 19(4):1437–1445, 1999.